Modelling, analysis and control of plantain plant-parasitic nematodes

Israël Tankam Chedjou

Modelling, analysis and control of plantain plant-parasitic nematodes

by :

TANKAM CHEDJOU Israël

Defended publicly on April 09, 2021

in fulfillment of the requirements for the degree
Doctor of Philosophy, Ph.D.
In the Department of Mathematics, Faculty of Science
University of Yaoundé I, Yaoundé, Cameroon

Jury:

President:	BEKOLLE David, Professor	University of Yaoundé I
Supervisors:	TEWA Jean-Jules, Professor	University of Yaoundé I
	TOUZEAU Suzanne, Senior Researcher	Inria Sophia-Antipolis, France
Reviewers:	EMVUDU WONO Yves Sébastien, Professor	University of Yaoundé I
	HAMELIN Frédéric, Senior Researcher	University of Rennes, France
Members:	AYISSI Raoul Domingo, Professor	University of Yaoundé I
	BOWONG Samuel, Associate Professor	University of Douala

Academic year 2019 - 2020

Dedication

To my parents.

Acknowledgements

It is always particularly challenging to write acknowledgements, because there is a risk of neglecting people. The immense scientific, moral and financial support that I received during this doctoral adventure involves so many people that it would take more pages than there are in this manuscript to thank them. However, if we had to retain a minimum of names, it would certainly be those of my various supervisors whose immense role could not be rendered by words. I would like to thank them here as sincerely as possible. Without Mr Jean Jules Tewa, Mrs Suzanne Touzeau, Mr Frédéric Grognard and Mr Ludovic Mailleret, I would not have had to write these lines. The first nominee, after having previously introduced me to mathematical modeling in a master's course, and directed my master's thesis, agreed to supervise this thesis despite its fluctuating availability. Mrs. Suzanne Touzeau and Mr. Frédéric Grognard, whom we affectionately call Fred, gave all their energy to not only follow this work and correct it whenever necessary, but also to forge the researcher that I have become. To this excellent supervision were added the experience and benevolence of Ludovic Mailleret, whom we affectionately call "Ludo". Thank you, madam, gentlemen, I enjoyed.

I would also like to thank Mr Samuel Bowong (University of Douala), co-leader of the Epitag project. Through him, I also want to express my gratitude to my Epitag project team as well as to all of its members. It was a real pleasure to evolve within this team with this wonderful atmosphere. Special thanks go to Yves Fotso, who was my companion during the whole adventure in Epitag. Our exchanges have always been fruitful, and I want to thank you for your friendship. I would also like to thank INRIA (hosted institute of my internships), IRD (through UMMISCO funds), EMS-simmons for Africa and the CETIC project for the financial support during my doctoral studies.

I cannot fail to thank Doctors Christian Chabrier and Douglas Marin for the enriching discussions we had on biology. I could not have started the modelling work without their input.

I would like to thank the members of my thesis defence jury for agreeing to be part of this jury.

I would also like to express my sincere gratitude to every teacher of the Departments of Mathematics of the University of Yaoundé I and the Department of mathematics and Computer Sciences of the University of Dschang. Particularly, I would like to reserve special acknowledgements for Mr. Joseph Mbang, Mr. Boulchard Mewoli, Mr. Yves Emvudu, Mr. Nicolas Gabriel Andjiga, Mr Christophe Fomekong, Mrs. Anne-Marie Tiaya, Mr. Calvin Tadmon, Mr. Celestin Lele, Mr. Gabriel Deugoué, Mr. Samuel Njipouakouyou. They all contribute to my graduate studies.

For the wonderful environment they helped to develop during my stays at INRIA in Sophia An-

tipolis, I would like to thank all the members of my host team (Biocore), as well as all those who exchanged a smile, a sweet word, in the hallway or at lunch. A special thank goes to the very attentive team leader, Jean-Luc Gouzé, and his second, Olivier Bernard. For the pleasant time we spent working on an issue that occupied my mind, I also want to express my gratitude to Pierre Bernhard. I cannot forget Walid Djema, Carlos Martinez, Lucy Chambon, Marjorie Morales, Ouassim Barra and others. Thank you for your welcome and your friendship. I would also like to warmly thank Samuel Nilusmas, thesis and thematic companion, who offered me his friendship and camaraderie.

The colleagues from my laboratories in Cameroon with whom I spent most of my time here deserve my gratitude for the pleasant exchanges and the beautiful company. Special thanks go first to my fellow graduate student, Luther Mann. Your support has been unwavering. I also want to thank all the others, Émilie Peynaud, Abdoulaye Mendy, Plaire Tchinda Mouofo (my very first co-author), Ramsès Djidjou Demasse, Myriam Tapi, Rodrigue Simon Tega II, Blériot Tchiengang, and those I forget.

Finally, I would like to thank people from my personal life who made the hours spent working more pleasant. They are friends, brothers, sisters, and sometimes proofreaders of my work. I'm thinking of Andrée Nenkam Mentho, Armel Fotsoh, Arsène Megaptche, Maxime Junior Teyou, Richard Dadji, Ghislain Takam, Ntsanyem Bounkeu, Dimitri Djamen, George-Michael Nkamsi, Wally Mbassi, and Fogo Miguel, who was very concerned with the management of the often complicated administrative affairs for this thesis. I am very especially grateful to Sadate Yves Nanfack for his invaluable support. Of course, I am grateful to my family for their patience and love. Thanks for the love.

Abstract

The aim of this thesis is to propose, on the one hand, a framework for mathematical analysis and simulation of the burrowing nematode *Radopholus similis* dynamic interaction with banana or plantain roots, and the other hand to identify the best control mean in order to optimize the economical yield of banana and plantain crops.

In the first step, we study the infestation dynamics of banana or plantain plants by *R. similis*. Two control strategies are analyzed: pesticides, which are widely used, and fallow deployment, which is more environmentally friendly. To represent the host-parasite dynamics, two semi-discrete models are proposed. In these models, during each cropping season, free nematodes enter the plant roots, on which they feed and reproduce. At the end of the cropping season, fruits are harvested. In the first model, the parent plant is cut down to be replaced by one of its suckers and pesticides are applied. In the second model, the parent plant is uprooted and a fallow period is introduced, inducing the decay of the free pest populations; at the beginning of the next cropping season, a pest-free vitro-plant is planted. For both models, we find a condition of global stability of the pest-free equilibrium. Then, the effective reproduction number of the pest is computed, assuming that the infestation dynamics is fast compared to the other processes, which leads to the model order reduction. Conditions on the pesticide load or the fallow duration are then derived to ensure the stability of the pest-free equilibrium. Finally, numerical simulations illustrated these theoretical results.

In a second step, we propose an eco-friendly optimization of banana or plantain yield by the control of the burrowing nematode. This control relies on fallow deployment. The optimization is based on the multi-seasonal model in which fallow periods follow cropping seasons. The aim is to find the best way, in terms of profit, to allocate the durations of fallow periods between the cropping seasons, over a fixed time horizon spanning several seasons. The existence of an optimal allocation is proven and an adaptive random search algorithm is proposed to solve the optimization problem. For a relatively long time horizon, deploying one season less than the maximum possible number of cropping seasons allows us to increase the fallow period durations and result in a better multi-seasonal profit. For regular fallow durations, the profit is lower than the optimal solution, but the final soil infestation is also lower.

In the last step, we propose a strategy of mixed control where cropping seasons can succeed each other by vegetative growth of the plant or by planting a healthy vitro-plant, after eventually a fallow. We derive an optimization problem in order to know when to implement one or the other reproductive

strategy and to know how long to make the fallow period last in case of fallow deployment. We obtain initial results and present perspectives.

Keywords: epidemiological modelling, semi-discrete model, singular perturbation, stability, host-parasite interactions, pest management, yield optimization, burrowing nematode, banana (Musa spp.).

Résumé

Le but de cette thèse est de proposer d'une part un cadre d'analyse mathématique de l'interaction dynamique du nématodes endoparasite *Radopholus similis* avec les racines de bananier ou de plantain. D'autre part, nous avons pour objectif d'identifier le meilleur moyen d'optimiser le rendement des cultures de bananiers et plantains via le contrôle du nématode.

Dans un premier temps, nous étudions la dynamique d'infestation des bananiers/plantains par *R. similis*. Deux stratégies de lutte sont ainsi analysées : la lutte chimique, qui est encore largement utilisées, et le déploiement de jachère, qui est plus écologique. Pour représenter la dynamique hôte-parasite, nous proposons deux modèles semi-discrets. Dans ces modèles, au cours de chaque saison de culture, les nématodes libres pénètrent dans les racines des plantes dont ils se nourrissent et se reproduisent. À la fin de la saison de culture, le régime de fruit est récolté. Dans le premier modèle, la plante mère est coupée pour être remplacée par l'un de ses rejets et des pesticides sont appliqués. Dans le deuxième modèle, la plante mère est déracinée et une période de jachère est introduite, induisant la décroissance de la population de nématodes libres dans le sol. Au début de la saison de culture suivante, un rejet sain est planté. Pour les deux modèles, nous trouvons une condition de stabilité globale de l'équilibre sans ravageur. Ensuite, nous calculons le taux de reproduction effectif du ravageur en supposant que la dynamique d'infestation est rapide par rapport aux autres processus, ce qui conduit à la réduction des modèles. Nous trouvons ensuite des conditions sur la charge de pesticides ou la durée de la jachère qui entrainent la stabilité locale de l'équilibre sans ravageurs. Des simulations numériques illustrent ces résultats théoriques.

Dans un deuxième temps, nous proposons une optimisation écologique du rendement de banane/plantain en contrôlant le nématode via le déploiement en jachère. L'optimisation est basée sur le modèle multi-saisonnier avec jachère précédent. L'objectif est de trouver la meilleure distribution des durées de jachère entre les saisons de culture, sur un horizon temporel fixe s'étalant sur plusieurs saisons. Nous prouvons l'existence d'une distribution optimale et proposons un algorithme de recherche aléatoire adaptative pour résoudre le problème d'optimisation. Pour un horizon de temps relativement long, le déploiement d'une saison de moins que le nombre maximum de saisons de culture pouvant être déployé nous permet d'augmenter les durées de jachère et de générer ainsi un meilleur rendement multi-saisonnier. Nous obtenons, après des régularations des durées de jachère, un rendement inférieur à la solution optimale non régulée, mais l'infestation finale est meilleure dans ces cas.

Pour finir, nous proposons une stratégie de lutte mixte où les saisons de culture peuvent se succéder par croissance végétative de la plante ou en plantant un rejet sain, après éventuellement une jachère. Nous obtenons ainsi un problème d'optimisation dont le but est de savoir quand mettre en œuvre l'une ou l'autre des deux stratégies de reproduction, et de savoir combien de temps durera la période de jachère en cas de déploiement

de jachère. Nous obtenons les premiers résultats et présentons les perspectives.

Mots-clés: modélisation épidémiologique, modèle semi-discret, perturbation singulière, stabilité, interactions hôte-parasite, gestion de ravageurs, optimisation du rendement, nématode endoparasite, bananier(Musa spp.).

Contents

I Introduction **1**

II Mathematical Preliminaries **8**

1 Mathematical preliminaries **9**

1.1 Semi-discrete modelling and overview on impulsive differential equations 9

1.1.1 Floquet theory 10

1.1.2 Comparison principle 11

1.2 Singular perturbation theory for slow-fast dynamics 12

1.3 Random search algorithms 15

1.3.1 General random search and convergence 15

1.3.2 Adaptive Random Search on the simplex 16

III Literature Review **19**

2 Biological background **20**

2.1 Biology and cultivation of banana and plantain 20

2.2 Biology of *Radopholus similis* 21

3 Existing soilborne pest, plant epidemic and crop rotation mathematical models **25**

3.1 Soilborne pest and plant epidemics mathematical models 25

3.1.1 The model of Gilligan and Kleczkowski [40] 25

3.1.2 The model of Madden and Van den Bosch [65] 27

3.1.3 The model of Mailleret et al. [66] 28

3.1.4 A cohort model adapted to *Radopholus similis* : the model of Tixier et al.[133] 30

3.2 Some crop rotation mathematical models 33

3.2.1 Taylor and Rodrìguez-Kábana's model of rotation of peanuts and cotton to manage soilborne organisms [127] 33

3.2.2 The model of Van Den Berg and Rossing [139] 37

3.2.3 The model of Nilusmas et al. [83] 38

IV Results and discussion 42

4 Modelling and analysis of the dynamics of the banana burrowing nematode *Radopholus similis* in a multi-seasonal framework 43

4.1 Modelling . . . 43
4.1.1 Core model . . . 43
4.1.2 Chemical control model . . . 46
4.1.3 Fallow deployment model . . . 47
4.1.4 Well-posedness of the problem . . . 48
4.2 Analysis and results . . . 49
4.2.1 Chemical control . . . 49
4.2.2 Sufficient fallow deployment . . . 61
4.3 Discussion . . . 66
4.4 Conclusion . . . 67

5 Optimal fallow deployment for the sustainable management of *Radopholus similis* 71

5.0.1 Yield and profit . . . 71
5.0.2 Parameter values . . . 72
5.1 Optimization . . . 73
5.1.1 Location of the optimal solutions . . . 74
5.1.2 Optimization algorithm . . . 78
5.2 Numerical results . . . 79
5.2.1 Small dimensions . . . 79
5.2.2 High dimensions . . . 80
5.2.3 Regulation of high dimension solutions . . . 81
5.2.4 Comparisons . . . 86
5.3 Discussion and future work . . . 86

6 Toward a mixed control strategy 90

6.1 Optimization problem . . . 90
6.2 Optimization with fixed-size chains and constant fallow . . . 91
6.2.1 Resolution . . . 91
6.2.2 A case study . . . 92
6.3 Optimization with fixed-size chains and varying fallows . . . 93
6.3.1 Resolution . . . 94
6.3.2 A case study . . . 95
6.4 Conclusion . . . 97

V Conclusion 99

VI Bibliography 102

List of Figures

1 Musa (Banana & Plantain) producer in West Africa (The "Banana Belt"). Source : Institute for Tropical Agriculture (IITA) (www.crop-mapper.org/banana/). 2

2 Plantain production in West Africa, 1990-2011 [11]. The production of main producers has almost triple as same as the overall production, and Cameroon has strengthened a leading position. West Africa here additionally includes Cameroon, Equatorial Guinea, Gabon, and the Republic of the Congo. 3

3 Banana production in West Africa, 1990-2011 [11]. The production of main producers has increased, and the lead of Cameroon is more than notable. West Africa here additionally includes Cameroon, Equatorial Guinea, Gabon, and the Republic of the Congo. 3

4 Plantain per-hectare yields in West Africa, 1990-2011 [11]. West Africa here additionally includes Cameroon, Equatorial Guinea, Gabon, and the Republic of the Congo. Globally, the per-hectare yield of plantain in Cameroon has increased during those two decades. 4

5 Banana per-hectare yields in West Africa, 1990-2011 [11]. West Africa here additionally includes Cameroon, Equatorial Guinea, Gabon, and the Republic of the Congo. Globally, the per-hectare yield of plantain in Cameroon has decreased during those two decades. 4

2.1 (a) Isolated root at different levels of infestation, from simple roots lesions to black necrosis; credits: Jesus et al. (2015) [54]. (b) Photo of a nematode inside the root; credits: Michael MacClure, University of Arizona. (c) Root pool at different levels of infestation; credits: Zhang et al. (2012) [153]. 22

2.2 Banana fall caused by R. Similis; credits: Danny Coyne, Consultative Group on International Agricultural Research. 23

2.3 Life cycle of *Radopholus similis* according to Marin et al. (1998) [71]. 23

3.1 Schematic drawing of disease Madden and Van den Bosch model, representing within-season dynamics of disease-free (S), latently infected (E), infectious (I), and postinfectious (R) plants; the production of inoculum or pathogen individuals (P); and mortality of inoculum within and between seasons. 28

3.2 Structure of the SIMBA-NEM model. At each time step t of the model for each species, $Rs_i(t)$ and $Pc_i(t)$ represent the number of nematodes in cohort i, $Rsmat(t)$ and $Pcmat(t)$ represent the number of mature nematodes, $K_{Rs}(t)$ and $K_{Pc}(t)$ the carrying capacity and $c_{Rs}(t)$ and $c_{Pc}(t)$ the population growth parameter for *R. similis* (Rs) and *P. coffeae* (Pc) respectively and $RootsStock(t)$, $Wat(t)$ and $Pest(t)$ represent the banana fresh root biomass, percentage of soil water and soil nematicide quantity, respectively. 31

4.1 Schematic representation of the core model (4.2). P, S, and X denote the population of free nematodes, respectively. Function f is a Holling type II functional response, and constant α is the conversion rate of the ingested fresh roots that are used to reproduce inside the root with a proportion γ and outside with a proportion $(1-\gamma)$. The constants μ and γ are natural mortalities, and constant β is a rate of infection that depends on the biomass of available fresh roots. The arrow from S to S illustrates the root growth during the root growing period. 45

4.2 Schematic representation of the course of the plant-pest dynamics over two cropping seasons for the model (4.2)-(4.7). On the time axis, plain lines represent the continuous course of time whereas the dotted line represents a discrete time, when switching occurs. Interactions during continuous periods are based on the core model in Figure 4.1. At the switching, the fresh root biomass (S) is initialized as a fraction q of the biomass inherited from the preceding season, the free nematode population (P) is initialized as the population of free nematodes inherited from the preceding season plus a portion $(1-q)$ of the infesting nematodes inherited from the preceding season, all with a survival rate λ to the instantaneous action of the nematicide. The infecting nematode population (X) is initialized as the fraction q of the population of infecting nematodes inherited from the preceding season, with a survival rate λ to the instantaneous action of the nematicide. 47

4.3 Schematic representation of the course of the plant-pest dynamics from one cropping season to the next. On the time axis, plain lines represent the continuous course of time whereas dotted lines represents discrete instants, where discrete phenomena occur (uprooting, planting). Interactions during cropping seasons are based on the core model in Figure 4.1. When switching from a cropping season to a fallow period, infecting nematodes convert into free nematodes with a conversion faction r. Crossed-out boxes represent the uprooting, i.e. the fresh root removal. When switching from a fallow period to a cropping season, i.e. planting a new sucker, the fresh root biomass is initialized at S_0 and infesting pest at 0 whereas free pest population stays the same. 49

4.4 Schematic representation of the reduced model, with first subsystem of model (4.2) reduced into model (4.21). During the root growing period, the system is reduced to a Rosenzweig-MacArthur model where the population of free nematodes is null, and the state variable N represents the sum of nematodes populations that stands for the population of infesting nematodes.At the flowering $t_n + d$, the nematode population from the end of the root growing period becomes the pest population at the start of fruit growing period, whereas the population of free nematodes is initialized as zero. The circled arrow represents the growth of fresh roots (S) that is effective before the flowering and null after, during the fruit growing period. 53

4.5 Pest population evolution over a single cropping season for different values of the infestation rate β. The infesting pests (red lines) and the free pests (blue lines) are represented for the full model (4.2) (plain lines) and the reduced model (4.21) (dashed lines). Paramater values are given in Table 4.1. 59
4.6 Infesting pest dynamics of model (4.2) - (4.7) over several cropping seasons for different values of λ. The infestation rate is $\beta = 0.1$, so that the reduced model approximates the full model well. Remaining parameter values are given in Table 4.1, leading to the threshold value $\lambda_0 = 0.010$ defined in equation (4.34). 60
4.7 Pest-root dynamics over four seasons without chemical control ($\lambda = 1$) of model (4.2) - (4.7). At the beginning t_i of each season, root biomass grows until either the growth stops (at $t_i + d$) or the pest populations are so high that they overeat the roots. The jumps in the root dynamics at t_i are due to the switch (4.7), where a portion of the root pool of the parent plant turns into a pool of old roots that die quickly by senescence. The remaining portion represents the root pool of the sucker from which the new plant grows. The jumps in the pest dynamics are also due to the switch (4.7), with in particular a proportion of the infesting pests which become free pests because of the senescence of the part of the roots they are in. The level of infesting pests goes up very quickly because the free pests return quickly in the fresh roots, since β is high. . 61
4.8 Infesting pest dynamics of model(4.2)-(5.1) over several cropping seasons for different values of τ. The infestation rate is $\beta = 0.1$, so that the reduced model approximates the full model well. Remaining parameter values are given in Table 4.1, leading to the threshold value $\tau_0 = 36.79$ defined in equation (4.48). 66

5.1 Local sensitivity analysis to assess the impact of the epidemiological and economic parameters, on the single season profit R_k defined in Equation (5.3). Sensitivities correspond to the directional derivatives of the profit with respect to these parameters. 73
5.2 Possible occurrences of T_{max}. In (a) T_{max} occurs in the middle of a cropping season, in (b) during a fallow period, and in (c) at the end of a cropping season, at the same time as the harvest. 74
5.3 Curves of pests populations (X and P) and fresh root biomass (S) for different values of the initial infestation $P(t_k^+)$. For initial infestations lower than 200, (a) the greater the initial infestation, the lower the curves of fresh root biomass on the domain $(t_k, t_k + D]$; (b) and (c) The greater the initial infestation, the higher the curves of pests on the domain $(t_k, t_k + D]$. 76
5.4 Counterexample: loss of monotonicity when $r = 100\%$ and $P_0 = 300$. (a) Root biomass during the second cropping season for two different values of $P(t_1^+)$ arising from $\tau_1 = 2$ days (blue curve) and $\tau_1 = 10$ days (red curve). At the beginning, the blue curve is below the red curve, which is consistent with the monotonicity assumption as $P(t_1^+)$ is higher for the blue curve. However, shortly after $t_1 + d$, the relative position of the two curves switches and so the monotonicity Assumption 5.2 is not verified. (b) Profit for the first two seasons as a function of fallow duration τ_1. The fallow duration $\tau_1 = 2$ days (blue cross) yields a better profit than the fallow duration $\tau_1 = 10$ days (red cross), although the former corresponds to a higher infestation $P(t_1^+)$ than the latter. This is due to the loss of monotonicity. 77

5.5 Profit as a function of the fallow period distribution on the A^3 simplex of size 80 days ($T_{max} = 1400$ days). The simplex is projected on its first two coordinates (τ_1, τ_2) and $\tau_3 = 80-(\tau_1+\tau_2)$. The lighter the colour, the higher the profit. The maximum is indicated by a blue square and corresponds to $\tau_1 = 80$ days and $\tau_2 = \tau_3 = 0$ day. 79

5.6 Profit as a function of the fallow period distribution on the A^3 simplex of size 20 days ($T_{max} = 1340$ days). The simplex is projected on its first two coordinates (τ_1, τ_2) and $\tau_3 = 20-(\tau_1+\tau_2)$. The lighter the colour, the higher the profit. The maximum is indicated by a blue square and corresponds to $\tau_3 = 20$ days and $\tau_1 = \tau_2 = 0$ day. 80

5.7 Profit as a function of the fallow period distribution on the A^3 simplex of size 20 days ($T_{max} = 1340$ days), for a very high initial infestation ($P_0 = 10000$ nematodes). The simplex is projected on its first two coordinates (τ_1, τ_2) and $\tau_3 = 20 - (\tau_1 + \tau_2)$. The lighter the colour, the higher the profit. The maximum is indicated by a blue square and corresponds to $\tau_1 = 20$ days and $\tau_2 = \tau_3 = 0$ day. 81

5.8 Optimal distribution of fallow periods for time horizon $T_{max} = 4000$ days. The maximal profit is obtained for 11 cropping seasons and 10 fallows: $\vec{\tau}^* = (192, 81, 14, 39, 42, 0, 2, 0, 0, 0)$ (in days). The red line corresponds to the average fallow period $\tau = 37$ days. 82

5.9 Optimal distribution of fallow periods for time horizon $T_{max} = 4000$ days, when fallow durations are upper-bounded by $\tau_{sup} = 60$ days. The maximal profit is obtained for 11 cropping seasons and 10 fallows: $\vec{\tau}^* = (60, 60, 59, 44, 58, 34, 48, 7, 0, 0)$ (in days). The red line corresponds to the average fallow period $\tau = 37$ days. 83

5.10 Optimal distribution of fallow periods for time horizon $T_{max} = 4000$ days, when far from average fallow durations are penalized. The maximal profit is obtained for 11 cropping seasons and 10 fallows: $\vec{\tau}^* = (71, 54, 46, 42, 39, 35, 32, 27, 20, 4)$ (in days). The red line corresponds to the average fallow period $\tau = 37$ days. 84

5.11 Profit R as a function of fallow duration τ (logarithm scale) for time horizon $T_{max} = 4000$ days. The set $\Xi = \{4, 37, 78, 129, 194, 282, 404, 588, 893, 1505\}$ (in days), defined in equation (5.11), is represented by dashed red bars. Elements of Ξ correspond to discontinuities of the profit function, when the number of fallows n (upper axis) that fit in T_{max} is incremented (from right to left). The maximal profit $R^* = 52000$ XAF (79.27 euros) is obtained for $n = 10$ fallows of duration $\tau^* = 37$ days, which belongs to Ξ. 86

5.12 Soil infestation after each harvest for the optimal non-regulated and regulated fallow deployment strategies over time horizon $T_{max} = 4000$ days. The non-regulated strategy (blue bars) corresponds to Figure 5.8. Regulations consist in bounding (green bars), penalizing (red bars) and setting constant (cyan bars) fallows; they correspond to Figures 5.9, 5.10 and 5.11, respectively. Soil infestations $P(t_0 + D^+)$ after the first harvest are the same for all strategies, as initial conditions are the same. All strategies involve 10 fallows, but as their durations differ among strategies, times t_k ($k = 1, \ldots, 9$) also differ. 87

5.13 Seasonal profits of banana crop under different strategies of fallow deployment. for the optimal non-regulated and regulated fallow deployment strategies over time horizon $T_{max} = 4000$ days. The non-regulated strategy (blue bars) corresponds to Figure 5.8. Regulations consist in bounding (green bars), penalizing (red bars) and setting constant (cyan bars) fallows; they correspond to Figures 5.9, 5.10 and 5.11, respectively. Profits of the first season are the same for all strategies, as initial conditions are the same. 88

6.1 Illustration of the first three chains of a mixed strategy. Each chain C_i contains l_i cropping seasons (CS) and one fallow (F). Cropping seasons have a fixed duration (D) but fallow durations τ_i may vary. 91

6.2 Visual representation of the optimal mixed deployment strategy with fixed-size chains and variable fallows. The optimum is obtained for chains of size 1 and the fallow distribution (192, 81, 14, 39, 42, 0, 2, 0, 0, 0). The blue bars correspond to the planting of nematode-free vitroplant while the red bars correspond to the uprooting of plants after the harvest of the fruit bunch. The filled spaces over the course of time correspond to banana cropping seasons while the white spaces correspond to fallows whose durations are indicated at the top. Some fallows last 0 days and in these cases, the old plant is still uprooted and a nematode-free vitroplant is planted. . . 96

6.3 Visual representation of the optimal mixed deployment strategy with fixed-size chains and variable fallows. The optimum is obtained for chains of size 3 and the fallow distribution (699, 0, 1). The vitroplant cost here is $c = 2300$ XAF. The blue bars correspond to the planting of nematode-free vitroplant while the red bars correspond to the uprooting of plants at the end of the chain. The filled spaces over the course of time correspond to banana cropping seasons while the white spaces correspond to fallows whose durations are indicated at the top. In this strategy, a single 370-day long fallow is deployed. 96

List of Tables

3.1 Variables, parameters and functions used in Gilligan and Kleczkowski's models. 26
3.2 Variables and parameters used in Mailleret et al.'s models. 29
3.3 Variables and parameters of the SIMBA-NEM model, where t is the time step of the model (in weeks) and i is the cohort rank. 32
3.4 Equations of the SIMBA-NEM model, where t is the time step of the model (in weeks) and i is the cohort rank. 34
3.5 Variables of Taylor and Rodrìguez-Kábana's model. 35
3.6 Dynamic population models for soilborne organisms and markovian price relationships in Taylor and Rodrìguez-Kábana's model 36
3.7 Variables and parameters of the model of Nilusmas et al. 39

4.1 Parameter values used in model simulations 58

6.1 Optimal fallow durations and generated profits for different chain sizes obtained for mixed deployment strategies with fixed-size chains and constant fallows. The line in bold print indicates the overall optimum, obtained here for chains of size 1. 93
6.2 Optimal fallow durations and profits obtained for different chain sizes obtained for mixed deployment strategies with fixed-size chains and constant fallow. The vitroplant cost here is $c = 2300$ XAF. The line in bold print indicates the overall optimum, obtained here for chains of size 7. 94
6.3 Optimal fallow duration distributions and profits obtained for different chain sizes for the mixed deployment strategy with fixed-size chains and varying fallow. The line in bold print indicates the overall optimum, obtained here for chains of size 1. 95
6.4 Optimal fallow durations and yields obtained for different chain sizes in the mixed control strategy with fixed-size chains and varying fallow when the cost of a healthy vitroplant is $c = 2300$ XAF. The line in bold print indicates the overall optimum, obtained here for chains of size 3. 97

Part I

Introduction

Introduction

Banana and plantain in Cameroon

With a world production of 145 million tonnes in 2014, banana (Musa spp.) is the most popular fruit in the world, and one of the most important staple crops in the world [30] . Collectively called banana, banana and plantain (Musa spp.) are grown in more than 135 countries and are found in most tropical and subtropical regions of the world. These are non-seasonal crops that provide a source of food all year round, making them vital for nutrition and food security. In sub-Saharan Africa, in general, bananas and plantains play a vital role in maintaining food/nutrition security [129]. In addition to its export value, banana plantations and small plantain farms are an important source of employment [129, 88]. In Western and Central Africa, the banana and plantain production is mostly concentrated in long strip of land called "the banana belt" (Figure 1). In the following, we name "West Africa" the countries of the banana belt. This includes countries of the Western African Region, to which are added the four main producers in the Central African region that are Cameroon, Equatorial Guinea, Gabon, and the Republic of the Congo (Congo-Brazzaville).

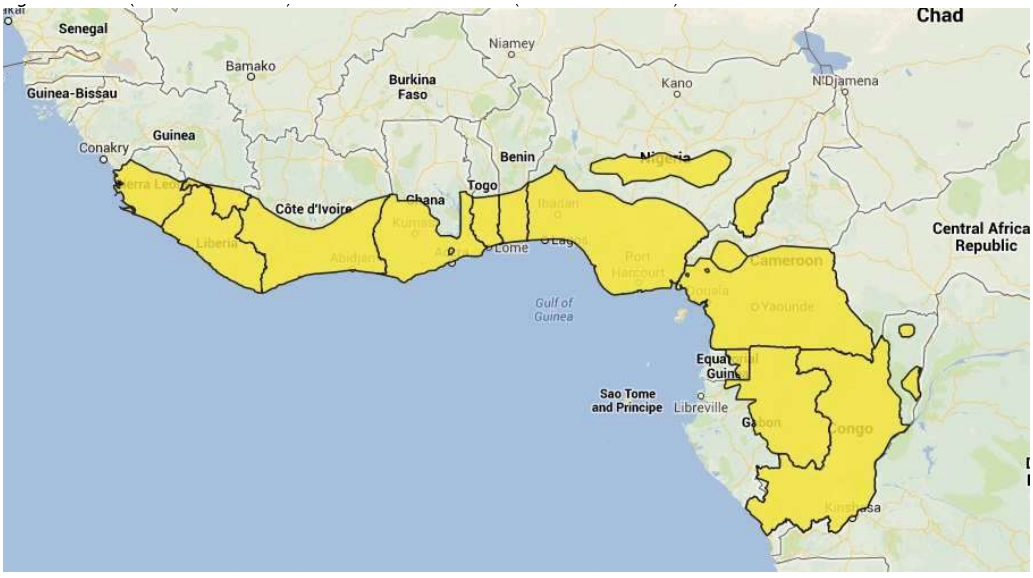

Figure 1 – Musa (Banana & Plantain) producer in West Africa (The "Banana Belt"). Source : Institute for Tropical Agriculture (IITA) (www.crop-mapper.org/banana/).

Cameroon has a good position in Central and West Africa as a banana and plantain producer. Its production increased steadily from 2001 (631,766 tonnes) to 2016 (1,187,547 tonnes), ranking fifteenth in the world at 1.5% (FAOSTAT). From the 90s to the beginning of the 2010s, its share in the production of the countries of

this region has never ceased to grow [11]. From the 90s to the 2010s, the production of banana and plantain has more than doubled. Figures 2 and 3 illustrate the increase of the production of respectively plantain and banana in different country of West Africa, and the evolution of their share of production from 1990 to 2011.

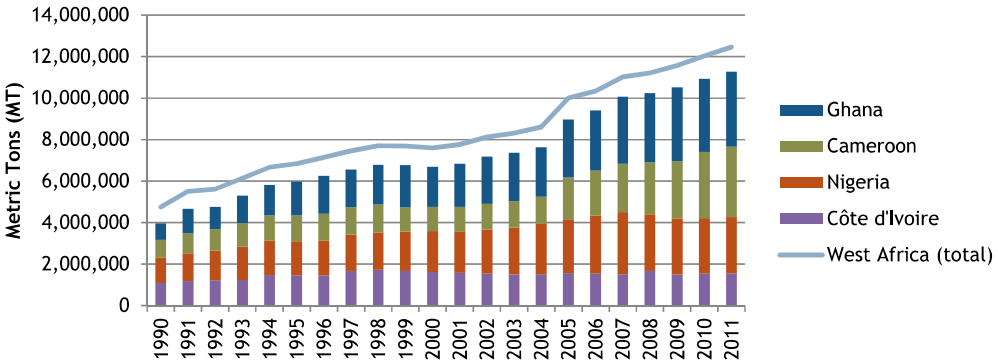

Figure 2 – Plantain production in West Africa, 1990-2011 [11]. The production of main producers has almost triple as same as the overall production, and Cameroon has strengthened a leading position. West Africa here additionally includes Cameroon, Equatorial Guinea, Gabon, and the Republic of the Congo.

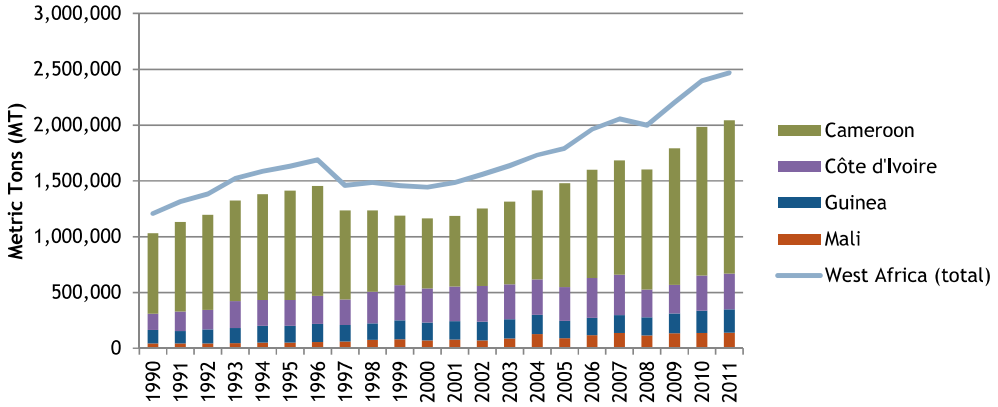

Figure 3 – Banana production in West Africa, 1990-2011 [11]. The production of main producers has increased, and the lead of Cameroon is more than notable. West Africa here additionally includes Cameroon, Equatorial Guinea, Gabon, and the Republic of the Congo.

In parallel to the production, the per-hectare yield for plantains in West Africa have increased slightly since 2004 overall, with large increases in Cameroon (Figure 4). Also, Yields for bananas vary widely (Figure 5).

Encouraged by the overall positive dynamics of agriculture in general, and of the banana/plantain sector in particular, the Cameroon government gave a large share to agro-industrial sectors in its Growth and Employment Strategy Paper (GESP) [21]. In a value-chain approach, the Government intends to negotiate and systematically implement development plans for processing industries for local products, including banana and plantain. The development plan of the banana sector negotiated with operators began to be implemented in the early 2010s. However, Figure 5 shows that per-hectare yields of banana in Cameroon did not improve. It has been even lower in 2011 than in 1990. The growth in production has been thus more related to the increase in agricultural areas than to the optimization of agricultural practices. Low yields can be explained by poor soils, bad climatic factors, plant diseases, or crop pests.

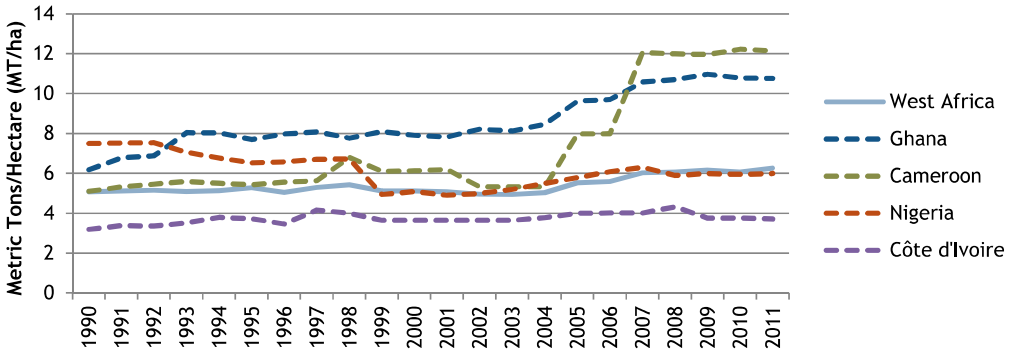

Figure 4 – Plantain per-hectare yields in West Africa, 1990-2011 [11]. West Africa here additionally includes Cameroon, Equatorial Guinea, Gabon, and the Republic of the Congo. Globally, the per-hectare yield of plantain in Cameroon has increased during those two decades.

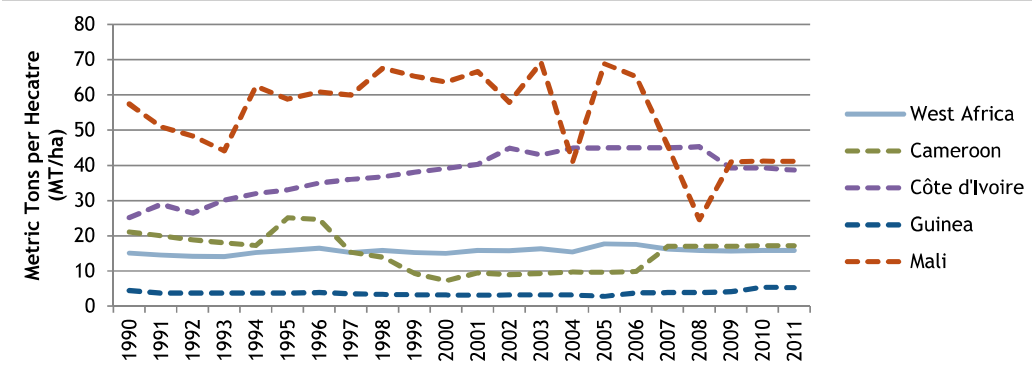

Figure 5 – Banana per-hectare yields in West Africa, 1990-2011 [11]. West Africa here additionally includes Cameroon, Equatorial Guinea, Gabon, and the Republic of the Congo. Globally, the per-hectare yield of plantain in Cameroon has decreased during those two decades.

Worldwide impact of the burrowing nematode an its chemical control

The burrowing nematode *Radopholus similis* is the most significant parasitic nematode of banana and plantain plants in the world [109, 91]. In Côte d'Ivoire, Vilardebo reported that *Radopholus similis* was causing average yield reductions of 80% in dessert banana plantations [146]. Fogain also recorded high overall yield losses of 60% on plantain production in Cameroon [35]. Smallholder farmers have increasingly come to view plantain crops as single-cycle, as opposed to perennial, crops because of nematode infection [84, 18]. This reduced crop number of cycles has major implications, impacting on farmer returns and on farmer decisions on whether or not to cultivate plantain [18].

Chemical control is somehow an efficient method to control infestations by the burrowing nematode. In the 70s, Vilardebo had already noticed that the application of nematicides increased yields up to 211% in Côte d'Ivoire. More recent studies showed that percentage efficacy in nematode control by chemical agents varied from 23 to 42% [106]. The application of nematicide increased the bunch weight by 41% when applied three times a year, and 27% when applied two times a year at six or seven months interval [106]. The efficacy of a lot of nematicides have been proven in the literature. As non exhaustive examples, we can think about tannic acid that can have an efficient mortality rate that goes up to 94% in a fine sand [51]. Fenamiphos can reach a mortality of 77% in in vitro tests[69]. A good efficacy has also been reported for the systemic nematicides aldicarb, carbofuran and phorate [58]. However, many problems arise from using chemical nematicides because they are highly toxic to animals and humans. Indeed, the use of chemical nematicides has been restricted because of their carcinogenicity, teratogenicity, high and acute residual toxicity, ability to create hormonal imbalances, spermatotoxicity, long degradation period and food residues [22, 92]. Also, chemical nematicides pollute soil and groundwater and their excessive use eradicates beneficial organisms in the soil and disturb ecological equilibrium. Ultimately, they cause environmental degradation. Also, some of them are absorbed by plants and sometimes contribute to impact plant growth via phytotoxicity [100]. Besides, nematicides are often only partially effective because of the large volumes of soil to be treated and the enormous nematode population involved [28]. Consequently, sustainable management might depend on an integration of agricultural methods. To minimize application of nematicides in banana fields, alternative crop systems have been developed for example in French West Indies [16]. These crop systems are based on the hostless survival of *R. similis*. Indeed, some studies have noticed that the nematode population undergoes a fast decay in the absence of hosts. Therefore, rotating cropping seasons with fallow periods appears to be a sustainable mean of control of fields infestation [16, 15, 17].

Specific issues and contribution of mathematics

If it is identified rotating cropping seasons with fallow periods or non-host crops can control field infestation in a sustainable way, it remains to be seen how to deploy these rotations. It is thus necessary to know when to set up rotations and how to alternate them. If the rotations are done with fallow periods, it is important to know the duration and the policy of deployment. To do this, it is important to understand beforehand the dynamics of the pest with its host and with the soil.

Mathematical modelling and computer simulation are becoming major tools for the study of the evolution of soilborne pests and optimization of pest control. Several mathematical and computational models have been proposed for such soilborne pests in the literature. Gilligan [41], followed by Gilligan and Kleczkowski

[40] have proposed some mathematical models for soilborne pathogens. Madden and Van den Bosch [65] and Mailleret et al. [66] introduced the semi-discrete formalism in soilborne pathogen models to obtain multi-seasonal dynamics of crop-pathogen interactions. To our knowledge, only one model has been specifically proposed for *R. similis* [133]. The latter is a cohort-based model, is fairly complex and requires extensive data to be calibrated.

Optimization models, in which an host plant cropping is alternated with either an off-season, a non-host cropping or a poor host cropping, also exist in the mathematical modelling literature. Van den Berg et al. [140, 141], for instance, rely on an extended Ricker model to optimize potato yield losses due to the potato cyst nematode by rotating different potato cultivars. Van den Berg and Rossing model do the same for the root lesion nematode *Pratylenchus penetrans*; the main crops are rotated with fallow or alternative crops [139]. Taylor and Rodrìguez-Kábana optimize the economical yield of peanut crops by rotating peanuts (good host) and cotton (bad host) in order to control the peanut root-knot nematode *Meloidogyne arenaria* [127]. Nilusmas et al. provide optimal rotation strategies between susceptible and resistant crops to control root-knot nematodes and maximize crop yield [83].

The aim of this thesis is to build a simple model that is adapted to the dynamics of the burrowing nematode in interaction with banana or plantain roots, and, basing on this model, to describe optimal fallow deployment in order to optimize the crop yields. Throughout this thesis, banana plants designate banana or plantain plants indifferently. Contrary to previous rotations models in which the seeded crop is chosen optimally, we always have the same crop and we optimize the duration of fallow periods between cropping seasons.

Work organisation

This dissertation is organized into five chapters, excepting the introduction, the conclusion and the appendix.

- Chapter 1 presents the main mathematical tools we rely on in this thesis. We present the semi-discrete models and some usual methods for their analysis. We also present the singular perturbation theory for slow-fast dynamics. We finally present the random search algorithm that is used for the optimization in Chapter 5.

- Chapter 2 presents the general biological background of this thesis. First, the biology of banana and plantain (Musa) and the usual agricultural practices related to them are presented. Secondly, we present the biology of *R. similis*, its life cycle, its range of host plants, its mechanisms of survival and dissemination.

- Chapter 3 is a reminder of different soilborne pests and crop rotation models existing in the literature in their chronological order.

- Chapter 4 is concerned with our first contribution in the mathematical modelling of the burrowing nematodes dynamics. Two semi-discrete models are proposed and the impact of chemical control and fallow deployment on the dynamics and the survival of *R. similis* is investigated.

- Chapter 5 is concerned with contribution in optimal pest control. We propose an eco-friendly optimization of banana or plantain yield by optimal fallow deployment. The optimization is based on the multi-seasonal model of the previous chapter in which fallow periods follow cropping seasons. We find the best way, in terms of profit, to allocate the durations of fallow periods between the cropping seasons, over a fixed time horizon spanning several seasons.

- Chapter 6 aims to state a more general optimization problem whose solutions could generalize those of the preceding chapter. In this chapter, vegetative breeding of plants is included so that there is no systematic deployment of fallow. In this optimization, it is therefore a question of determining both when and how to deploy the fallow. We get first results and discuss perspectives.

  The document ends with a bibliography of the sources used throughout the write up.

Part II

Mathematical Preliminaries

CHAPTER ONE

MATHEMATICAL PRELIMINARIES

We introduce some of the key mathematical theories and methodologies relevant to the thesis. The materials presented in this chapter are mostly standard definition and results obtained from the literature.

1.1 Semi-discrete modelling and overview on impulsive differential equations

Mathematical models are description of systems using mathematical language and concepts. Usually, they are composed of relationships between variables, that are abstractions of system parameters that can be quantified. Dynamic models are those that account for time-dependant changes in the state of systems, in opposition to static models. They are typically represented by differential equations or difference equations. The two latter are representative of two classes of dynamical systems. The first class is the class of discrete dynamical systems, in which the variables depend on the time represented by a discrete set. Generally, their form is given by a recurrence relationship :

$$x_{t+1} = f(x_t) \tag{1.1}$$

The second class is the class of continuous dynamical systems, in which the time flows continuously. Generally, their form is given by :

$$\frac{dx}{dt} = f(t, x) \tag{1.2}$$

A third class of systems arises from the two classes above. This is the class of semi-discrete models. Semi-discrete models are hybrid dynamical that undergoes continuous dynamics in ordinary differential equations most of the time and that experiences discrete dynamics at some given time instants [67]. If x denotes the vector of state variables at time t and t_k the instants when the discrete changes occur, then a semi-discrete model reads :

$$\begin{cases} \dfrac{dx(t)}{dt} = f(t, x), & t \neq t_k \\ x(t_k^+) = F(x(t_k), t_k), \end{cases} \tag{1.3}$$

with t_k^+ denoting the instant just after $t = t_k$. $f(\cdot)$ is the continuous ordinary differential equation, possibly time-varying, followed by the system, and $F(\cdot)$ is the discrete component also termed "pulse".

More generally, we can write an impulsive system as follows [50] :

$$\begin{cases} \dfrac{dx(t)}{dt} = f(t,x), & t \neq t_k \\ \Delta x = I_k(x(t)), & t = t_k, \\ x(t_0^+) = x_0, & t_0 \geq 0, \end{cases} \tag{1.4}$$

with $\Delta x = x(t_k^+) - x(t_k^-)$ (the "$-$" superscript denoting the instant that directly precedes $t = t_k$), f continuous on $\mathbb{R} \times \Omega$, with Ω an open set of $\mathbb{R}^n$, $I_k : \Omega \to \Omega$.

We define what is a periodic solution for such a system.

Definition 1.1. Periodic solution [64]

A map $x : \mathbb{R}^+ \to \mathbb{R}^n$ is said to be a periodic solution of equation (1.4) with period ω if :

1. It satisfies the equalities of equation (1.4) and is a piecewise continuous map with jump discontinuities.
2. It satisfies $x(t+\omega) = x(t)$ for $t \neq t_k$ and $x(t_k + \omega^+) = x(t_k)$, for $k \in \mathbb{Z}$.

1.1.1 Floquet theory

Floquet theory helps studying the behaviour of periodic solutions. Let's consider the following linear impulsive differential system :

$$\begin{cases} \dfrac{dx(t)}{dt} = A(t)x(t), & t \neq t_k, t \in \mathbb{R} \\ x(t^+) = x(t) + B_k x(t), & t = t_k, k \in \mathbb{Z} \end{cases} \tag{1.5}$$

Let's consider the following hypothesis :

H_1) $A(\cdot) \in PC(\mathbb{R}, C^{m\times n})$ and $A(t+T) = A(t)$, where $C^{m\times n}$ is the set of $(m \times n)$-matrix.

H_2) $B_k \in C^{m\times n}$ and $det(I + B_k) \neq 0 \qquad (k \in \mathbb{Z})$

H_3) There exists $q \in \mathbb{N}$ such that $B_{k+q} = B_k$ and $t_{k+q} = t_k + T \qquad (k \in \mathbb{Z})$.

Where $PC(\mathbb{R}, C^{m\times n})$ denotes the set of functions $\Psi : \mathbb{R} \to C^{m\times n}$ that are continuous on $t \in \mathbb{R}$, $t \neq t_k$, and admitting jump discontinuities at t_k.

Theorem 1.1. (Lakshmikantham, Bainov and Simeonov) [59]

If hypothesis H_1) to H_3) are satisfied, then each fundamental matrix of equation (1.5) can be written in the following form :

$$X(t) = \phi(t)e^{\Lambda t} \qquad (t \in \mathbb{R}),$$

where the matrix $\Lambda \in C^{m\times n}$ is constant, and the matrix $\phi \in PC^1(\mathbb{R}, C^{m\times n})$ is non-singular and periodic with period T.

If $X(t)$ is a fundamental matrix solution of equation (1.5), then there exists a unique constant matrix $M \in C^{m\times n}$ such that :

$$X(t+T) = X(t)M, \qquad t \in \mathbb{R}.$$

The matrix M is called monodroomy matrix. The representation $X(t) = \phi(t)e^{\Lambda t}$ is called a Floquet normal form for the fundamental matrix $X(t)$. The eigenvalues of $e^{\Lambda t}$ are called the characteristic multipliers of the system. They are also the eigenvalues of the (linear) Poincaré maps $x(t) \mapsto x(t+T)$. A Floquet exponent (sometimes called a characteristic exponent), is a complex μ such that $e^{\mu T}$ is a characteristic multiplier of the system. Notice that Floquet exponents are not unique, since $e^{(\mu+\frac{2\pi i\eta}{T})T} = e^{\mu T}$, where η is an integer. The real parts of the Floquet exponents are called Lyapunov exponents. The zero solution is asymptotically stable if all Lyapunov exponents are negative, Lyapunov stable if the Lyapunov exponents are non-positive and unstable otherwise.

Practical computation of Floquet multipliers

To compute the Floquet multipliers of equation (1.5), one chooses arbitrary a fundamental matrix solution $X(t)$ of (1.5) and one computes the eigenvalues of the matrix

$$M = X(t_0 + T)X^{-1}(t0),$$

If $X(0) = I$ (or $X(0^+) = I$) then on can choose

$$M = X(T) \qquad (\text{or } M = X(T^+))$$

as monodromy matrix. Otherwise, most of the time the monodromy matrix of equation (1.5) is given by the following :

$$M = X(T^+) = \prod_{k=1}^{q}(I + B_k)\exp\big(\int_0^T A(t)dt\big) \tag{1.6}$$

1.1.2 Comparison principle

This principle helps to establish the global stability of an impulsive system. Let's consider the system (1.4). We first give some definitions.

Definition 1.2. Let $r(t) = r(t, t_0, u_0)$ be a solution of (1.4) defined on the interval $(t_0, t_0 + T)$. The solution $r(t)$ is maximal if for each solution $u(t) = u(t, t_0, u_0)$ of (1.4), we have

$$r(t) \leq u(t) \qquad \text{for all } t \in (t_0, t_0 + T)$$

Definition 1.3. Let $V : \mathbb{R}^+ \times \mathbb{R}^n \mapsto R^+$. V is said to be of class ν_0 if :

1. V is continuous on $(t_k, t_{k-1}] \times \mathbb{R}^n$ and $\lim_{(t,y)\to(t^+,x)} V(t, y) = V(t_k^+, x)$, for all $x \in \mathbb{R}$, $k \in \mathbb{Z}$.
2. V is continuous and locally Lipschitz according to the second variable.

Definition 1.4. Let $V \in \nu_0$ on (t_k, t_{k+1}), $(k \in \mathbb{Z})$. The Dini derivative of V according to system (1.4) is given by :

$$D^+V(t,x) = \lim_{h\to 0^+}\sup\frac{1}{h}[V(t+h, x+hf(t,x)) - V(t,x)]$$

and

$$D_-V(t,x) = \lim_{h\to 0^-}\inf\frac{1}{h}[V(t+h, x+hf(t,x)) - V(t,x)]$$

Definition 1.5. Comparison system

Let $V \in \nu_0$ and let's assume that

$$\begin{cases} D^+V(t,x) \leq g\big(t, V(t,x)\big), & t \neq t_k, \\ V(t, x + I_k(x)) = \psi_k\big(V(t_k, x)\big), & t = t_k, k \in \mathbb{Z} \end{cases} \tag{1.7}$$

with

- $g : \mathbb{R}^+ \times \mathbb{R} \mapsto \mathbb{R}$ a continuous function on (t_k, t_{k+1}), and, for all $x \in \mathbb{R}$, $k \in \mathbb{Z}$, we have $\lim\limits_{(t,y)\to(t_k^+,x)} g(t,y) = g(t^+, x)$ that exists.
- $\psi_k : \mathbb{R}^+ \mapsto \mathbb{R}^+$ is a non decreasing function.

Then, the following systems is called comparison system of system (1.4) :

$$\begin{cases} \dfrac{dw}{dt} = g(t,w), & t \in (t_k, t_{k+1}], \\ w(t^+) = \psi(w(t_k)) \\ w(t_0) = w_0 \geq 0 \end{cases} \tag{1.8}$$

Theorem 1.2. [119] Assuming that, given a solution x^* of system (1.4), we have :

1. There exists a function $V \in \mu_0$ such that
$$V(t, x^*(t)) = 0, t \in (t_0, \infty).$$
2. There exists $a, b \in \mathcal{K}$ such that
$$a\big(||x - x^*||\big) \leq V(t,x) \leq b\big(||x - x^*||\big), \text{ for all} (t,x) \in (t_0, \infty) \times \mathbb{R}^n,$$
with $\mathcal{K} = \big\{a \in \mathcal{C}(\mathbb{R}^+, \mathbb{R}^+) : \text{a is strictly increasing and } a(0) = 0\big\}$
3. $V\big(t_k^+, x(t_k^+)\big) \leq V\big(t_k, x(t_k)\big)$.
4. $D^+V(t,x) \leq 0$, $t \neq t_k$ ($k \in \mathbb{Z}$) is satisfied for $t \in (t_0, \infty)$

Then, the solution $x*$ of system (1.4) is globally stable.

The results of this section are used in Chapter 4 where a semi-discrete model describes the coupled dynamics of plant-parasitic nematodes with plantain roots. The result we present in the next section helps reducing the dimension of this model.

1.2 Singular perturbation theory for slow-fast dynamics

In this appendix, we remind the application of singular perturbation theory for slow-fast dynamics [145, 116]. It leads to the approximation of a high dimensional system by a smaller dimensional system when a very small parameter is assumed to be equal to 0. The smaller dimension system that arises from the full system is the "slow system". This terminology implies that the zero approximation above assumes the understood "fast dynamics" to be instantaneous.

Consider the system of ordinary differential equations :

$$\begin{cases} \dfrac{dx}{dt} = f(x, y, t, \varepsilon), \\ \varepsilon \dfrac{dy}{dt} = g(x, y, t, \varepsilon), \end{cases} \tag{1.9}$$

with $x \in \mathbb{R}^m, y \in \mathbb{R}^n, t \in \mathbb{R}$, and ε is a small positive parameter. Such systems are called *singular perturbed systems*. The most common approach of the qualitative study of system (1.9) is to consider the following first degenerated system ($\varepsilon = 0$) :

$$\begin{cases} \dfrac{dx}{dt} = f(x, y, t, 0), \\ 0 = g(x, y, t, 0), \end{cases} \tag{1.10}$$

and to drw conclusions about the qualitative behaviour of the full system (1.9) for sufficiently small ε. We introduce some definitions and assumptions.

Definition 1.6. (Slow subsystem, fast subsystem [116])

The system of equations :

$$\frac{dx}{dt} = f(x, y, t, \varepsilon) \tag{1.11}$$

is called the *slow subsystem* of (1.9), x is called the *slow variable*, and the system of equation :

$$\varepsilon \frac{dy}{dt} = g(x, y, t, \varepsilon) \tag{1.12}$$

is called the *fast subsystem* of (1.9). Here $x \in \mathbb{R}^m$, $y \in \mathbb{R}^n$, $t \in \mathbb{R}$.

Definition 1.7. (Integral manifold [116])

A smooth surface S in $\mathbb{R} \times \mathbb{R}^m \times \mathbb{R}^n$ is called an integral manifold of the system (1.9) if any integral curve of the system that has at least one point in common with S lies entirely on S. Formally, if $(t_0, x(t_0), y(t_0)) \in S$, then the integral curve $(t, x(t, \varepsilon), y(t, \varepsilon))$ lies entirely on S.

Definition 1.8. (Manifold of slow motions)

The integral manifolds of system (1.9) which are graphs of vector -valued functions $y = h(x, t, \varepsilon)$, with h sufficiently smooth in ε, are called *manifold of slow motions* or *slow integral manifold*.

The motion along an integral manifold of the system (1.9) is governed by the equation :

$$dx/dt = f(x, h(x, t, \varepsilon), t, \varepsilon), \tag{1.13}$$

where $y = h(x, t, \varepsilon)$ is a slow integral manifold. If $x(t, \varepsilon)$ is a solution of (1.13), then the pair $\big(x(t, \varepsilon), y(t, \varepsilon)\big)$, where $y = h(x(t, \varepsilon), t, \varepsilon)$, is a solution of the original system (1.9) since it defines a trajectory on the integral manifold.

Definition 1.9. (Slow surface, slow curve [116])

The surface described by the equation :

$$g(x, y, t, 0) = 0 \tag{1.14}$$

is called a *slow surface*. When the dimension of this surface is equal to one, it is called a *slow curve*.

The slow surface can be considered as a zero-order approximation of the slow integral manifold, since $h(x,t,0)=\phi(x,t)$, with $\phi(x,t)$ a function whose graph is a sheet of the slow surface.

Definition 1.10. (Boundary layer)

If we set the time variable $\tau = t/\varepsilon$ (called *fast time*), then the equation

$$\frac{dy}{dt} = g(x,y,t,0) \tag{1.15}$$

is called the boundary layer equation of (1.9), or simply the layer equation.

We now look for the conditions under which the degenerate system (1.10) can be considered like the zero-approximation of the full system (1.9).

Let's consider the following hypothesis on system (1.9):

(i) The functions f and g are uniformly continuous and bounded, together with their partial derivatives with respect to all the variables in some open domain of the space (x,y), $t\in[t_0,t_1]$, $\varepsilon\in[0,\varepsilon_0]$.

(ii) The boundary layer equation (1.15) has a solution for a given initial value.

(iii) For every fixed x and t, $y=\phi(x,t)$ is an isolated root of $g(x,y,t,0)=0$, i.e. $g(x,\phi(x,t),t,0)=0$ and there exists a positive number $\delta>0$ such that the conditions $||y-\phi(x,t)||<\delta$ and $y\neq\phi(x,t)$ imply $g(x,y)\neq 0$.

(iv) The equation $dx/dt = f(x,\phi(x,t),t,0)$ with a given initial condition has a solution $x=\bar{x}(t) ont\in[t_0,t_1]$.

(v) There exists $\gamma>0$ such that $g_\gamma(x,\phi(x,t),t,0)\leq-\gamma$. This implies that $\phi(x,t)$ is an asymptotically stable equilibrium solution to (1.15).

(vi) The point y_0 belongs to the basin of attraction of the steady state solution $y=\phi(x_0,t_0)$.

We have the following theorem :

Theorem 1.3. (Tychonov's Theorem [132, 116, 145])

If hypothesis (i) to (vi) are holds, then the solution $\big(x(t,\varepsilon),y(t,\varepsilon)\big)$ of the initial value problem (1.9) exists in $[t_0,t_1]$ and the following conditions hold :

$$\lim_{\varepsilon\to 0} x(t,\varepsilon)=\bar{x}(t),\quad t_0\leq t\leq t_1; \tag{1.16}$$

$$\lim_{\varepsilon\to 0} y(t,\varepsilon)=\phi(\bar{x}(t),t),\quad t_0\leq t\leq t_1. \tag{1.17}$$

The convergence in (1.16) and (1.17) is uniform in the interval $t_0\leq t\leq t_1$ for $x(t,\varepsilon)$ and in any interval $t_0<\nu\leq t\leq t_1$ for $y(t,\varepsilon)$.

Remark 1.1. Theorem (1.3) means that, under conditions of Tychonov's theorem, the solution travels to the slow surface and is the limit of the exact solution as $\varepsilon\to 0$.

For a large share of systems, the use of degenerate equation (1.10), obtained setting $\varepsilon=0$, instead of the full equation (1.9), give acceptable results. The accuracy of the approximation can be numerically evaluated in most of the cases. When such approximation is too crude, more exact approximations of the singular perturbed system (1.9) can be provided by asymptotic methods such as the averaging method [107], the multi-scale method [81], the regularization method [60] or the boundary layer method [144].

1.3 Random search algorithms

1.3.1 General random search and convergence

We consider the following problem:

Problem 1.1. Given a function f from $\mathbb{R}^n$ to R and S a subset of $\mathbb{R}^n$. We seek a point x in S which minimizes f on S or at least which yields an acceptable approximation of the minimum of f on S.

Convergence Criteria [134]

For convenience several probabilistic convergence criteria are listed below. Let $x_1, x_2, \ldots$ be a random sequence in R^n, i.e., $x_i = x(\omega)$ where $\omega \in \Omega$ and (Ω, σ, P) is a probability space.

Definition 1.11. (Convergence with probability 1)

The sequence x_i converges to the random vector x with probability 1 if

$$P\{\omega | \lim_{i\to\infty} x_i(\omega) = x(\omega)\} = 1.$$

Definition 1.12. (Convergence with probability)

The sequence x_i converges to the random vector x with probability if

$$\lim_{i\to\infty} P\{\omega | (|x_i(\omega) - x(\omega)|) > \varepsilon\} = 0$$

for each $\varepsilon > 0$.

Definition 1.13. (Convergence in distribution)

Let $F_i(y)$ and $F(y)$ denote the distribution function of x_i and x respectively. The sequence x_i converges to x in distribution if $F_i(y)$ converges to $F(y)$ at all points of continuity of $F(y)$.

Convergence in probability follows from convergence with probability 1. Convergence in probability implies convergence in distribution.

To exclude global minima that will be impossible to detect it is assumed that the global minimum of $f(x)$ in Problem 1.1 is the essential infimum f_e^* of $f(x)$. The convergence to a point in the optimality region $R_{\varepsilon,M}$ is considered where

$$R_{\varepsilon,M} = \begin{cases} (x | x \in S, f(x) < f_e^* + \varepsilon), & \text{if } f_e^* \text{ is finite} \\ (x | x \in S, f(x) < M), & \text{if } f_e^* = -\infty \end{cases} \tag{1.18}$$

We present the following Solis and Wets' algorithm which generalizes random search algorithms.

Conceptual algorithm [118]

Step 0 Find x_0 in S and set $k = 0$.

Step 1 Generate ζ_k from the sample space $(\mathbb{R}^n, \mathcal{B}, P_k)$.

Step 2 Set $x_{k+l} = D(x_k, \zeta_k)$, choose t_{k+l}, set $k = k + 1$ and return to Step 1.

The map D with domain $S \times \mathbb{R}^n$ and range S satisfies the following condition:

(H1) $f(D(x,\zeta)) \leq f(x)$ and if $\zeta \in S$, $f(D(x,\zeta)) \leq f(\zeta)$.

The P_k are probability measures corresponding to distribution functions defined on $\mathbb{R}^n$. By M_k we denote the support of μ_k, i.e., M_k is the smallest closed subset of $\mathbb{R}$ of measure 1. Nearly all random search methods are adaptive by which we mean that P_k depends on the quantities, in particular $x_0, x_1, \ldots, x_{k-1}$, generated by the preceding iterations; the P_k are then viewed as conditional probability measures. Let (Ω, σ, P) be a probability space with the sequence of σ-algebras $\sigma_0 \subset \sigma_1 \subset \cdots \subset \sigma$. The trial vector ζ_k is defined as the function $g_k(\omega) \in \mathbb{R}^n$ measurable with respect to σ_k and

$$P_k(B) = P(\omega \in g_{k-1}(B) | \sigma_{k-1})$$

for $B \in \mathcal{B}$. Therefore the features of $P_k(\cdot)$ below should be regarded as taking place with probability 1.

(H2) For any non-negligible Borel subset $B \subset A$, the following equality holds: $\prod_{k=0}^{\infty}(1 - P_k(B)) = 0$.

The following theorem gives the convergence result for global random search algorithm.

Theorem 1.4. (Convergence [118])

Suppose that f is a measurable function, S is a measurable subset of $\mathbb{R}^n$ and hypotheses (H1) and (H2) are satisfied. Let $\{x_k\}_{k=0}^{\infty}$ be a sequence generated by the conceptual algorithm above. Then

$$\lim_{k\to\infty} P[x_k \in R_{\varepsilon,M}] = 1$$

where $P[x_k \in R_{\varepsilon,M}]$ is the probability that at step k, the point x_k generated by the algorithm is in $R_{\varepsilon,M}$.

1.3.2 Adaptive Random Search on the simplex

The adaptive random search (ARS) algorithm consists in exploring a given bounded space, by alternating variance-selection and variance-exploitation phases [72, 148]. It will be used in Algorithm 5.1 to solve maximization Problem 5.2. We adapted this algorithm to the simplex A^n as follows. First, from a current point on the simplex, the displacement towards a new point of the simplex requires to randomly choose a direction $\vec{d} = (d_k)_{k=1\ldots n}$ such that $\sum_{k=1}^{n} d_k = 0$, and $||\vec{d}|| = 1$. Then, if the length of the displacement, drawn from a normal distribution $\mathcal{N}(0,\sigma)$, is too large and such that the new point falls the limit of the simplex, this point is discarded and another displacement is drawn randomly.

The ARS algorithm, adapted to the n-simplex A^n, is described below. It aims at determining the optimal fallow distribution $\text{ARS}(n) = \vec{\tau}^{n,*} = (\tau_1^*, \ldots, \tau_n^*)$ that maximizes the profit R defined in equation (5.4) for a given number of fallows n.

(Initialization)

Step 1 – Start as the center of the simplex:

$$\vec{\tau}^{n,*} := [T_{max} - (n+1)D]\left(\frac{1}{n}, \ldots, \frac{1}{n}\right)$$

and initialize the standard deviation at the "size" of the simplex:
$\sigma^* = \sigma^0 := T_{max} - (n+1)D$.

(Variance-selection)

It aims at finding the best standard deviation σ^*.

Step 2 – 5 decreasing standard deviations $\sigma^{i\in\{1,\dots,5\}} < \sigma^0$ are chosen. For each standard deviation, $2 \times n^2$ fallow distributions are drawn randomly in the simplex and their profit is evaluated. The best standard deviation, selected for the next step, is the one corresponding to the highest profit.

$\vec{\tau}_{sel} := \vec{\tau}^{n,*}$
for *i := 1 to 5* **do**
  $\sigma^i := 0.3 \times \sigma^{i-1}$
  for *j := 1 to* $2 \times n^2$ **do**
    Draw $\vec{d^j}$ (cf. below)
    Draw $r^j \sim \mathcal{N}(0, \sigma^i)$
    $\vec{\tau}^j := \vec{\tau}_{sel} + r^j \vec{d^j}$
    while $\vec{\tau}^j$ *is outside of the simplex* **do**
      Draw $r^j \sim \mathcal{N}(0, \sigma^i)$
      $\vec{\tau}^j := \vec{\tau}_{sel} + r^j \vec{d^j}$
    end
    if $R(\vec{\tau}^j) > R(\vec{\tau}^{n,*})$ **then**
      $\vec{\tau}^{n,*} := \vec{\tau}^j$ and $\sigma^* := \sigma^i$
    end
  end
end

$\vec{d^j}$ draw:

1. $\vec{d^j} \sim \mathcal{U}\big([0,1]^n\big)$;
2. project $\vec{d^j}$ on the hyperplane $H = \{(d_k) \in \mathbb{R}^n | \sum_{k=1}^n d_k = 0\}$;
3. normalize $\vec{d^j}$.

(Variance-exploitation)

It aims at finding the best fallow distribution $\vec{\tau}^{n,*}$.

Step 3 – $5 \times n^2$ fallow distributions are drawn randomly in the simplex, using the best standard deviation σ^* selected from the previous variance-selection phase, and their profit is evaluated. The best fallow distribution is the one with the highest profit.

for *j := 1 to* $5 \times n^2$ **do**
  Draw $\vec{d^j}$ (cf. above)
  Draw $r^j \sim \mathcal{N}(0, \sigma^*)$
  $\vec{\tau}^j := \vec{\tau}^{n,*} + r^j \times \vec{d}$
  while $\vec{\tau}$ *is outside of the simplex* **do**
    Draw $r^j \sim \mathcal{N}(0, \sigma^*)$
    $\vec{\tau}^j := \vec{\tau}^{n,*} + r^j \vec{d^j}$
  end
  if $R(\vec{\tau}^j) > R(\vec{\tau}^{n,*})$ **then**
    $\vec{\tau}^{n,*} := \vec{\tau}^j$
  end
end

(Stopping criteria)

Steps 2 and 3 are repeated until one of the following stopping criteria is achieved:

- The smallest standard deviation σ^5 is used in more than 4 successive variance-exploitation phases.
- The optimum is not improved in more than 4 successive variance-exploitation phases.
- The profit is evaluated more than $100 \times n^2$ times.

Part III

Literature Review

CHAPTER TWO

BIOLOGICAL BACKGROUND

2.1 Biology and cultivation of banana and plantain

Banana and plantain are subspecies of the genus Musa [102]. Worldwide, there is no sharp distinction between "bananas" and "plantains". Especially in the Americas and Europe, "banana" usually refers to soft, sweet, dessert bananas [138], particularly those of the Cavendish group, which are the main exports from banana-growing countries [1]. By contrast, Musa cultivars with firmer, starchier fruit, used for cooking are called "plantains", distinguishing them from dessert bananas. In some regions, many more kinds of banana are grown and eaten, so the binary distinction is not useful and is not made in local languages [138].

The term "banana" is also used as the common name for the plants that produce the fruit. It is a perennial herbaceous plant widely cultivated in the tropical and subtropical regions, and, as a non-seasonal crop, bananas are available fresh year-round. It is perennial because it produces succeeding generations of crops. The first cycle after planting is called the plant crop. The ratoon is the sucker (also called the follower) succeeding the harvested plant. The plant propagates itself by producing such suckers which are outgrowths of the vegetative buds set on the rhizome during leaf formation. During their initial development, the suckers share their parent rhizome [26]. Hence, if the parent plant is infested, so are the suckers [24, 26]. The second cropping cycle after planting is called the first ratoon crop. The third cycle is the second ratoon crop, and so on.

The growth cycle of banana consists of two phases. The vegetative phase (or 'shooting') begins with the production of leaves by the planted tissue culture plant and ends when the inflorescence appearing at the top of the plant. During this phase, banana produces roots continuously. After it, the absorbed nutrients are essentially directed to the growing of the fruit bunch [6]. The reproductive phase begins with the transition of the vegetative meristem into a floral shoot. The division of phases is arbitrary, and it takes normally about 7-8 months after planting before the inflorescence emerges at the top of the plant [80]. The fruit filling period, that is,the time between flowering and harvest, completes the reproductive phase and the growth cycle.

During the growth cycle, plants develop essentially three major components : an underground corm producing suckers and roots, a pseudo stem consisting of encircling leaf sheaths and carrying the leaves and an inflorescence, containing female flowers that develop into fruits. At the end of the growth cycle, the fruit bunch is harvested and after harvest, the aerial portions of a banana plant (leaves, pseudostem and fruit stalk) are normally cut down, or else they will die back naturally. The roots that are not involved in the growth of the sucker quickly lose their freshness by senescence [76].

The length of the growth cycle depends on the cultivar. The parent plant and the ratoon are in competition for resources and ratooning is generally followed only in those areas where there is an assured source of irrigation. During the vegetative phase, most of the resources are directed to the growing parent plant. During

flowering, ratoon development increases. Hence ratoon management or de-suckering becomes very important. As a rule, a sucker is allowed only after the emergence of the inflorescence in the planted crop and the same package of practices are followed as that of the planted crop before allowing a sucker for the second ratoon. In commercial plantings, usually only one of the suckers is selected to grow out and regenerate the plant [102], in order to keep constant the number of plants by hectare.

In East, West and Central Africa, where most of the world's plantains are grown, very little attention has been given to them in terms of research. This was evidently because there were no major production problems in the context of limited input and small-scale subsistence farming systems, thus research was not considered a high priority. However, research is now critically important due to the serious threat of black Sigatoka [70], Xanthomonas wilt [136], and banana bunchy top virus (BBTV) [34], as well as rapid yield decline due to banana weevil, poor weed control, poor soil fertility and nematodes.

2.2 Biology of *Radopholus similis*

Overview

Radopholus similis is commonly known as the burrowing nematode and belongs to the nematodes phylum, Tylenchida order and Pratylenchidae family [117]. It is with, among others, *Radopholus kahikateae sp.*, *Radopholus nelsonensis sp. nov.*, *Radopholus nativus* and *R. vacuus*, one of the many representatives of the genus Radopholus [105].

Radopholus similis has six life stages: egg, juvenile (4 stages), and adult. The sexual dimorphism is very pronounced in *Radopholus similis*: the male has a highly developed cephalic cap, thin labial rings, an aborted stylet, a reduced oesophagus and is probably incapable of feeding [143]. On the other hand, females and juveniles have a large stylet with strong basal buttons and thick labial rings. The type specimen is $580\ \mu m$ long by $21\ \mu m$ in diameter [152]. The size and especially the diameter of the adults can indeed vary from one individual to another. In general, males are slightly thinner than females and pregnant females are thicker than young adult females. Examining the offspring of an isolated female, adults can be ranged in size from 580 to $785\ \mu m$ and 22 to $26\ \mu m$ in diameter [142].

Host plants and impact

Since *Radopholus similis* is one of the most important root pathogens of banana crops [87], it has long been considered to be linked to banana. But in fact, R. similis is able to attack more than 1200 species belonging to many botanical groups [23]. It is an especially important pest of bananas and citrus, and it can be found on coconut, avocado, coffee, sugar cane, other oily, and ornamental. Depending on geographical origins, host weed ranges are highly variable. In Costa Rica, grasses are little or not attacked by R. similis, unlike fabaceae [27]. In Martinique, several grasses, Solanaceae and especially an urticaceae (*Phenax sonneratii*) are good hosts [99].

When it penetrates the banana root, travels and feeds on the root cortex, *R. similis* directly destroys cells and also facilitates the entry and development of saprophagous and secondary parasites [7, 63]. At the macroscopic scale, this damages result in the appearance of brown-red necrosis then black (Figure 2.1) [62]. These necroses can develop and cause a decrease in the capacity of the roots to feed the banana. Its growth can therefore be

delayed, and its bunches are smaller. In Ivory Coast, yield reductions ranging from 30% to more than 50% have been observed [113, 111].

Necrosis also causes an alteration of the mechanical resistance of the roots. Their ability to maintain anchorage of the plant is then reduced, the risk of toppling (Figure 2.2) is seriously increased [8, 120]. For some authors, the proportion of plants harvested, which depends on the proportion of not fallen plants, is the main yield factor affected by *R. similis* [16, 14].

The most important damage of R. similis is observed near the bulbs [89]. When they are affected, necrosis develops along the cortex and at the base of strains causing the Black Head Disease (BHD) [62]. These necroses lead often to the toppling of the plant, usually shortly after flowering [8, 120].

Figure 2.1 – (a) Isolated root at different levels of infestation, from simple roots lesions to black necrosis; credits: Jesus et al. (2015) [54]. (b) Photo of a nematode inside the root; credits: Michael MacClure, University of Arizona. (c) Root pool at different levels of infestation; credits: Zhang et al. (2012) [153].

Life cycle

Radopholus similis is a phytophagous nematode that attacks the roots of host plants. Radopholus similis usually breeds by sexual reproduction. However, in the absence of males, unfertilized females can reproduce by parthenogenesis [55]. The females lay four to five eggs per day during two weeks in root necrotic areas [71]. These eggs in the root, or in soil close by and hatch in a few days. The young nematodes, called juveniles or larvae, moult several times before they become adult. Whether it hatches on the spot or penetrates its host, this nematode joins the cortical zone where it feeds [9] and in which it can move [7]. When the cells die, the nematodes migrate through the root of healthier parts, or they return to the soil and search for another root [53]. At each developmental stage, juvenile stages 2 to 4 (J2 to J4) and adults of both sexes are able to move. It is thus described as migratory endoparasite. However, *R. similis* is able to complete its entire life cycle in a single root. This life cycle is 2-3 weeks, depending on moisture and temperature. Figure 2.3 summarizes its life cycle.

Figure 2.2 – Banana fall caused by R. Similis; credits: Danny Coyne, Consultative Group on International Agricultural Research.

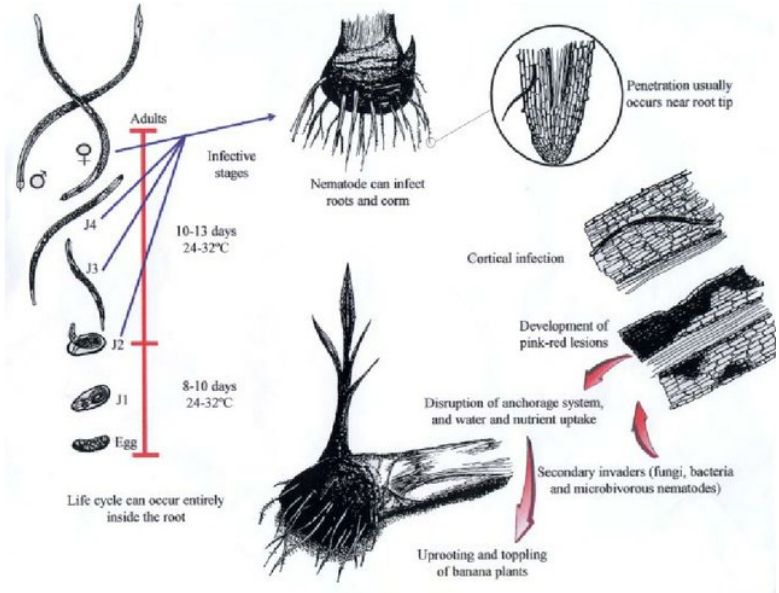

Figure 2.3 – Life cycle of *Radopholus similis* according to Marin et al. (1998) [71].

Survival and dissemination

In the absence of food resources, temperature, humidity and soil oxygenation are considered to be the main limiting factors for *R. similis* survival [73]. The nematode survives without breeding at 16 ° C, develops moderately at 20 ° C and very well above 25 ° C [90]. Its thermal optimum for reproduction is between 27 and 33 ° C [29]. Anyway, the R. similis population declines in the absence of a host plant.

Teissier's model [128] adequately describes the survivorship curves of several plant parasitic nematodes, including endoparasitic nematodes in the same family as *R. similis* [101]. This model is based on the hypothesis that the effect of aging and starvation increases constantly, so that nematode life expectancy decreases exponentially over time. However, in some types of soil, exponential model satisfactorily describe trends of nematode populations in soil. In nitisols, both models describe well the decline of adult populations [12]. Teissier's model is a bit better adapted to females. But for males, the exponential model is on the contrary the most suitable [17]. Similarly in wet andosols, both models are close to the data observed with nematode populations. On the other hand, in dry andosols, the two models do not describe the evolutions of populations [12]. Interactions with other soil organisms may also have a role in the survival of *R. similis* in the soil.

Regarding the dissemination of *R. Similis*, the nematode mainly spreads in the soil by the following ways:

- The human factor through the transportation of contaminated suckers from one banana plantation to another [25], which has more impact at the regional level than at the plantation level.
- Transport by agricultural machinery, which is marginal.
- Transport by water [33, 13] which is highly dependent on rainfall in the region. Thus, the contamination by runoff can be done over very long distances (several tens, or even hundreds of meters) in favour of high precipitation. The term "high" is deliberately imprecise: on soils with high hydraulic conductivity (andosols and nitisols from Martinique or the region of Penja in Cameroon), rain leading to runoff will be 10 or 20 times stronger than rain that will cause runoff on laterite or wet vertisols.
- Migration, which gives its qualification of migratory endoparasite to *R. Similis* [13]. This migration is induced by a tactism that attracts the nematodes to the hosts [150]. Yet, R. similis does not have a broad diffusive spread in the soil [10]. Studies have shown, for example, that in soil containing 92% sand and 6% clay, that is to say relatively easy to cross, *R. similis* was unable to actively join a plant planted at 1.6 meters from the point of inoculation, while the roots of this plant had spread less than 1 meter from the point of inoculation [24]. The same authors observed that colonization by *R. similis* of a land without another plant cover closely follows the colonization by the roots of the original host plants; in the absence of a host plant *R. similis* did not spread.

CHAPTER THREE

EXISTING SOILBORNE PEST, PLANT EPIDEMIC AND CROP ROTATION MATHEMATICAL MODELS

Introduction

In this chapter we first remind several soilborne pest and plant epidemic models that exist in literature respecting their chronological order. Secondly, we briefly remind some mathematical models of crop rotation that are essentially statistical models. The aims of this chapter is to present soilborne pests modeling evolution, to understand the modelling evolution, to understand the different improvements and the improvements that are needed.

3.1 Soilborne pest and plant epidemics mathematical models

3.1.1 The model of Gilligan and Kleczkowski [40]

Gilligan and Kleczkowski proposed two general models for the temporal spread of plant infections basing on a previous model of Gilligan [41], and the model of Walker & Smith [147]. On model deals with root as units, the other with lesions. They are adapted to soilborne epidemics including ectotrophic pathogens and necrotrophic root rotting fungi.

The root model

Naming N_i the density of infected roots, N the density of susceptible roots and P the pest inoculum, the Gilligan and Kleczkowski root model is given by the following equation :

$$\begin{cases} \dfrac{dN_i}{dt} = (r_p P + r_s N_i)(N - N_i), \\ \dfrac{dN}{dt} = r_n f(N), \\ \dfrac{dP}{dt} = -r_d P, \end{cases} \tag{3.1}$$

in which r_n is the rate of root production, r_d is the rate of decay of the inoculum, $f(N)$ is a general growth term that incorporates exponential $\big[f(N) = N\big]$ and logistic $\big[f(N) = N\big(1 - N/Nmax\big)\big]$ growths.

The parameter r_p is the rate of primary infectation, and r_s is the rate of secondary infectation. The primary infection is driven by contact between inoculum (P) and susceptible roots $(N - N_i)$, while secondary depends on contact between infected and susceptible individuals.

The lesion model

Naming U the root lesions or single infections, L_i the length of infected roots, L the total root length and P the pest inoculum, the Gilligan and Kleczkowski root model is given the following equation :

$$\begin{cases} \dfrac{dU}{dt} = (r_p P + r_s N_i)(N - N_i), \\ \dfrac{dL_i}{dt} = r_1 U\Big(1 - \dfrac{L_i}{L}\Big), \\ \dfrac{dL}{dt} = r_n f(L), \\ \dfrac{dP}{dt} = -r_d P, \end{cases} \tag{3.2}$$

in which r_n, r_d and $F(L)$ are analogously defined for the root model (3.1) above, except that the host growth now refers to growth in length rather than in number of roots. We summarize in Table 3.1 the variables, parameters and functions used in Gilligan and Kleczkowski models.

symbol	description	unit (root model)	unit (lesion model)
variables			
N_i	infected roots	numbers	–
N	total roots	numbers	–
P	propagules	numbers	numbers
U	lesions	–	numbers
L_i	infected root Length	–	cm
L	total roots	–	cm
parameters			
N_{max}	maximal root numbers	–	number
L_{max}	maximal root length	–	cm
r_p	primary infection rate	day^{-1}	(day cm)$^{-1}$
r_s	secondary infection rate	day^{-1}	(day cm^2) $^{-1}$
r_l	lesion growth	–	cm s^{-1}
r_n	host growth	day^{-1}	day^{-1}
r_d	inoculum death	day^{-1}	day^{-1}
functions			
f	functional response	numbers	cm

Table 3.1 – Variables, parameters and functions used in Gilligan and Kleczkowski's models.

Models (3.1) and (3.2) help understand the influence of host growth and inoculum decay on the dynamics of infection. From them, authors obtained criteria of equilibrium, as same as the showed that the amount of initial inoculum present in soil at the beginning of a season can influence carrying capacity. They also showed that the rate of decay of soilborne inoculum affect the switch from primary to secondary infection. They analysed how the distribution of lesions can affect the dynamics of an epidemics by comparing disease trajectories that arises from relatively few large lesions with those arising from small lesion.

This work however not includes temporal changes in host availability. Indeed, on long time scales, perturbations due to harvesting of crops or seasonal defoliation in perennial hosts might be considered. These models could include realistic within season host dynamics and synchronous removal at the end of each season. Within-season dynamics are required for a proper treatment of yield, and to explain paradoxical reductions in severity when host growth out-paces that of the pathogen [19].

3.1.2 The model of Madden and Van den Bosch [65]

In the early 2000s, Madden and Van den Bosch have developed a coupled differential equation model for the multi-seasonal dynamics of plant disease for annual crops. Their model is an SEIR model of a plant pathogen introduced in an annual cropping system with a semi-discrete formalism. They investigated to what extent plant pathogens may be used as biological weapons, and the conditions under which the pathogen may persist from season to season were given. Naming S the disease free plant individuals, E the latently infected individuals, I the infectious individuals, such that $Y = E+I+R$ is the total diseased individual, and naming P the abundance of pathogen incoculum. The model of Madden and Van den Bosch is given by the following equation :

$$\begin{cases} \dfrac{dS}{dt} = -\nu SP - \beta SI, \\ \dfrac{dE}{dt} = \nu SP + \beta SI - \sigma E, \\ \dfrac{dI}{dt} = \sigma E - \gamma I, \\ \dfrac{dR}{dt} = \gamma I, \\ \dfrac{dR}{dt} = -(\mu'_g + \nu')P, \end{cases} \tag{3.3}$$

where $P(0) = P_0$, $S(0) = S_0$. The constant ν is the primary infection rate parameter, such that νSP is the rate of occurrence of new infections, and νS is the mean number of new infected plant individuals produced per unit of inoculum per time. Infectious plants are first in latent state and become infectious at rate σ. Infectious plants become post-infectious or remove from epidemic at the rate γ. New infection occur from infectious plants at a rate βSI, with β being the secondary infection rate parameter. Thus, βS is the mean number of new infected individuals per infected individual per time.

The introduced pathogen decays exponentially at a natural mortality rate $\mu_g P$ and a depletion rate $\nu' P$. In the latter expression, $\mu' = \mu$ because each unit of inoculum that produces a plant infection is one less unit of inoculum available for infectiong another plant.

In this model, an epidemic ends at $t = T_g$, to represent crop harvest. All abundance are set to 0 immediately after the end of the T_g. This is $E(T_g^+) = I(T_g^+) = R(T_g^+) = S(T_g^+) = 0$; where the "+" superscript represents the instant after the end of the season.

Diseased individuals R, I and R produce each an amount of pathogen inoculum at the end of the growing season. If θ_E, θ_I, θ_R represent the amount of pathogen inoculum produced per diseaded individuals, then $k_E = \theta_E E(T_g^-)$, $k_I = \theta_I I(T_g^-)$, $k_R = \theta_R R(T_g^-)$ represent the total amount of inoculum at $t = T_g^+$ from latent, infectious and removed diseased individuals at time $t = T_g^-$. Hence, $P(T_g^+) = k_P + k_E + k_I + k_R$; $k_p = P_0 \exp -(\nu' + \mu_g)T_g^-$, and the "-" superscript represents the instant before the end of the season.

Between growing seasons, P decays exponentially with the rate $\mu_b(\varepsilon)$. This correspond to $dP/dt = -\mu_b(\varepsilon)P$. Hence, the single-season model (3.3) is expanded for multiple seasons, with new inoculum of

growing season given by the inoculum that survive from the preceding season, and initial susceptible individuals that are set to S_0.

Figure 3.1 gives a schematic representation of the epidemic within a growing season.

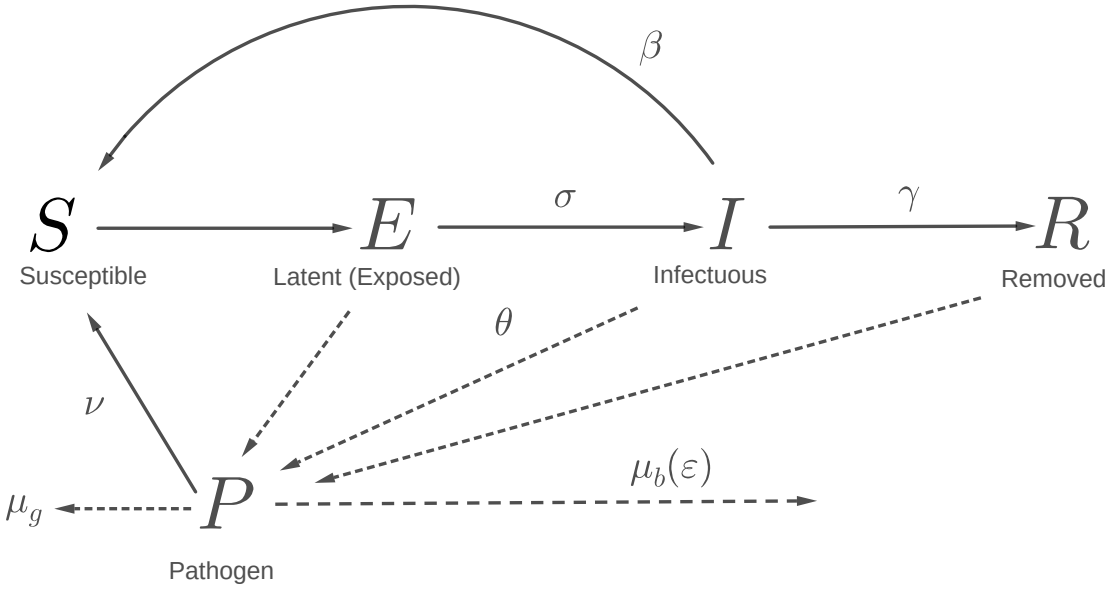

Figure 3.1 – Schematic drawing of disease Madden and Van den Bosch model, representing within-season dynamics of disease-free (S), latently infected (E), infectious (I), and postinfectious (R) plants; the production of inoculum or pathogen individuals (P); and mortality of inoculum within and between seasons.

Given this model, Madden and Van den Bosch have computed the basic reproduction number and the thresholds of persistence of the infection. However, this model, that covers multiple seasons, is still not adapted to *R. similis* since susceptible individuals (eventually root biomass) is not impacted by the pathogen via consumption.

3.1.3 The model of Mailleret et al. [66]

In their paper, Mailleret et al. present two models, an "airborne" model and a "soilborne" model depending on whether the primary inoculum depletion depends or not on the host availability. They build on Madden and Van den Bosch's model [65], and hence consider both primary and secondary infectation dynamics. Two sets of ordinary differential equations, coupled to two sets of recurrence equations, define the model. Table 3.2 summarizes the variables and parameters used in the models of Mailleret et al.

The models are subjected to environmental seasonality. This is the succession of two time periods : the growing season, during which the host plant is present, and the winter season, during which the host plant is absent.

Symbol	Description
Variables	
P	Primary inoculum density
S	Susceptible host plant density
I	Infected host plant density
Parameters	
τ	Growing season length (host plant is present)
$T-\tau$	Winter season length (host plant is absent)
T	Year length
β	Secondary infection rate
Θ	Primary infection rate
α	Infected host plants removal rate
π	Conversion rate from I to P (at the end of the season)
μ	Winter season mortality rate of primary inoculum
Λ	Primary inoculum density independent depletion rate
Ξ	Primary inoculum density dependent depletion rate

Table 3.2 – Variables and parameters used in Mailleret et al.'s models.

Airborne model

Since τ denote the length of growing season and T denote the length of the year, the k-th year's dynamics is governed by the following equation : For $t \in \big(kT, kT+\tau\big)$

$$\begin{cases} \dfrac{dP}{dt} = -\Lambda P, \\ \dfrac{dS}{dt} = -\Theta PS - \beta SI, \\ \dfrac{dI}{dt} = +\Theta PS + \beta SI - \alpha I. \end{cases} \tag{3.4}$$

The $\pm PS$ terms indicate that only a fraction of the released primary inoculum encounter healthy hosts and initiate primary infection, the remaining part being lost.

At the end of the growing season ($t = kT+\tau$), host plants are removed. At that time, infected host plants debris are assumed to convert into primary inoculum at a rate π. This is expressed by the following recurrence equation :

$$\begin{cases} P(kT+\tau^+) = P(kT+\tau) + \pi I(kT+\tau), \\ S(kT+\tau^+) = 0, \\ I(kT+\tau^+) = 0, \end{cases} \tag{3.5}$$

where the "+" superscript denotes the instant right after the end of the growing season.

During the winter, the parasites survive as primary inoculum (P), and their population undergoes an exponential decay with mortality μ. Thus, for $t \in \big(KT+\tau, (k+1)T\big)$,

$$\begin{cases} \dfrac{dP}{dt} = -muP, \\ \dfrac{dS}{dt} = 0, \\ \dfrac{dI}{dt} = 0. \end{cases} \tag{3.6}$$

At the begining of a new season ($t = (k+1)T$), new susceptible are made available with an initial density S_0. This is expressed by the recurrence equation :

$$\begin{cases} P((k+1)T^+) = P((k+1)T), \\ S((k+1)T^+) = S_0, \\ I((k+1)T^+) = 0, \end{cases} \tag{3.7}$$

The semi-discrete model composed of sub-models (3.4) to (3.7) depicts the course of an epidemic over one year through primary and secondary infection dynamics, with infected host plants conversion into primary inoculum at the end of the growing season, and survival to host absence until the next year. Mailleret et al. estimated that it remains the Madden and Van den Bosch's model [65].

Soilborne model

In this model, the authors consider that the promary inoculum depletion occurs only in contact with host plants. Indeed, many root parasites have a primary inoculum form that generates soilborne propagules upon reception of chemical signal of host. This is the case of the burrowing nematode *R. similis* [150]. The constant Ξ being a healthy host density-dependent- primary inoculum depletion rarten and equation (3.5) to (3.6) remaining unchanged, equation (3.4) takes the following form in the soilborne model :

$$\begin{cases} \dfrac{dP}{dt} = -\Xi PS, \\ \dfrac{dS}{dt} = -\Theta PS - \beta SI, \\ \dfrac{dI}{dt} = +\Theta PS + \beta SI - \alpha I. \end{cases} \tag{3.8}$$

Assuming that primary inoculum is fast, this is primary infection rate parameters Θ, Λ and Ξ are large, Mailleret et al. reduced both airborne and soilborne model to a two-dimensional compact model using singular perturbation theory for slow-fast dynamic [145]. For both they computed a periodic disease free equilibrium around which they linearized the system, and from which they derived a basic reproduction number. The latter stands here for the quantity of primary inoculum at the beginning of the year $(k+1)$ produced via the infections generated by one primary unit at the beginning of year k in a disease-free context [20, 65]. They also regarded the coexistence issue and chaos.

The Mailleret et al.'s soilborne model seems to fit well to the dynamics of *R. similis*, but still there is no feeding of pests on host (root). Also, there is no interruption in host growth during growing season at it is for the banana root growth after plant flowering. Besides, there is a fixed off-season here, that is the winter which does not exist in tropical region where banana grows. The next model is pretty much more adapted to *R. similis*.

3.1.4 A cohort model adapted to *Radopholus similis* : the model of Tixier et al.[133]

Tixier et al. describe the development of SIMBA-NEM, a cohort-based model aimed at simulating the dynamics of populations of banana plant-parasitic nematode at field scale, in relation to environmental factor and banana root system.

In SIMBA-NEM, the growth of the population is assumed to follow a logistic function with an intrinsic growth rate and a carrying capacity that depends on banana root biomass. The model also takes in account the competition between two nematode species for banana root biomass, and the use of nematicide. The two species of nematodes are *Pratylenchus coffeae* (Pc) and *Radopholus similis* (Rs). Both population are divided in cohorts as follows ; a cohort represents a pool of individuals at the same age in number of weeks. The model assumes that the nematodes are mature 3 weeks after hatching and have a life-cycle of 6 weeks, so that cohorts 1 to 2 are juveniles and cohorts 3 to 6 are adults. The time step is discrete with one week as a step. Table 3.3 summarizes the variables and parameters of the model, and Figure 3.2 describes the structures of the model.

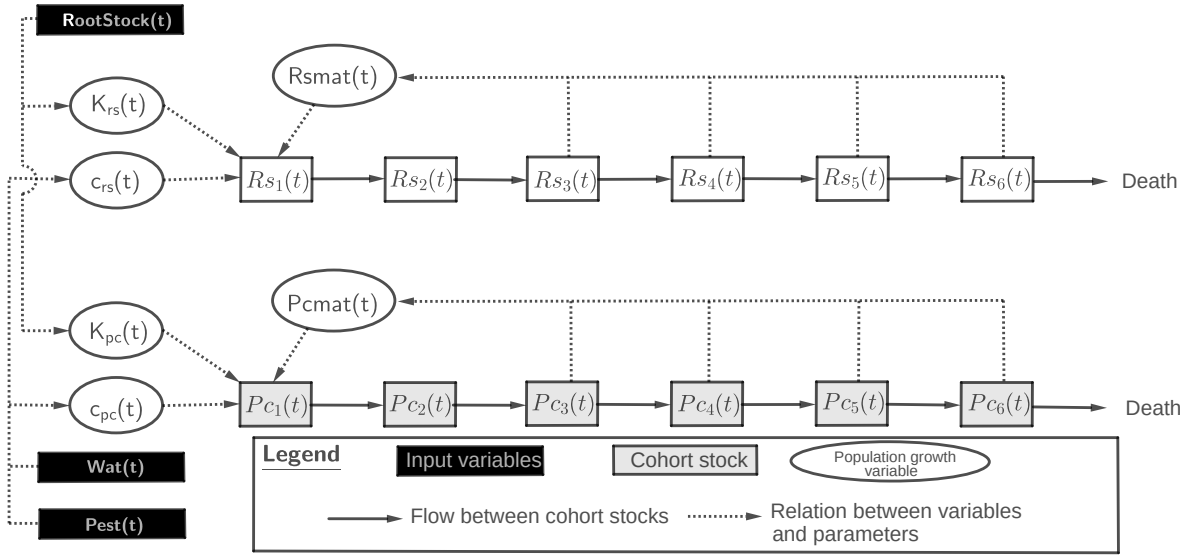

Figure 3.2 – Structure of the SIMBA-NEM model. At each time step t of the model for each species, $Rs_i(t)$ and $Pc_i(t)$ represent the number of nematodes in cohort i, $Rsmat(t)$ and $Pcmat(t)$ represent the number of mature nematodes, $K_{Rs}(t)$ and $K_{Pc}(t)$ the carrying capacity and $c_{Rs}(t)$ and $c_{Pc}(t)$ the population growth parameter for *R. similis* (Rs) and *P. coffeae* (Pc) respectively and $RootsStock(t)$, $Wat(t)$ and $Pest(t)$ represent the banana fresh root biomass, percentage of soil water and soil nematicide quantity, respectively.

All the equations of the model are given in Table 3.4. We give more comments on the equations in Table 3.4:

- Eq. (1) : The total carrying capacity of the environment for the two species $K_{nem}pot(t)$ is calculated with the banana root biomass $RootsStock(t)$ and the maximal carrying capacity $KnemMax$.
- Eqs. (2a) and (2b) : Carrying capacities $K_{Rs}(t)$ and $K_{Pc}(t)$ are calculated with the total carrying capacity $K_{nem}pot(t)$ and to the total number of nematodes of other species $Rstotal(t)$ and $Pctotal(t)$.
- Eqs. (3a) and (3b) : The growth rates $c_{Rs}(t)$ and $c_{Pc}(t)$ are calculated at each step of the model using the intrinsic growth rate of each species $c_{Rs}pot$ and $c_{Pc}pot$ and correction factors relative to the soil water content and the quantity of nematicides in the soil .
- Eqs. (4a) and (5a) : The total population of nematodes is calculated.

	Meaning
Input variables	
$RootsStock(t)$	Banana root fresh biomass at step t (g.ha^{-1})
$Wat(t)$	Soil water content at step t in percentage of stock (%)
$Pest(t)$	Grams of nematicide active product in soil per hectare at step t (g.ha^{-1})
$Rs_1(1)$; $Pc_1(1)$	Initial nematode number for Rs and Pc (in number of nematode per hectare, nb.ha $^{-1}$)
Output variables	
$K_{nem}pot(t)$	Total carrying capacity in nematodes per hectare at step t (ha^{-1})
$K_{Rs}(t)$; $K_{Pc}(t)$	Carrying capacity per hectare for Rs and Pc at step t (ha^{-1})
$c_{Rs}(t)$; $c_{Pc}(t)$	Growth rate at step t for Rs and Pc
$FX_{pest}(t)$	Nematicide effect at step t
$FX_{wat}(t)$	Soil water content effect at step t
$Rs_i(t)$; $Pc_i(t)$	Number of nematodes in cohort i per hectare at step t for Rs and Pc (ha^{-1})
$Rsmat(t)$; $Pcmat(t)$	Total number of mature nematodes per hectare at step t for Rs and Pc (ha^{-1})
$Rstotal(t)$; $Pctotal(t)$	Total number of nematodes per hectare at step t for Rs and Pc (ha^{-1})
$Rs(t)$; $Pc(t)$	Nematode population per gram of root at step t for Rs and Pc (g^{-1})
Parameters	
$K_{nem}Max$	Maximum carrying capacity per gram of root (g^{-1})
$c_{Rs}pot$; $c_{Pc}pot$	Intrinsic growth rate for Rs and Pc
a_{pest}, b_{pest}	Parameters of the nematicide effect curve $FX_{pest}(t)$
a_{wat}, b_{wat}, c_{wat}	Parameters of the soil water content effect curve $FX_{wat}(t)$
	Rs for *R. similis* and Pc for *P. coffeae*.

Table 3.3 – Variables and parameters of the SIMBA-NEM model, where t is the time step of the model (in weeks) and i is the cohort rank.

- Eqs. (4c) and (5c) : The logistic growth patterns corresponding to new individuals (eggs) are given.
- Eqs. (4d) and (5d) : The passage of individuals from cohort i to cohort $i+1$ is described.
- Eq. (7a) : The nematicide effect on intrinsic growth rates $c_{Rs}(t)$ and $c_{Pc}(t)$ is accounted for through a corrective factor $FX_{pest}(t)$ ranging from 0 to 1, $FX_{pest}(t)$ follows a curve whose parameters are a_{pest} and b_{pest}.
- Eq. (7b) : The effect of soil water content on the intrinsic growth rates is accounted for through a corrective factor $FX_{wat}(t)$ ranging from 0 to 1, $FX_{wat}(t)$ follows a curve whose parameters are a_{wat}, b_{wat} and c_{wat}. The parameter a_{wat} defines the optimum soil water content, b_{wat} and c_{wat} are the maximum corrections for minimum and maximum soil water content respectively (drought and water excess).

SIMBA-NEM has been calibrated to some experimental data, from which arose some results on multi-species competition in long-term simulations and an optimisation of pest management strategies. The model arises to be an excellent computational model, which in addition takes into account competitive interactions between nematode species, a step forward toward the modelling of ecological community. The latter appear to be an important issue in modelling plant disease [93]. Indeed, modelling quantitative disease resistance in populations facing multiple pathogens is a key challenge in predicting disease dynamics and evolutionary responses of pathogens and hosts [19]. However, SIMBA-NEM being computational, it has no analytic result or qualitative description and its outputs and conclusions strongly depend on the value of the parameters and precision in their estimation, which often requires extensive data [3]. But we have not found in the literature quantitative studies that count nematodes by sorting them by age, stage or cohort; possibly because it is difficult to set up this type of experiment for microscopic worms. Also, the model does not allow fallowing or crop rotation with non-host plants, whereas it has been shown empirically that these are effective strategies to fight the spread of R. similis [17, 16, 15].

3.2 Some crop rotation mathematical models

In this section we analyse some crop rotation models in the literature. These models give us an overview on the use of mathematical modelling in the management of crop rotation, and is going to somehow give us a good base to deal with crop rotation in chapters 5 and 6. The models in this section deal with the rotation of a main crop with either a resistant poor-host or non-host crop or a resistant crop, whereas in chapters 5 and 6 we rotates the crop with a fallow period which can eventually serve for the deployment of a non-host plant.

3.2.1 Taylor and Rodrìguez-Kábana's model of rotation of peanuts and cotton to manage soilborne organisms [127]

Taylor and Rodrìgues-Kábana proposes a model that maximises the profit of cotton and peanut crops over a multi-year planning horizon. The model accounts the stochastic population dynamics of two major pests which are the root-knot nematode (*Meloidogyne arenaria*) and Southern blight (white mold), and the beneficial microbivorous nematodes. In their model, the price of cotton and the world price of peanuts are also treated with stochastic dynamic relationships in the model.

	Equations
(1)	$K_{nem}pot(t) = RootsStock(t) \times K_{nem}Max$
(2a)	$K_{Rs}(t) = K_{nem}pot(t) - Pctotal(t-1) \quad (\text{for } t > 1)$
(2b)	$K_{Pc}(t) = K_{nem}pot(t) - Rstotal(t-1) \quad (\text{for} t > 1)$
(3a)	$c_{Rs}(t) = c_{Rs}pot \times FX_{pest}(t) \times FX_{wat}(t)$
(3b)	$c_{Pc}(t) = c_{Pc}pot \times FX_{pest}(t) \times FX_{wat}(t)$
(4a)	$Rstotal(t) = Rs_1(t) + Rs_2(t) + Rs_3(t) + Rs_4(t) + Rs_5(t) + Rs_6(t)$
(4b)	$Rsmat(t) = Rs_3(t) + Rs_4(t) + Rs_5(t) + Rs_6(t)$
(4c)	$Rs_1(t) = (c_{Rs}(t) \times Rsmat(t-1)) \times ((K_{Rs}(t) - Rstotal(t-1))/K_{Rs}(t)) \quad (\text{for } t > 1)$
(4d)	$Rs_i(t) = Rs_{i-1}(t-1) (\text{for } i > 1 \text{ and for} t > 1)$
(5a)	$Pctotal(t) = Pc_1(t) + Pc_2(t) + Pc_3(t) + Pc_4(t) + Pc_5(t) + Pc_6(t)$
(5b)	$Pcmat(t) = Pc_3(t) + Pc_4(t) + Pc_5(t) + Pc_6(t)$
(5c)	$Pc_1(t) = (c_{Pc}(t) \times Pcmat(t-1)) \times ((K_{Pc}(t) - Pctotal(t-1))/K_{Pc}(t)) \quad (\text{for } t > 1)$
(5d)	$Pc_i(t) = Pc_{i-1}(t-1) \quad (\text{for } i > 1 \text{ and for } t > 1)$
(6a)	$Rs(t) = Rstotal(t)/RootsStock(t)$
(6b)	$Pc(t) = Pctotal(t)/RootsStock(t)$
(7a)	$FX_{pest}(t) : \{\text{if } Pest(t) > a_{pest}\}, \{\text{then } b_{pest}\}, \{\text{otherwise } ((b_{pest}-1)/a_{pest}) \times Pest(t) + 1\}$
(7b)	$FX_{wat}(t) : \{\text{if } Wat(t) < a_{wat}\}, \{\text{then } (((1-b_{wat})/a_{wat}) \times Wat(t)) + b_{wat}\}, \{\text{otherwise } (((1 - c_{wat})/(a_{wat}-1)) \times Wat(t)) + (c_{wat} - ((1-c_{wat})/(a_{wat}-1)))\}$
	For $t = 0$, $Pctotal(t-1)$ and $Rstotal(t-1)$ are considered equal to the initial nematodes populations. See Table 3.3 for variables and parameters description.

Table 3.4 – Equations of the SIMBA-NEM model, where t is the time step of the model (in weeks) and i is the cohort rank.

The dynamic population models for soilborne pathogenes depend on population levels of other organisms, on pesticide use, and on previous crops. The decision rule that gives the optimal crop rotation (between cotton and peanuts) and use of nematicide arises from a stochastic dynamical programming. Thus, decision variables in the model are whether to plant cotton or peanuts, and whether to use nematicide and fungicide on peanuts. Table 3.5 summarizes the variables used in the model. Table 3.6 describes the relationship between the variables.

	Meaning
Stochastic variables	
RK_t	Root-knot nematode infestation in the Fall of crop year t
MB_t	Microbivorous nematode level in the Fall of crop year t
WM_t	Southern blight infestation in peanuts at harvest time in crop year t
PCT_t	Market price of cotton lint in crop year
PPN_t	Market price of additional (non-quota) peanuts in crop year t
Deterministic variables	
L_{t-1}, L_{t-2}	land use in each of the previous 2 years
Decision variables	
C_t	Binary variable that indicates whether the crop planted in crop year t is peanuts ($C_t = 0$) or cotton ($C_t = 1$)
N_t	Binary variable indicating whether a nematicide is used if the crop is peanuts in crop year t
F_t	Binary variable indicating whether a fungicide is used if the crop is peanuts in crop year t
R_t	Function showing annual returns over variable production cost in t

Table 3.5 – Variables of Taylor and Rodrìguez-Kábana's model.

The optimal value function is given by the following expression :

$$V_t(PPN_t, PCT_t, RK_t; WM_t; MB_t, L_{t-1}, L_{t-2}) = \max_{C_t, N_t, F_t} \Big\{ \mathbb{E}\Big[R_t\big(PPN_t, PCT_t, RK_t, WM_t, MB_t, L_{t-1}, L_{t-2}, C_t, N_t, F_t\big) + \beta V_{t+1}\big(PPN_{t+1}; PCT_{t+1}, RK_{t+1}, WM_{t+1}, MB_{t+1}, L_t, L_{t-1}\big)\Big] \Big\} \tag{3.9}$$

where, β is the annual discount factor; and $\mathbb{E}$ is the expectation operator, with the expectation taken with respect to the set of stochastic variables (Table 3.5) in the state transition equations (Table 3.6). Maximization of V_t is done subject to the set of state-transition equations and the return equation based on crop yields. A Dynamical Approach [5] is used to maximize the function V_t. The economical return is given by the following equation :

$$R_t = \big\{PCT_t - ucct)YCT_t - vcct\big\}C_t + \big\{PPN_t - ucpn)YPN_t - vcpn\big\}(1 - C_t), \tag{3.10}$$

where YCT_t and YPN_t are per-acre yields of cotton and peanuts, respectively; $ucct$ and $ucpn$ are the variable costs of producing cotton and peanuts which are proportional to yield; $vcct$ and $vcpn$ are the variable costs of cotton and peanuts which are fixed per acre. The peanut component of this return equation is modified for scenarios assuming a peanut quota, by adding to returns the value of the fixed quota above PPN_t.

Soilborne organisms	
Organism	Stochastic equation $^{(a)}$
Root-knot nematode in peanuts after peanuts	$log(RK_t+1) = 6.650 + 0.234log(RK_{t-1}+1) - 0.435log(MB_{t-1}+1) - 0.542N_t + \epsilon_{1,t}$ $\sigma = 0.512$
Root-knot nematode in peanuts after cotton	$log(RK_t+1) = 2.636 + 0.392log(MB_{t-1}+1) - 2.805N_t + \epsilon_{2,t}$ $\sigma = 0.1251$
Microbivorous nematodes in peanuts after peanuts	$log(MB_t+1) = 4.151 + 0.299log(RK_t+1) + 0.166log(RK_{t-1}+1) - 0.198log(MB_{t-1}+1)$ $+ 0.229N_t + \epsilon_{3,t}$ $\sigma = 0.453$
Microbivorous nematodes in peanuts after cotton	$log(MB_t+1) = 8.507 - 0.560log(MB_{t-1}+1) - 0.204N_t + \epsilon_{4,t}$ $\sigma = 0.357$
Microbivorous nematodes in cotton after peanuts	$log(MB_t+1) = 5.559 + 0.125log(RK_{t-1}+1) - 0.364log(MB_{t-1}+1) + \epsilon_{5,t}$ $\sigma = 0.390$
Microbivorous nematodes in cotton after cotton	$log(MB_t+1) = 4.193 + \epsilon_{6,t}$ $\sigma = 0.428$
Southern blight in peanuts after peanuts	$log(WM_t+1) = 4.333 - 0.183log(MB_{t-1}+1) - 1.034F_t + \epsilon_{7,t}$ $\sigma = 0.443$
Southern blight in peanuts after 1 year of cotton	$log(WM_t+1) = 4.011 - 0.199log(MB_{t-1}+1) - 0.956F_t + \epsilon_{8,t}$ $\sigma = 0.345$
Southern blight in peanuts after 1 year of cotton	$log(WM_t+1) = 3.739 - 0.199log(MB_{t-1}+1) - 0.956F_t + \epsilon_{9,t}$ $\sigma = 0.345$
Markovian prices	
Commodity	Estimated equation$^{(b)}$
Cotton price	$PCT_t = 0.271482 + 0.643422PCT_{t-1} + \epsilon_{10,t}$ $(2.11) \quad (4.42)$ $\sigma = 0.126$
Additional peanut price	$PPN_t = 0.070243 + 0.656116PPN_{t-1} + \epsilon_{11,t}$ $(1.92) \quad (4.52)$ $\sigma = 0.049$

(a) In each of the equations above, σ is the estimated standard deviation of the additive random error term, $\epsilon_{m,t}$ for the m-th equation.
(b) Student's t-values are given in parentheses below their respective estimated coeffcients.

Table 3.6 – Dynamic population models for soilborne organisms and markovian price relationships in Taylor and Rodrìguez-Kábana's model

From this model, Taylor and Rodrìguez-Kábana determined the optimal peanuts-cotton rotation strategies to optimize the economical. However, from their own word, it would be practically impossible to fully explain its optimal decision rule to a producer untrained in statistics and dynamic optimization

3.2.2 The model of Van Den Berg and Rossing [139]

The model of Van Den Berg and Rossing deals with the optimisation of the yield of crops through the control of the lesion nematode *Pratylenchus penetrans* via dynamic crop rotations. The authors use the Metropolis algorithm [38] to fit the model to data and find the parameters of optimal rotation. The model aims to describe optimal rotation strategies between host crops and non-host crops (or fallow) over n-year cycles.

On a single year, the final density (P_f) of pest is linked to the initial density (P_i) by the following formula :

$$P_f = \frac{P_i}{\alpha + \beta P_i}, \tag{3.11}$$

in which $1/\alpha$ and $1/\beta$ define respectively the slope of the curve of evolution of pest density and its horizontal asymptote. Both can arise from the logistic growth equation applied to pest densities.

During a year with non-host plant or fallow, a fraction of nematodes is assumed to survive. The surviving fraction is estimated with equation (3.11) as $1/\alpha$ by setting β to 0 :

$$P_f = \frac{P_i}{\alpha}, \tag{3.12}$$

The yield (Y) of each year cropping of the host crop is assessed from initial density of pest by the following equation :

$$Y = \frac{1}{1 + \lambda P_i}, \tag{3.13}$$

where λ is a rate parameter.

Gross margin (GM expressed in euros.ha.$^{-1}$.year^{-1}) of a crop in absence of nematodes is equal to financial output (FO in euros.ha.$^{-1}$.year^{-1}), the product of yield, and value of the crop minus the specific costs (SC in euros.ha.$^{-1}$.year^{-1})) of the crop :

$$GM = F0 - SC. \tag{3.14}$$

When nematodes are present it is assumed that yield is a function of P_i; therefore FO in equation (3.14) is multiplied with relative yield Y from equation(3.13) :

$$GM(P_i) = \frac{F0}{1 + \lambda P_i} - SC. \tag{3.15}$$

In a crop rotation, n crops are grown on the same field for n consecutive years. This process is repeated every n years, so the period of the rotation is n years. Each crop is denoted as a phase of the rotation, with crop 1 being phase 1, crop 2 being phase 2, and so on [151]. The size of nematode population at the start of year t is P_t. The dynamics are modeled by the equation :

$$P_{t+1} = f(t, P_t) = \frac{P(t)}{\alpha(\tau(t)) + \beta(\tau(t))P_t} \qquad P_1 = \pi_0, \tag{3.16}$$

in which $\tau(t) = t \mod n$ and $1 \leq \tau \leq n$. Function $t \mod n$ is such that $\tau(t)$ is equal to 1 in year 1, equal to 2 in year 2, equal to n in year n, and again equal to 1 in year $n + 1$, and so on.

The nematode density before the first crop is grown for the first time, π_0, is a field-specific parameter of the model. The parameters $\alpha(\tau(t))$ and $\beta(\tau(t))$ are dependent on the crop grown in year $t \mod n$. When P_t and P_{t+1} in equation (3.16) are replaced by their inverse R_t and R_{t+1} and $\rho_0 = 1/\pi_0$, equation (3.16) becomes

$$R_{t+1} = R(t, P_t) = \beta(\tau(t)) + \alpha(\tau(t))R_t) \qquad R_1 = \rho_0, \tag{3.17}$$

The development of equation (3.17), using among others some properties of geometric series, leads to the equation :

$$R_{t=pn+1} = \left(\sum_{k=1}^{n-1} \beta(k) \prod_{m=k+1}^{n} \alpha(m) + \beta(n) \right) \frac{1 - \prod_{s=1}^{n} \alpha(s)^p}{1 - \prod_{s=1}^{n} \alpha(s)} + R_1 \prod_{s=1}^{n} \alpha(s)^p. \tag{3.18}$$

Maximizing the Gross Margin (3.14) passes through the optimization of rotations via equation (3.18), by choosing the years k for which $\beta(k) = 0$. Such years are years of non-host plant cropping or fallow, according to equation (3.12).

The model of Van den Berg and Rossing and its output is easy to understand and to apply. However, it considers the same duration for the cropping of the host plant and the cropping of the non-host plant (or the fallow). Besides, it puts asides the decline of carrying capacity (root density) of nematodes due to their feeding.

3.2.3 The model of Nilusmas et al. [83]

Nilusmas et al. propose an epidemiological model that describes the within-season dynamics of avirulent ant virulent root-knot nematodes (RKNs) of the species *Meloidogyne incognita* and their between-season survival. They then propose a yield-maximizing rotation strategy between resistant and non-resistant plants basing on their model.

The use of nematode-resistant plants is a promising strategy for eco-friendly pest management [78]. However, the long-term deployment of resistant plants creates a selection pressure that allows nematode populations to develop resistance. Thus appears in the population of nematodes virulent strains. If avirulent nematodes can only attack non-resistant (susceptible) plants, virulent nematodes can attack resistant plants. In addition, they attack susceptible plants with even more aggressiveness. Over-long-term deployment of resistant plants may change the entire population of nematodes into virulent nematodes. It is therefore necessary to alternate the deployment of resistant plants with susceptible plants.

The Nilusmas et al.'s model aims to determine the optimal rotation between susceptible host plants (termed H^S) and resistant host plants (termed H^R).

The within-season model describes, in continuous time, the changes in free living nematode densities (P), healthy susceptible plant root density (H), latent nematode feeding site size (E) and infectious nematode deeding site size (I). The latent deeding site is a state of in-root nematodes in which they do not produce free-living progeny, contrary to infectious sites.

Each of the state variables above are subdivide in two particular substates. Free living nematodes (P) are subdivided into virulent (P_ν) and avirulent (P_a) strains. Healthy roots are subdivided into resistant (H^R) and susceptible (H^S) densities. Latent sites are subdivided into virulent nematode feeding sites (E_ν) and avirulent nematode feeding sites (E_a). Infectious sites are subdivided into virulent nematode feeding sites (I_ν) and avirulent nematode feeding sites (I_a). Table 3.7 summarizes the variables and parameters in the model of Nilusmas et al.

	Meaning
Variables	
H^X	Density of healthy plant root (UR); H^S for susceptible plants, H^R for resistant plants
P	Density of free living nematodes (UN); P_a for avirulent nematodes, P_ν for virulent nematodes
E	Density of latently infected feeding sites (UR); E_a for sites of avirulent nematodes, E_ν for sites of virulent nematodes
I	Density of infectious feeding sites UR; I_a for sites of avirulent nematodes, I_ν for sites of virulent nematodes
Parameters	
H_0	Initial root biomass (UR)
P_0	Initial nematode density in the soil (UN)
p_ν	Initial proportion of virulent nematodes
β	Infection rate (UR^{-1}day$^{-}1$)
w_β	Fitness cost on infectiveness
λ	Transition rate from E to I (day^{-1})
r	Nematode reproduction rate (UN UR^{-1} day^{-1})
w_r	Fitness cost on reproduction
δ	Fraction of virulent offspring
α	Nematode mortality rate in roots (day^{-1})
η	Nematode mortality rate in the soil (day^{-1})
ϕ	Between-season survival probability
ε_y^X	Nematode infection success (UN UR^{-1}); 0 if $X = R$ and $y = a$, 1 otherwise
μ	Plant root growth rate (mg day^{-1})
x	Conversion factor between root mass and density of feeding sites (UR mg^{-1})
k	Impact of infection prevalence on root growth rate
τ	Duration of a cropping season
	Units: UR: number of feeding sites per gram of soil; UN: number of nematodes per gram of soil.

Table 3.7 – Variables and parameters of the model of Nilusmas et al.

Given the varaibles and parameters in Table 3.7, the model of Nilusmas et al. reads :

$$\begin{cases} \dfrac{dP_a}{dt} = -\beta P_a H^X - \eta P_a + (1-\delta) r I_a, \\ \dfrac{dP_\nu}{dt} = -\beta P_\nu H^X - \eta P_\nu + \delta r I_a + (1-w_r) I_\nu, \\ \dfrac{dH^X}{dt} = \mu x f(H^X, E_a + E_\nu, I_a + I_\nu) - \varepsilon_a^X \beta P_a H^X - (1-w_\beta)\varepsilon_\nu^X \beta P_\nu H^X, \\ \dfrac{dE_a}{dt} = \varepsilon_a^X \beta P_a H^X - \lambda E_a \\ \dfrac{dE_\nu}{dt} = (A - w_\beta)\varepsilon_\nu^X \beta P_\nu H^X - \lambda E_\nu, \\ \dfrac{dI_a}{dt} = \lambda E_a - \alpha I_a, \\ \dfrac{dI_\nu}{dt} = \lambda E_\nu - \alpha I_\nu. \end{cases} \tag{3.19}$$

with initial conditions $H^X(0) = H0$, the initial root biomass of newly planted individuals, $P_a = (1-p_\nu)P_0$ and $P_\nu = p_\nu P_0$, where P_0 refers to the initial nematode density in the soil and p_ν to the initial proportion of virulent nematodes in the soil. Initial values of I_a, E_a , I_ν and E_ν are set to 0 because plants are assumed to be healthy at the time they are planted.

When a free living nematode P_ϱ, ($\varrho = a$ or $\varrho = \nu$) comes into contact with a portion of healthy plant root H^X, the latter becomes latently infected E_ϱ at rate $\varepsilon_\varrho^X \beta P_\varrho H^X$, where β is the infection rate and ε_ϱ^X is a conversion factor between nematode and root densities. Avirulent and virulent nematodes compete for healthy plant roots H^X in the following way: avirulent nematodes P_a can infect susceptible plants ($\varepsilon_a^S = 1$) but are unable to infect resistant plants ($\varepsilon_a^R = 0$), while virulent nematodes P_μ are able to infect both resistant ($\varepsilon_\nu^R = 1$) and susceptible plants ($\varepsilon_\nu^S = 1$). After a time period 1λ, the infected root portion becomes infectious (I_a) and starts producing free living avirulent nematodes (P_a) at rate r. Free living nematodes in the soil and infectious nematodes in the roots die at rates η and α, respectively. Roots are assumed to grow linearly with time at basic rate μx, where x is a conversion factor between root biomass and root density. Root infection by nematodes impacts root growth through function $f(\dot{})$ that discounts the basic growth rate by a decreasing exponential function of infection prevalence $\pi = \frac{E_a + I_a}{H^S + E_a + I_a}$ multiplied by a scaling factor k : $f(H^S, E_a, I_a) = e^{-k\pi}$.

At the end of each cropping season, plants are removed. At the beginning of the next cropping season, healthy and infected roots are thus reset to their initial values, H_0 and 0, respectively. Nematode densities P_a and P_ν are set to their value at the end of the previous cropping season, multiplied by a survival probability ϕ. The full model of plant nematode interaction over multiple cropping seasons is therefore a hybrid model, with a continuous part to describe the nematode infection dynamics during a cropping season of length τ, and a discrete part to describe nematode survival between seasons and crop planting as in the model of Mailleret et al. (Subsection 3.1.3).

The optimization here operates on the choice of the strain of plants (resistant or susceptible) that are planted each season. Nilusmas et al consider several resistance deployment strategies: the two "pure" strategies, resistant-only and susceptible-only strategies, consisting in planting one crop type all the time; periodic rotation strategies, alternating resistant and susceptible plants according to a repeated pattern; and unconstrained strategies, i.e. arbitrary sequences of susceptible and resistant plants.

Generally in crop rotation model, the rotations can be assessed in terms of mean nematode density per rotation, initial nematode density per rotation, healthy root density per rotation, or yield of crop per rotation.

The two last are linked each to other.

Deployment strategy assessment

The performance of each strategy in this model is quantified with the *Healthy root density* (HRD), a proxy of crop yield defined as the mean of the integral of healthy plant root densities over the n cropping seasons:

$$HRD = \frac{1}{n}\sum_{i=1}^{n}\int_{ith \text{ season}} H^X(t)dt \tag{3.20}$$

The optimal strategy over a given time horizon of n cropping seasons was defined as the strategy with best performance, i.e. maximising the HRD in equation 3.20. To identify optimal periodic strategies, authors compute all periodic rotation strategies between resistant and susceptible crops, beginning with resistant crops and alternating m and p seasons of resistant. They also find unconstrained optimal strategies by using a genetic algorithm, with particular attention the influence of the genetic parameters (fitness costs w_β , w_r, and the proportion of virulent offspring δ). The robustness of their results is evaluated in order to determine whether optimal periodic strategies remain effective if biological parameters are not known with perfect precision.

Part IV

Results and discussion

CHAPTER FOUR

MODELLING AND ANALYSIS OF THE DYNAMICS OF THE BANANA BURROWING NEMATODE *Radopholus similis* IN A MULTI-SEASONAL FRAMEWORK

Introduction

In this chapter, we study the infestation dynamics of banana plants by *Radopholus similis*. Two control strategies are implemented: pesticides, which are widely used, and fallows, which are more environmentally friendly. To represent the host-parasite dynamics, two semi-discrete models are proposed. During each cropping season, free nematodes enter the plant roots, on which they feed and reproduce. At the end of the cropping season, fruits are harvested. In the first model, the parent plant is cut down to be replaced by one of its suckers and pesticides are applied. In the second model, the parent plant is uprooted and a fallow period is introduced, inducing the decay of the free pest populations; at the beginning of the next cropping season, a pest-free vitroplant is planted. For both models, the basic reproduction number is computed, assuming that the infestation dynamics is fast compared to the other processes, which leads to the model order reduction. Conditions on the pesticide load or the fallow duration are then derived to ensure the stability of the pest free equilibrium. Finally, numerical simulations illustrate these theoretical results.

4.1 Modelling

4.1.1 Core model

This work considers several cropping seasons and assumes a homogeneous repartition of nematodes in the roots. We therefore build a multi-seasonal compartmental model which represents the root growth, the pest dynamics and their interaction with the roots. Two cases are considered for banana plant reproduction. In the first case, a sucker of the parent plant is selected to form the new plant. Dying roots of the parent plant are assigned the term *old root pool* in our model. In the second case, a new nematode-free vitroplant is planted after the uprooting of the parent plant. Some root tips are then left in the soil, the uprooting being hardly perfect. These tips are also included in the *old root pool*.

We consider a single plant and make the following additional modelling assumptions:

1. The nematode population is divided into three compartments: free nematodes in the soil (P), infesting nematodes in the roots (X), infesting nematodes inside the old root pool (Y). Since the absence of males is not limiting because the females can reproduce by parthenogenesis, we do not pay attention to the sex of the pests.

2. There is one compartment for the biomass of functional roots (S).

3. During a cropping season, banana roots grow logistically [45] until the flowering at which moment root development stops. The duration of the growth period, *i.e.* the time elapsed between the start of the cropping season and the flowering of the plant, is termed d; the total duration of a cropping season is termed D. We denote the starting point of the $(n+1)$-th season by t_n, and we set $t_0 = 0$ as the starting point of the first season. The logistic growth of the roots during a cropping season is therefore given by:

$$\frac{dS}{dt} = \rho(t)S\Big(1 - \frac{S}{K}\Big),$$

where

$$\rho(t) = \begin{cases} \rho & \text{for } t \in (t_n, t_n + d], \\ 0 & \text{for } t \in (t_n + d, t_n + D]. \end{cases}$$

4. Free pests (P) infest the plant roots (rate β). They undergo natural mortality (rate ω).

5. Infesting pests (X) feed on the plant roots with a Holling type II-like functional response $\frac{aSX}{S+\Delta}$ that is well-suited for invertebrates [52]. They undergo natural mortality (rate μ). This mortality rate differs from the mortality rate in the soil because the environments are different. The root, which serves both as host and food for the nematode, is more favourable to pest survival than the soil ($\mu < \omega$).

6. When infesting nematodes feed, the ingested root biomass is used for growth and for reproduction. Reproduction occurs inside (proportion γ) or outside (proportion $1-\gamma$) the roots [53]. α is the conversion rate of ingested biomass into pests.

7. The old root pool quickly loses its freshness and degrades in the soil. The infesting pests in those roots are then free in the soil (rate δ). They also undergo natural mortality (rate μ).

Under the assumptions above, free nematodes (P), infesting nematodes (X), and infesting nematodes in the old root pool (Y) interact with the functional roots (S) during the cropping season, *i.e.* for $t \in (t_n, t_n + D]$, according to the following system:

$$\begin{cases} \dfrac{dP(t)}{dt} = \delta Y(t) - \beta P(t)S(t) + \alpha a(1-\gamma)\dfrac{S(t)X(t)}{S(t)+\Delta} - \omega P(t), \\ \dfrac{dS(t)}{dt} = \rho(t)S(t)\Big(1 - \dfrac{S(t)}{K}\Big) - a\dfrac{S(t)X(t)}{S(t)+\Delta}, \\ \dfrac{dX(t)}{dt} = \beta P(t)S(t) + \alpha a\gamma\dfrac{S(t)X(t)}{S(t)+\Delta} - \mu X(t), \\ \dfrac{dY(t)}{dt} = -(\delta + \mu)Y(t). \end{cases} \tag{4.1}$$

with the initial conditions at the beginning of the first season $P(0^+) = P_0$, $S(0^+) = S_0$, $X(0^+) = X_0$, $Y(0^+) = Y_0$; where 0^+ stands for the instant that directly follows the initial time 0.

If the senescence rate δ is very large, then the Y population is transferred into P very quickly with the old root pool disappearing. Hence, we assume that the transfer from Y to P is instantaneous and rewrite system (4.1) as follows:

$$\begin{cases} \dfrac{dP(t)}{dt} = -\beta P(t)S(t) + \alpha a(1-\gamma)\dfrac{S(t)X(t)}{S(t)+\Delta} - \omega P(t), \\ \dfrac{dS(t)}{dt} = \rho(t)S(t)\Big(1 - \dfrac{S(t)}{K}\Big) - a\dfrac{S(t)X(t)}{S(t)+\Delta}, \\ \dfrac{dX(t)}{dt} = \beta P(t)S(t) + \alpha a\gamma\dfrac{S(t)X(t)}{S(t)+\Delta} - \mu X(t). \end{cases} \tag{4.2}$$

with the initial conditions $P(0^+) = P_0 + Y_0$, $S(0^+) = S_0$, $X(0^+) = X_0$. To simplify the notation, we will assume in what follows that $Y_0 = 0$, which has no impact on the analysis as we could just change the value of the parameter P_0. By taking a larger value of parameter P_0, we compensate for what is lost when taking $Y_0 = 0$.

In this paper, the dynamics of (4.2) during the $(t_n, t_n + d]$ intervals will be called "the first subsystem of (4.2)", while "the second subsystem of (4.2)" will concern interval $(t_n + d, t_n + D]$ with $\rho = 0$.

Figure 4.1 displays a diagram representing the parasitism process within the cropping season.

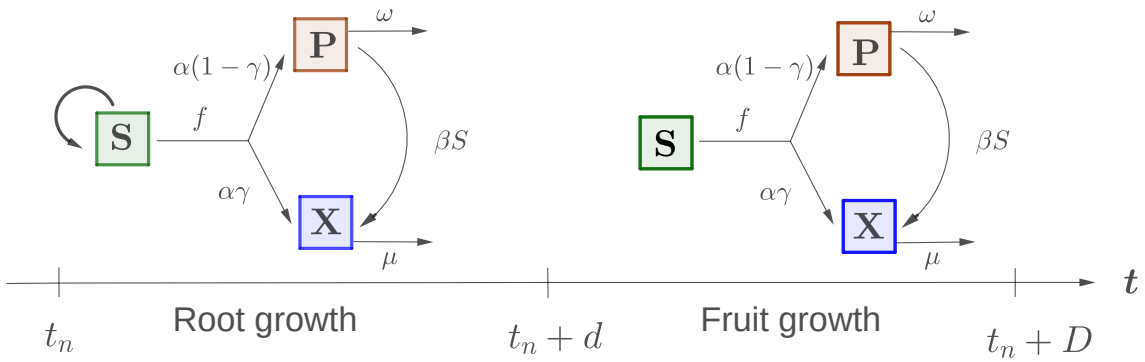

Figure 4.1 – Schematic representation of the core model (4.2). P, S, and X denote the population of free nematodes, respectively. Function f is a Holling type II functional response, and constant α is the conversion rate of the ingested fresh roots that are used to reproduce inside the root with a proportion γ and outside with a proportion $(1-\gamma)$. The constants μ and γ are natural mortalities, and constant β is a rate of infection that depends on the biomass of available fresh roots. The arrow from S to S illustrates the root growth during the root growing period.

Switching from a cropping season to the following can be done in two different ways:

i) In the first case, the banana plant has a vegetative growth and a new sucker arises from the existing roots. Chemical nematicides are used at the beginning of each cropping season to control the pest.

ii) In the second case, a pest-free vitroplant is planted. A fallow is introduced between two cropping seasons to control the pest.

The following subsections describe both cases.

4.1.2 Chemical control model

In this case, since there is no fallow, each season is immediately followed by the next season, so $t_n = nD$.

R. similis can be controlled by nematicides. These have two means of action on nematodes: contact effect and systemic effect. Contact nematicides directly kill nematodes after contact, whereas systemic nematicides are absorbed by the plant roots and distributed throughout the organs where they act against pests [85]. Some nematicides present both effects. We assume that the nematicide is used at the begining of each season and presents both systemic and contact effects.

The switching between seasons is supported by the following assumptions:

- At the end of a season, a proportion q of the total biomass of the plant roots corresponds to the sucker that will grow during the next season. Assuming an homogeneous distribution of nematodes in the roots, the sucker bears the same proportion q of infesting nematodes. The sucker becoming the new parent plant, remaining roots of the previous parent plant are transferred to the old root pool. The old root pool therefore bears the proportion $(1-q)$ of infesting pests.

  This leads to the following switching rule at the beginning of the next season:

$$\begin{cases} P(t_n^+) = P(t_n), \\ S(t_n^+) = qS(t_n), \\ X(t_n^+) = qX(t_n), \\ Y(t_n^+) = (1-q)X(t_n), \qquad n \in \mathbb{N}^*. \end{cases} \tag{4.3}$$

  As we have assumed that the infesting pests in the old root pool (Y) instantaneously turn into free pests, we can write the previous switching rule (4.3) as follows:

$$\begin{cases} P(t_n^+) = P(t_n) + (1-q)X(t_n), \\ S(t_n^+) = qS(t_n), \\ X(t_n^+) = qX(t_n). \end{cases} \tag{4.4}$$

To add the action of the nematicide, we make the following assumptions:

- We assume that the natural clearance of the nematicide is very fast, so that the action of the nematicide is instantaneous on the pest population [114, 121]. Hence, at time t_n^+, the nematicide contact action on free pests is given by:

$$P(t_n^+) = \lambda\big(P(t_n) + (1-q)X(t_n)\big), \tag{4.5}$$

  with $0 \leq \lambda \leq 1$ the nematode survival rate on the application of the nematicide.

- We assume that the systemic and contact effects are equivalent, *i.e.* that their efficiency is the same for both free pests and infecting pests, so we obtain:

$$X(t_n^+) = \lambda q X(t_n), \qquad \text{with } 0 \leq \lambda \leq 1. \tag{4.6}$$

According to all the previous assumptions, the switching rule between seasons is given by:

$$\begin{cases} P(t_n^+) = \lambda\big(P(t_n) + (1-q)X(t_n)\big), \\ S(t_n^+) = qS(t_n), \\ X(t_n^+) = \lambda q X(t_n). \end{cases} \tag{4.7}$$

Systems (4.2) and (4.7) with $t_n = nD$ form our multi-seasonal model with the use of nematicide. A schematic is shown in Figure 4.2.

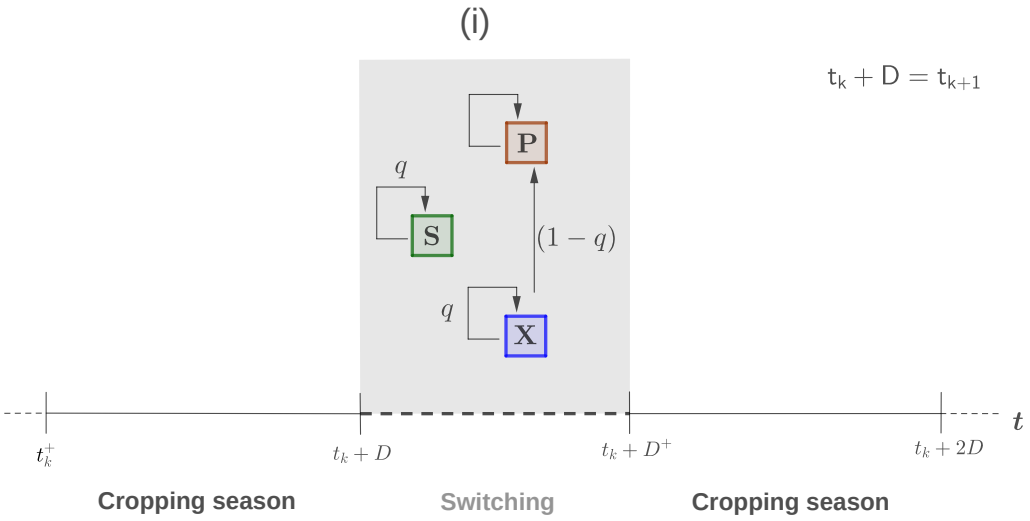

Figure 4.2 – Schematic representation of the course of the plant-pest dynamics over two cropping seasons for the model (4.2)-(4.7). On the time axis, plain lines represent the continuous course of time whereas the dotted line represents a discrete time, when switching occurs. Interactions during continuous periods are based on the core model in Figure 4.1. At the switching, the fresh root biomass (S) is initialized as a fraction q of the biomass inherited from the preceding season, the free nematode population (P) is initialized as the population of free nematodes inherited from the preceding season plus a portion $(1-q)$ of the infesting nematodes inherited from the preceding season, all with a survival rate λ to the instantaneous action of the nematicide. The infecting nematode population (X) is initialized as the fraction q of the population of infecting nematodes inherited from the preceding season, with a survival rate λ to the instantaneous action of the nematicide.

4.1.3 Fallow deployment model

In this case, banana crops are alternated with fallows or alternative non-host crops. Because of its mandatory parasitism, *R. similis* populations in the soil decline rapidly in the absence of hosts. In the following, we will term the period during which banana plants are not grown *fallow*, whether or not this is in fact due to fallowing or alternative non-hosts being deployed

We assume that all the fallow periods have the same duration designated by τ. A new season begins when both the cropping season and the fallow are completed. The season duration is hence $D + \tau$ and the starting point of the (n+1)-th season $t_n = n(D + \tau)$.

- At the beginning of each cropping season, a pest-free vitroplant is planted [16]. The initial condition $X(0^+)$ of system (4.2) becomes $X_0 = 0$. Moreover, $S(t_n^+) = S_0$ and $X(t_n^+) = 0$.

- At the end of a cropping season, *i.e.* at $t = t_n + D$, the plant is uprooted. Since uprooting is imperfect, so we assume that a fraction r of the roots remains in the soil and constitutes the old root pool, in which the nematodes Y are uniformly distributed. This leads to the following switching rule for $n \in \mathbb{N}^*$:

$$\begin{cases} P(t_{n-1} + D^+) = P(t_{n-1} + D), \\ S(t_{n-1} + D^+) = 0, \\ X(t_{n-1} + D^+) = 0, \\ Y(t_{n-1} + D^+) = rX(t_{n-1} + D). \end{cases} \tag{4.8}$$

  As we have assumed that the infesting pests (Y) in the old root pool instantaneously turn into free pests (P), we can rewrite the previous switching rule (4.8) as follows:

$$\begin{cases} P(t_{n-1} + D^+) = P(t_{n-1} + D) + rX(t_{n-1} + D), \\ S(t_{n-1} + D^+) = 0, \\ X(t_{n-1} + D^+) = 0. \end{cases} \tag{4.9}$$

- In the absence of hosts, during the fallow, free pests undergo an exponential decay [17]:

$$\frac{dP(t)}{dt} = -\omega P(t) \quad \text{for } t \in (t_{n-1} + D, t_n]. \tag{4.10}$$

Solving equation (4.10) with the initial condition given by (4.9) leads to the following transition rule:

$$\begin{cases} P(t_n^+) = \Big(P(t_{n-1} + D) + rX(t_{n-1} + D)\Big)e^{-\omega\tau}, \\ S(t_n^+) = S_0, \\ X(t_n^+) = 0, \end{cases} \tag{4.11}$$

where S_0 is the size of newly planted pest-free vitro-plant.

The system formed by equations (4.2) and (5.1) form the multi-seasonal model with fallow. This is schematically displayed in Figure 4.3.

4.1.4 Well-posedness of the problem

Considering system (4.2) with either the switching rule (4.7) or (5.1), the problem is well-posed.

Indeed, each subsystem of system (4.2) is a well-posed Cauchy problem. The first subsystem has $P = P_0$, $S = S_0$, $X = X_0$ as the initial conditions when $n = 0$ and the initial conditions are given by (4.7) or (5.1) when $n \geq 1$. The second subsystem of system (4.2) has the value of the solution of its first subsystem as the initial condition. Therefore, since S is bounded and the (P, X) dynamics are linearly bounded, system (4.2) admits a unique continuous solution on $(t_n, t_n + D]$.

The non-negativity of the trajectories is straightforward and given in the following Lemma.

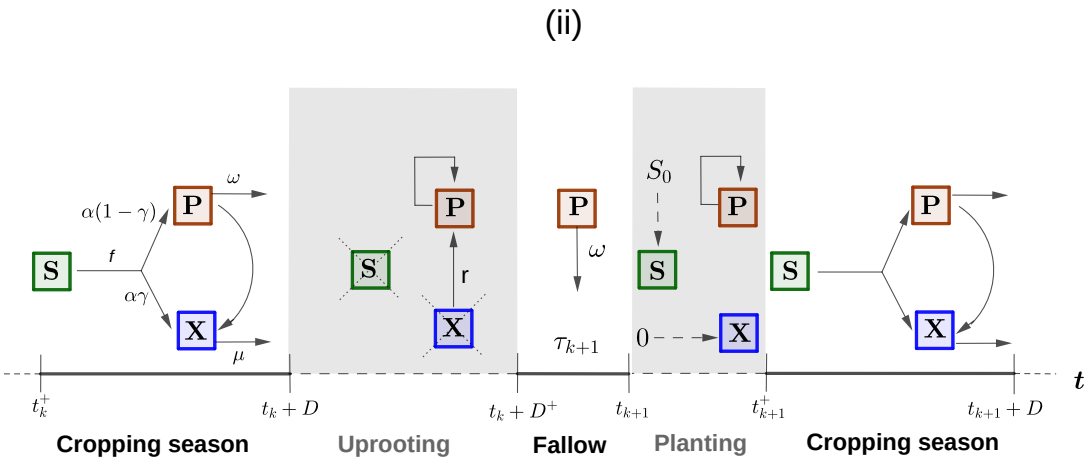

Figure 4.3 – Schematic representation of the course of the plant-pest dynamics from one cropping season to the next. On the time axis, plain lines represent the continuous course of time whereas dotted lines represents discrete instants, where discrete phenomena occur (uprooting, planting). Interactions during cropping seasons are based on the core model in Figure 4.1. When switching from a cropping season to a fallow period, infecting nematodes convert into free nematodes with a conversion faction r. Crossed-out boxes represent the uprooting, i.e. the fresh root removal. When switching from a fallow period to a cropping season, i.e. planting a new sucker, the fresh root biomass is initialized at S_0 and infesting pest at 0 whereas free pest population stays the same.

Lemma 4.1. The state variables of system (4.2) with either switching rule (4.7) or (5.1) remain non-negative.

Proof. We first consider $n = 0$ and denote by $W = (P, S, X)$ the state vector and by $W(0^+)$ the initial condition. As these state variables represent biological quantities, we set $W(0^+) \geq 0$. The structure of the model then ensures that the state variables remain non-negative in the course of time. Besides, the discrete rules (4.7) and (5.1) ensure that if the non-negative orthant is positively invariant for season n, then the initial condition for season $n + 1$ will be positive. Hence, the same conclusion holds for $n \geq 1$.

4.2 Analysis and results

The analysis of the two models in the previous section turns out to be very different from the analysis of similar models in the literature [66, 49]. This is because these models are more complex, their non-linearities are stronger and more numerous than those of the models in the literature, and the form of the growth function of the roots brings an additional hybridism to the models. We will reduce the models, at least on the intervals on which the Tychonov theorem holds, in order to obtain local stability results and some thresholds related to this stability.

4.2.1 Chemical control

In this subsection we consider the system formed by equations (4.2) and (4.7) with $t_n = nD$.

Solving the root equation in the absence of pests leads to the following solution:

$$S(t) = \begin{cases} \dfrac{S(t_n^+)K}{S(t_n^+) + (K - S(t_n^+))e^{-\rho(t-t_n)}} & \text{if } t \in (t_n, t_n + d], \\ \dfrac{S(t_n^+)K}{S(t_n^+) + (K - S(t_n^+))e^{-\rho d}} & \text{if } t \in (t_n + d, t_{n+1}] \end{cases} \tag{4.12}$$

such that:

$$S(t_{n+1}^+) = q\frac{S(t_n^+)K}{S(t_n^+) + \big(K - S(t_n^+)\big)e^{-\rho d}}. \tag{4.13}$$

If $S(t_{n+1}^+) < S(t_n^+)$ then the root biomass will decrease over time even if there is no pest. In order to avoid such unrealistic scenario, for small $S(t_n^+)$, we want $S(t_{n+1}^+) > S(t_n^+)$, that is:

$$q > e^{-\rho d} + \frac{S(t_n^+)}{K}\big(1 - e^{-\rho d}\big),$$

which is satisfied for small enough $S(t_n^+)$ when:

$$q > e^{-\rho d}. \tag{4.14}$$

Under condition (4.14), the discrete system (4.13) will be stabilized around the equilibrium S_0^* whose expression is given by:

$$S_0^* = \frac{K(q - e^{-\rho d})}{1 - e^{-\rho d}}$$

and upon which a periodic Pest Free Solution (PFS) of system (4.2,4.7) is built.

Theorem 4.1. (Global stability of the pest-free solution)

The pest-free solution of the system (4.2,4.7) is globally asymptotically stable under the condition $\alpha a < \mu$.

Proof. We can consider the growth rate of roots $\rho(t)$ as a state variable R that takes the value ρ on the $(t_n, t_n + d]$ intervals and the value 0 on the $(t_n + d, t_n + D]$ intervals. That allows us to write the system (4.2,4.7) as the autonomous 4-dimensions impulsive system (4.15 - 4.17) that follows :

$$\begin{cases} \dfrac{dP}{dt} = -\beta PS + \alpha a(1-\gamma)\dfrac{SX}{S+\Delta} - \omega P, \\ \dfrac{dS}{dt} = RS\Big(1 - \dfrac{S}{K}\Big) - a\dfrac{SX}{S+\Delta}, \\ \dfrac{dX}{dt} = \beta PS + \alpha a\gamma\dfrac{SX}{S+\Delta} - \mu, \\ \dfrac{dR}{dt} = 0, \\ \quad t \in (t_n, t_{n+1}], n \in \mathbb{N}, \text{and } P(0^+) = P_0,\ S(0^+) = S_0,\ X(0^+) = 0,\ R(0^+) = \rho. \end{cases} \tag{4.15}$$

$$\begin{cases} P(t_n + d^+) = P(t_n + d), \\ S(t_n + d^+) = S(t_n + d^+), \\ X(t_n + d^+) = X(t_n + d^+), \\ R(t_n + d^+) = 0. \end{cases} \tag{4.16}$$

$$\begin{cases} P(t_n^+) = \lambda\big(P(t_n) + (1-q)X(t_n)\big), \\ S(t_n^+) = qS(t_n), \\ X(t_n^+) = \lambda q X(t_n), \\ R(t_n^+) = \rho. \end{cases} \tag{4.17}$$

Let us introduce the function $V(t) = P(t) + X(t)$

- When $t \neq t_n$ and $t_n \neq t_n + d$,

$$\begin{aligned} D^+V(t) &= \alpha a \frac{SX}{S+\Delta} - \mu X - \omega P \\ &\leq (\alpha a - \mu)X - \omega P, \end{aligned}$$

because, S being positive according to Lemma 4.1, we have $\frac{S}{S+\Delta} \leq 1$. Hence, $D^+V < 0$, since $\alpha a < \mu$. We can thus write :

$$D^+V(t) = -\zeta, \quad \zeta > 0. \tag{4.18}$$

- When $t = t_n + d$,

$$\begin{aligned} V(t_n + d^+) &= P(t_n + d^+) + X(t_n + d^+) \\ &= P(t_n + d) + X(t_n + d) \\ &= V(t_n + d). \end{aligned} \tag{4.19}$$

- When $t = t_{n+1}$,

$$\begin{aligned} V(t_{n+1}^+) &= P(t_n^+) + X(t_n^+) \\ &= \lambda\big(P(t_n) + X(t_n)\big) \\ &= \lambda V(t_{n+1}) \\ &\leq V(t_{n+1}). \end{aligned} \tag{4.20}$$

Equations (4.18), (4.19), (4.20) lead for all $n \in N$, for all $t \in (t_n, t_{n+1}]$, $V(t) \leq -\zeta t + P_0$, from which $V(t) \to 0$ when $t \to \infty$, since $V(t)$ is positive according to Lemma 4.1.

Therefore, $P(t)$ and $X(t)$ tend to 0 when $t \to \infty$. □

Remark 4.1. This proof is same as the comparison principle (see 1.1.2) applied to the pest-free solution.

Remark 4.2. The condition $\alpha a < \mu$ means that nematodes breed on average less than they die.

Generally, in the presence of host plants, *Radopholus similis* population in the soil is very low [110, 31, 95, 79]. In this modelling, this can be interpreted as a high infestation rate, leading to the fast convergence of the free pest level to zero.

The following proposition allows us to reduce the order of the first subsystem of (4.2) by assuming that the infestation rate β is large and by using singular perturbation theory for the slow-fast dynamics [145].

Proposition 4.1. Assuming that the primary infestation β is large and considering the state variable $N = P + X$, the first subsystem of (4.2) can be approximated by the following Rosenzweig-MacArthur model [104] on the $(t_n, t_n + d]$ intervals:

$$\begin{cases} \dfrac{dS}{dt} = \rho S\Big(1 - \dfrac{S}{K}\Big) - a\dfrac{SN}{S+\Delta}, \\ \dfrac{dN}{dt} = \alpha a \dfrac{SN}{S+\Delta} - \mu N, \end{cases} \tag{4.21}$$

with initial conditions $S(0^+) = S_0$, $N(0^+) = P_0 + X_0$, $S(t_n^+) = S_0$ and $N(t_n^+) = P(t_n^+) + X(t_n^+)$.

Proof. Let's consider the first subsystem of equation (4.1), i.e. $t \in (t_n, t_n + d[$. Let $N = P + X$ and consider the system in (P, S, N).

Assuming that β is large, let $\beta = \frac{\beta'}{\varepsilon}$, $0 < \varepsilon \ll 1$ and $\zeta = \frac{t}{\varepsilon}$. The new time ζ is called *fast time*. The system with derivatives according to ζ is written:

$$\begin{cases} \dfrac{dP}{d\zeta} = -\beta' PS + \varepsilon\alpha a(1-\gamma)\dfrac{S(N-P)}{S+\Delta} - \varepsilon\omega P, \\ \dfrac{dS}{d\zeta} = \varepsilon\rho S\Big(1 - \dfrac{S}{K}\Big) - \varepsilon a\dfrac{S(N-P)}{S+\Delta}, \\ \dfrac{dN}{d\zeta} = \varepsilon\alpha a\gamma\dfrac{S(N-P)}{S+\Delta} + \varepsilon(\mu-\omega)P - \varepsilon\mu N, \end{cases} \tag{4.22}$$

When $\varepsilon = 0$, we then define the *fast equation* by

$$\frac{dP}{d\zeta} = -\beta' PS$$

Which admits an equilibrium $\bar{P} = 0$ that is asymptotically stable because $S > 0$ according to Lemma 4.1.

The *slow equation* is written as:

$$\begin{cases} \dot{S} = \rho S\Big(1 - \dfrac{S}{K}\Big) - a\dfrac{SN}{S+\Delta}, \\ \dot{N} = \alpha a\gamma\dfrac{SN}{S+\Delta} - \mu N, \end{cases} \tag{4.23}$$

Which corresponds to a Rosenzweig-MacArthur model. The Tychonov theorem ensures that

$$\lim_{\varepsilon\to 0} P(t,\varepsilon) = 0, \quad t \in (t_n, t_n + d[$$

$$\lim_{\varepsilon\to 0}(S(t,\varepsilon), N(t,\varepsilon)) = (\bar{S}(t), \bar{N}(t)), \quad t \in (t_n, t_n + d[$$

Where $(\bar{S}, \bar{N})$ is the solution of equation (4.23) and $(P(t,\varepsilon), S(t,\varepsilon), N(t,\varepsilon))$ is the solution of the perturbed system:

$$\begin{cases} \varepsilon\dot{P} = -\beta' PS + \varepsilon\alpha a(1-\gamma)\dfrac{S(N-P)}{S+\Delta} - \varepsilon\omega P, \\ \dot{S} = \rho S\Big(1 - \dfrac{S}{K}\Big) - a\dfrac{S(N-P)}{S+\Delta}, \\ \dot{N} = \alpha a\dfrac{S(N-P)}{S+\Delta} + (\mu-\omega)P - \mu N. \end{cases}$$

□

Remark 4.3. According to this proposition, the number of free pests is null in the reduced first subsystem. This is a good approximation when β has a high value. Thus, we are going to consider that the second second subsystem of (4.2) starts with a free pest population $P = P(t_n + d) = 0$ and an infesting pest population $X = N(t_n + d)$.

Figure 4.4 illustrates the dynamics of the reduced system (4.21) over the root growing period, and how it initializes the full model on the fruits growing period.

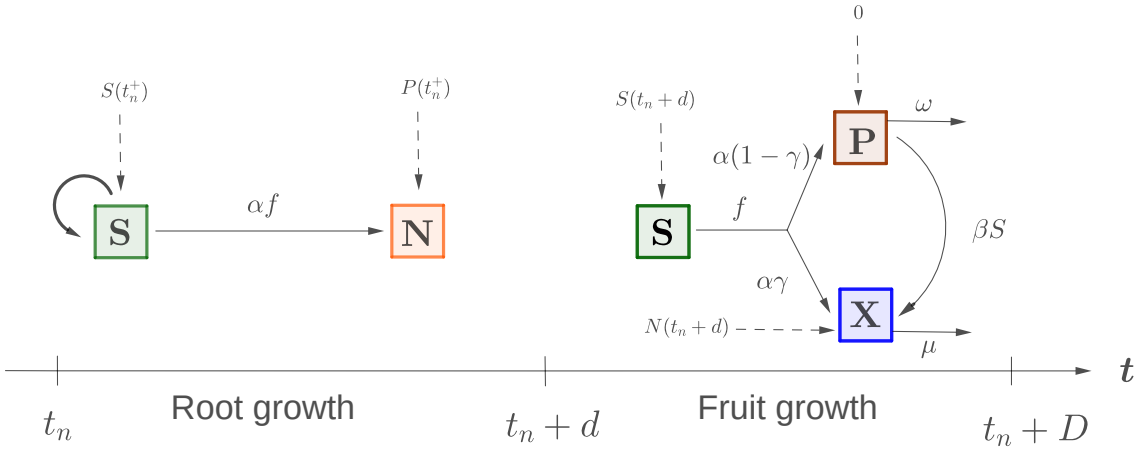

Figure 4.4 – Schematic representation of the reduced model, with first subsystem of model (4.2) reduced into model (4.21). During the root growing period, the system is reduced to a Rosenzweig-MacArthur model where the population of free nematodes is null, and the state variable N represents the sum of nematodes populations that stands for the population of infesting nematodes.At the flowering $t_n + d$, the nematode population from the end of the root growing period becomes the pest population at the start of fruit growing period, whereas the population of free nematodes is initialized as zero. The circled arrow represents the growth of fresh roots (S) that is effective before the flowering and null after, during the fruit growing period.

We can obtain the analytical solution of the reduced system (4.21) linearised around the pest free solution thanks to the following proposition.

Proposition 4.2. For $q > e^{-\rho d}$, the periodic pest free solution of system (4.2,4.7) is:

$$S^*(t) = \begin{cases} \dfrac{S_0^* K}{S_0^* + (K - S_0^*)e^{-\rho(t-t_n)}} & \text{if } t \in (t_n, t_n + d], \\ \dfrac{S_0^* K}{S_0^* + (K - S_0^*)e^{-\rho d}} & \text{if } t \in (t_n + d, t_{n+1}]. \end{cases} \tag{4.24}$$

Moreover, the following results hold:

- For all $n \in \mathbb{N}$, the solution of equations (4.21) linearised around the pest-free solution for $t \in (t_n, t_n + d]$ is given by:

$$N(t) = \left(P(t_n^+) + X(t_n^+)\right) \exp\left(-\mu(t \bmod D) + \int_{t_n}^{t} \frac{\alpha a S^*(\tau)}{S^*(\tau) + \Delta} d\tau\right), \tag{4.25}$$

$$\begin{aligned} S(t) = S^*(t) + \left[\int_{t_n}^{t} -F(\xi) \exp\left(-\int_{t_n}^{\xi} \rho\left(1 - \frac{2S^*(\tau)}{K}\right) d\tau\right) d\xi + \tilde{S}(t_n^+)\right] \\ \times \exp\left(\int_{t_n}^{t} \rho\left(1 - \frac{2S^*(\tau)}{K}\right) d\tau\right), \end{aligned} \tag{4.26}$$

where $F(t) := \frac{aS^*(t)}{S^*(t)+\Delta}\tilde{N}(t)$ and $\tilde{S}(t_n^+) = S(t_n^+) - S_0^*$.

- For all $n \in \mathbb{N}$ and $t \in (t_n + d, t_n + D]$, there exists a matrix $\Pi(t)$, detailed in the proof, such that:

$$\begin{pmatrix} P(t) \\ X(t) \end{pmatrix} = \Pi(t \pmod D - d). \begin{pmatrix} 0 \\ N(t_n + d) \end{pmatrix}$$

and

$$S(t) = S^*(t) - a\frac{S(t_n + d)}{S(t_n + d) + \Delta} \int_{t_n+d}^{t} X(\tau)d\tau + \big[S(t_n + d) - S^*(t_n + d)\big],$$

where $S(t_n + d)$ is obtained from (4.26).

Proof. • First, in absence of pest, the periodic solution occurs and we have $S(t_n^+) = S_0^*$. The Pest Free Solution is written for all $t \in [0, d]$, $\begin{pmatrix} S^*(t) \\ N^*(t) \end{pmatrix} = \begin{pmatrix} \frac{S_0^* K}{S_0^* + (K - S_0^*)e^{-\rho t}} \\ 0 \end{pmatrix}$,

with $S_0^* = \frac{K(q - e^{-\rho d})}{1 - e^{-\rho d}}$.

Considering the deviation variables $\tilde{S} = S(t) - S^*(t)$ and $\tilde{N} = N(t) - N^*(t) = N(t)$, one can write the deviation system as:

$$\begin{cases} \dot{\tilde{S}} = \rho(\tilde{S} + S^*(t))\Big(1 - \dfrac{\tilde{S} + S^*(t)}{K}\Big) - \dfrac{a(\tilde{S} + S^*(t))\tilde{N}}{\tilde{S} + S^* + \Delta} - \rho S^*(t)\Big(1 - \dfrac{S^*(t)}{K}\Big), \\ \dot{\tilde{N}} = \dfrac{\alpha a(\tilde{S} + S^*(t))\tilde{N}}{\tilde{S} + S^* + \Delta} - \mu\tilde{N}, \\ \tilde{S}(0^+) = q\tilde{S}_0,\ \tilde{N}(0^+) = N(0^+) = P_0 + X_0. \end{cases} \tag{4.27}$$

In a neighbourhood of the PFS, the system is equivalent to

$$\begin{pmatrix} \dot{\tilde{S}} \\ \dot{\tilde{N}} \end{pmatrix} = \begin{pmatrix} \rho\Big(1 - \dfrac{2S^*(t)}{K}\Big) & -\dfrac{aS^*(t)}{S^*(t) + \Delta} \\ 0 & -\mu + \dfrac{\alpha a S^*(t)}{S^*(t) + \Delta} \end{pmatrix} . \begin{pmatrix} \tilde{S} \\ \tilde{N} \end{pmatrix} \tag{4.28}$$

This leads to the equation in $\tilde{N}$

$$\dot{\tilde{N}} = \Big(-\mu + \frac{\alpha a S^*(t)}{S^*(t) + \Delta}\Big)\tilde{N},$$

whose solution is given by

$$\tilde{N}(t) = \big(P(0^+) + X(0^+)\big)e^{-\mu t + \displaystyle\int_0^t \frac{\alpha a S^*(\tau)}{S^*(\tau) + \Delta} d\tau}.$$

One can now replace this expression in (4.28) and let $F(t) := \frac{aS^*(t)}{S^*(t)+\Delta}\tilde{N}(t)$ to obtain the equation in $\tilde{S}$:

$$\dot{\tilde{S}} = \rho\Big(1 - \frac{2S^*(t)}{K}\Big)\tilde{S}(t) - F(t), \qquad \tilde{S}^+(0) = q\tilde{S}(0).$$

This leads to the solution

$$\tilde{S}(t) = \Big[\int_0^t -F(\xi) \exp\Big(-\int_0^\xi \rho\big(1 - \frac{2S^*(\tau)}{K}\big)d\tau\Big)d\xi + q\tilde{S}(0)\Big] \times \exp\big(\int_0^t \rho\Big(1 - \frac{2S^*(\tau)}{K}\Big)d\tau\big)$$

- On $(t_n + d, t_n + D]$, the second subsystem of equation (4.2) is written:

$$\begin{cases} \dot{P}(t) = -\beta P(t)S(t) + \alpha a(1-\gamma)\dfrac{S(t)X(t)}{S(t)+\Delta} - \omega P(t), \\ \dot{S}(t) = -a\dfrac{S(t)X(t)}{S(t)+\Delta}, \\ \dot{X}(t) = \beta P(t)S(t) + \alpha a\gamma\dfrac{S(t)X(t)}{S(t)+\Delta} - \mu X(t). \end{cases} \tag{4.29}$$

With initial conditions $P(t_n + d^+) = 0$, $X(t_n + d^+) = N(t_n + d)$ and $S(t_n + d^+) = S(t_n + d)$ from the system (4.21).

The pest free equilibrium (PFE) can be written $Y_P(t) = \begin{pmatrix} P_p(t) \\ S_p(t) \\ X_p(t) \end{pmatrix} = \begin{pmatrix} 0 \\ S^*(d) \\ 0 \end{pmatrix}$. Considering the deviation variables $\tilde{P}(t) = P(t) - P_p(t) = P(t), \tilde{S}(t) = S(t) - S_p(t), \tilde{X}(t) = X(t) - X_p(t) = X(t)$, one can write the equation in the new variables as:

$$\begin{cases} \dot{\tilde{P}} = -\beta\tilde{P}(\tilde{S} + S^*(d)) + \alpha a(1-\gamma)\dfrac{(\tilde{S} + S^*(d))\tilde{X}}{\tilde{S} + S^*(d) + \Delta} - \omega\tilde{P}, \\ \dot{\tilde{S}} = -a\dfrac{(\tilde{S} + S^*(d))\tilde{X}}{\tilde{S} + S^*(d) + \Delta}, \\ \dot{\tilde{X}} = \beta\tilde{P}(\tilde{S} + S^*(d)) + \alpha a\gamma\dfrac{(\tilde{S} + S^*(d))\tilde{X}}{\tilde{S} + S^*(d) + \Delta} - \mu\tilde{X} \end{cases} \tag{4.30}$$

And the Jacobian matrix $J = \begin{bmatrix} -\beta S^*(d) - \omega & 0 & \alpha a(1-\gamma)\frac{S^*(d)}{S^*(d)+\Delta} \\ 0 & 0 & -a\frac{S^*(d)}{S^*(d)+\Delta} \\ \beta S^*(d) & 0 & -\mu + \alpha a\gamma\frac{S^*(d)}{S^*(d)+\Delta} \end{bmatrix}$.

In the neighbourhood of the PFE, system (4.30) is then equivalent to the linearised system

$$\dot{\tilde{Y}} = J.\tilde{Y}, \quad \tilde{Y} = (\tilde{P}, \tilde{S}, \tilde{X}). \tag{4.31}$$

Since the second column of J is null, one just has to compute the exponential of At that will generate a local solution for $\tilde{P}$ and $\tilde{X}$, where $A := \begin{bmatrix} -\beta S^*(d) - \omega & \alpha a(1-\gamma)\frac{S^*(d)}{S^*(d)+\Delta} \\ \beta S^*(d) & -\mu + \alpha a\gamma\frac{S^*(d)}{S^*(d)+\Delta} \end{bmatrix}$.

We deduce $\tilde{S}$ from $\dot{\tilde{S}} = -a\frac{S^*(d)}{S^*(d)+\Delta}\tilde{X}$, i.e.

$$\tilde{S}(t) = -a\frac{S^*(d)}{S^*(d)+\Delta}\int_0^d \tilde{X}(\tau)d\tau + \tilde{S}(d).$$

And so one for each season, assuming the trajectories remain close enough to the PFS. Since A is a Metzler matrix, it admits two distinct real eigenvalues $\lambda_{1,2} = \frac{tr(A)}{2} \pm \frac{1}{2}\sqrt{tr^2(A) - 4det(A)}$ and we

have $\Pi(t) = \begin{pmatrix} \Pi_{1,1}(t) & \Pi_{1,2}(t) \\ \Pi_{2,1}(t) & \Pi_{2,2}(t) \end{pmatrix}$, where

$$\Pi_{1,1}(t) = \frac{1}{\lambda_2 - \lambda_1}\Big(e^{\lambda_1 t}(\lambda_2 + \beta S^*(d) + \omega) - e^{\lambda_2 t}(\lambda_1 + \beta S^*(d) + \omega)\Big)$$
$$\Pi_{1,2}(t) = -\frac{1}{\lambda_2 - \lambda_1}\Big(\frac{\alpha a(1-\gamma)}{S^*(d) + \Delta}(e^{\lambda_1 t} - e^{\lambda_2 t})\Big)$$
$$\Pi_{2,1}(t) = -\frac{1}{\lambda_2 - \lambda_1}\Big(\beta S^*(d)(e^{\lambda_1 t} - e^{\lambda_2 t})\Big)$$
$$\Pi_{2,2}(t) = \frac{1}{\lambda_2 - \lambda_1}\Big(e^{\lambda_1 t}\big(\lambda_2 + \mu - \frac{\alpha a S^*(d)}{S^*(d) + \Delta}\big) - e^{\lambda_2 t}\big(\lambda_1 + \mu - \frac{\alpha a S^*(d)}{S^*(d) + \Delta}\big)\Big)$$

□

We can finally use Proposition 4.2 to study the discrete dynamics of the total pest population $N(t_n^+)$ in the neighbourhood of the pest free solution. This leads to the computation of the seasonal effective reproduction number $\mathcal{R}$, which corresponds to the quantity of free pest at the beginning of a season produced by a single free pest at the beginning of the previous season, in a pest-free context under control measures [66, 131] . If this number is larger than 1, pests tend to persist over time. If it is smaller, pests tend to decline. These results are given in the following proposition.

Proposition 4.3. Pest persistence and effective reproduction number $\mathcal{R}$

1. For all $n \in \mathbb{N}$, the discrete pest dynamics in the neighbourhood of the pest free solution are defined by:

$$N(t_n^+) = (\lambda\theta)^n N_0, \tag{4.32}$$

where:

$$\theta = \big(\Pi_{1,2}(D-d) + \Pi_{2,2}(D-d)\big)e^{-\mu d + \int_0^d \frac{\alpha a S^*(\tau)}{S^*(\tau) + \Delta} d\tau},$$

$N_0 = P_0 + X_0$, S^* is given by equation 4.24, and the $\Pi_{i,j}$ are the inputs of the matrix Π defined in the proof.

2. The effective reproduction number is given by:

$$\mathcal{R} = \lambda\theta. \tag{4.33}$$

3. The pest free solution is locally asymptotically stable for nematode survival rate to pesticide load $\lambda < \lambda_0$, with:

$$\lambda_0 = \frac{1}{\theta} \tag{4.34}$$

Proof. 1. From Proposition 4.2, when the pests remain in a neighbourhood of the PFS,

$$\begin{pmatrix} P(t) \\ X(t) \end{pmatrix} = \Pi\big(t - (t_n + d)\big).\begin{pmatrix} 0 \\ N(t_n + d) \end{pmatrix}$$

Hence,

$$\begin{aligned} N(t_{n+1}) &= P(t_{n+1}) + X(t_{n+1}) \\ &= \big(\Pi_{1,2}(D-d) + \Pi_{2,2}(D-d)\big)N(t_n+d) \\ &= \big(\Pi_{1,2}(D-d) + \Pi_{2,2}(D-d)\big)N(t_n^+)e^{-\mu d + \int_0^d \frac{\alpha a S^*(\tau)}{S^*(\tau)+\Delta} d\tau} \\ &\quad (from\ \ equation(4.25)) \\ &= \theta N(t_n^+). \end{aligned}$$

Thus, $N(t_{n+1}^+) = \lambda\theta N(t_n^+)$

Therefore, $\forall n \in \mathbb{N}$,

$$\begin{aligned} N(t_n^+) &= (\lambda\theta)^n N(0^+) \\ &= (\lambda\theta)^n (P_0 + X_0). \end{aligned}$$

2. Since for $(P_0 + X_0) \neq 0$, $N(t_n^+) \longrightarrow 0$ iff $(\lambda\theta) < 1$, we deduce $\mathcal{R} = \lambda\theta$.

□

Proposition 4.3 shows that the effective reproduction number depends on the nematode survival rate to pesticide load λ. Thereby, if this number is greater than the threshold λ_0, the effective reproduction number will be greater than 1 and the population or *R. similis* will persist over time; otherwise this population undergoes a decline. We are going to illustrate this numerically.

Numerical simulations

In these simulations, we first show how well the reduced system (4.21) approximates the first subsystem of equation (4.2). Then, we illustrate the pest behaviour in the reduced model, in terms of persistence or decline, according to the values taken by λ and $\mathcal{R}$ on both sides of their critical values.

Most parameters were set to realistic values obtained from experimental studies in the literature and are given in Table 4.1. However, some parameters cannot be easily measured and were estimated indirectly:

- The consumption rate a of *Radopholus similis* is evaluated from the size, and therefore the mass, of a single pest [143]. Given the value of this consumption rate, the consumption efficiency α and the half-saturation constant Δ are evaluated in order to keep an appropriate range of pest population over the time.
- The growth rate of roots ρ is chosen such that, when there is no pest, the roots almost reach their maximum biomass at the end of their growing period.

Generally, infestation is about $[400, 51400]$ nematodes per 100 g of roots [154]. However in this work, in order to compare the two strategies exposed, we consider that both studies begin with a pest-free sucker $X_0 = 0$ and a rather large value of nematodes in the soil $P_0 = 100$.

In Figure 4.5, we first compare, over a single cropping season, the full model described by equation (4.2) and the reduced model defined by equation (4.21) combined to the second subsystem of (4.2), according to several values of parameter β ranging from 0.001 to 1. As expected, the reduced system approximates the full model better when β gets larger. $\beta = 0.1$ leads to a very good approximation.

We hence set $\beta = 0.1$ for the remaining simulations. With this parameter value and the other parameter values given in Table 4.1, the critical threshold for the nematode survival rate to pesticide load is $\lambda_0 = 0.01$. Figure 4.6 illustrates the pest dynamics when the λ survival rate λ varies:

Param.	Description	Literature values	Value (s)
d	Duration of the roots growth	210-240 days (Berangan), 180-210 days (Cavendish) [2]	210 days
D	Duration of the cropping season	$300 - 360$ days [2]	330 days
β	Infestation rate	\	$1,\ 10^{-1},\ 10^{-2},\ 10^{-3}$
K	Maximum roots biomass	$\geq$ 143 g [115]	150 g
ρ	Roots growth rate	\	0.025 day^{-1} (1)
ω	Mortality rate of free pests	0.0495 day^{-1} [13]	0.0495 day^{-1}
μ	Mortality rate of infested pests	$0.05 - 0.04$ day^{-1} [112]	0.045
a	Consumption rate	magnitude 10^{-4} g (2) [143]	2.10^{-4} g.day^{-1}
α	Conversion rate of ingested roots	\	400 g^{-1} (3)
Δ	Half-saturation constant	\	60 g (3)
γ	Proportion of pests laid inside	\	0.5
q	Proportion of roots forming the new sucker	\	$1/3$ (4)
r	Proportion of roots forming the old pool after uprooting	\	5% (5)
S_0	Initial root biomass	60 g [115]	60 g (6)
P_0	Initial soil infestation	small [31, 79, 95, 110]	100
X_0	Initial roots infestation	0 [16]	0

(1) ρ is estimated such that $S(d) \simeq K$.

(2) The magnitude of a is evaluated from the size of *R. similis*.

(3) α and Δ are estimated to maintain a sensible population size.

(4) The proportion q of the maximum biomass is close to the pest survival critical level;

(5) We assume that the uprooting is carefully done.

(6) The initial root biomass corresponds to the sucker survival critical level.

\ No data available in the literature.

Table 4.1 – Parameter values used in model simulations

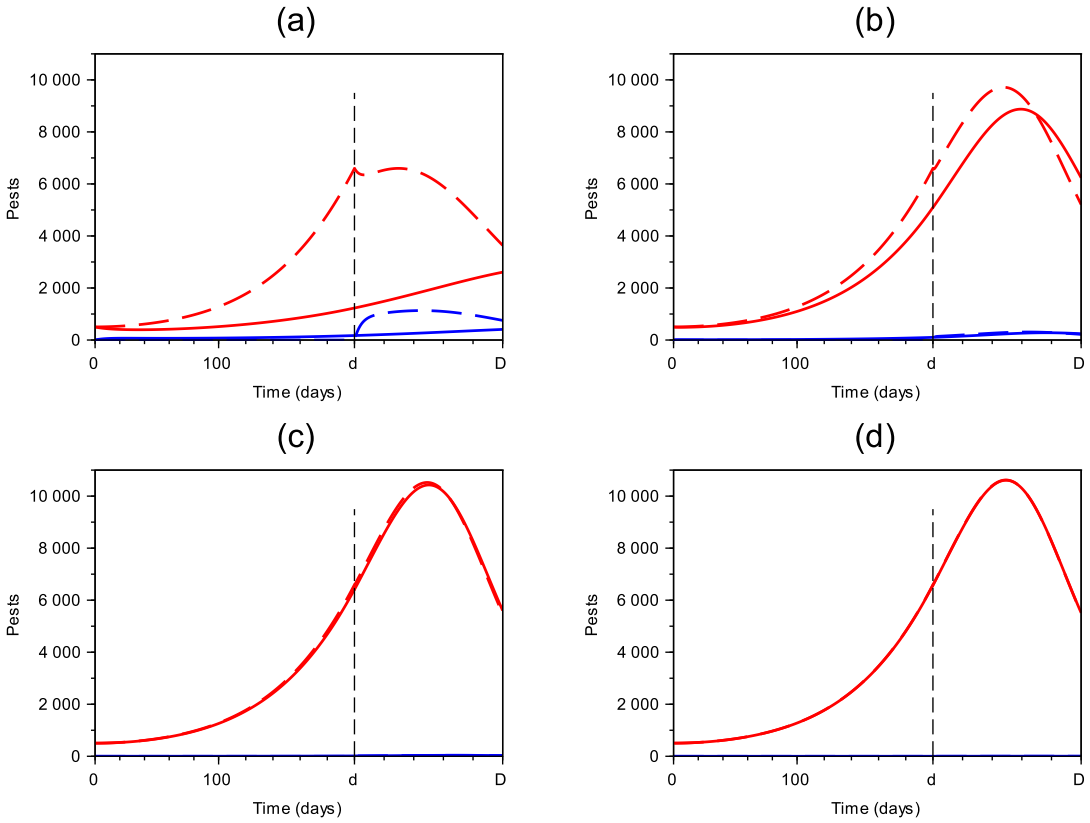

(a) $\beta = 0.001$; **(b)** $\beta = 0.01$; **(c)** $\beta = 0.1$; **(d)** $\beta = 1$.

Figure 4.5 – Pest population evolution over a single cropping season for different values of the infestation rate β. The infesting pests (red lines) and the free pests (blue lines) are represented for the full model (4.2) (plain lines) and the reduced model (4.21) (dashed lines). Paramater values are given in Table 4.1.

(a) A small value of the effective reproduction number $\mathcal{R} = 0.1$ is obtained when $\lambda = 0.001 \ll \lambda_0$. It leads to a very fast decline of the pests since $\mathcal{R} \ll 1$.

(b) A value $\mathcal{R} = 0.9$ close to but less than 1 is obtained when $\lambda = 0.009 < \lambda_0$. It leads to a slower decline of the pests.

(c) A value $\mathcal{R} = 1.1$, obtained when $\lambda = 0.011 > \lambda_0$, induces pest persistence. Nematodes first steadily decrease and then persist with small oscillations. No nematode eradication is achieved.

(d) When the nematicide is not applied $\lambda = 1 \gg \lambda_0$. The effective reproduction number takes its larger possible value $\mathcal{R} = \mathcal{R}_0 = 97.7 \gg 1$. This value of $\mathcal{R}$ is realistic in this multi-seasonal formalism, as it measures the average number of pests that a single pest, introduced at the beginning of a season in a pest-free context, produces for the following season. Indeed, a nematode of the species *R. similis* has a life cycle of 21 days and a single female produces about 18 larvae (hatched eggs) during its life cycle [61]. Throughout a cropping season that lasts until 330 days, several generations of descendants follow each other, and surviving descendants produce each about 18 larvae. Without control, a single original pest can therefore produce a huge number of pests. The saturation of resources (roots) is the reason

why exponentially high numbers are not reached. The pests persist with large oscillations and a doubled periodicity that we analyse in Figure 4.7. A periodicity over two periods arises. A first season starts with a large root biomass (t_5), which allows an explosion of pests that ravage the root in the second half of the season. A second season (t_6) therefore starts with a much lower root biomass, which prevents the quick development of nematodes during the first part of the season and therefore gives a large root in the second half of the season; which in turn will favour the explosion of nematodes. And so on.

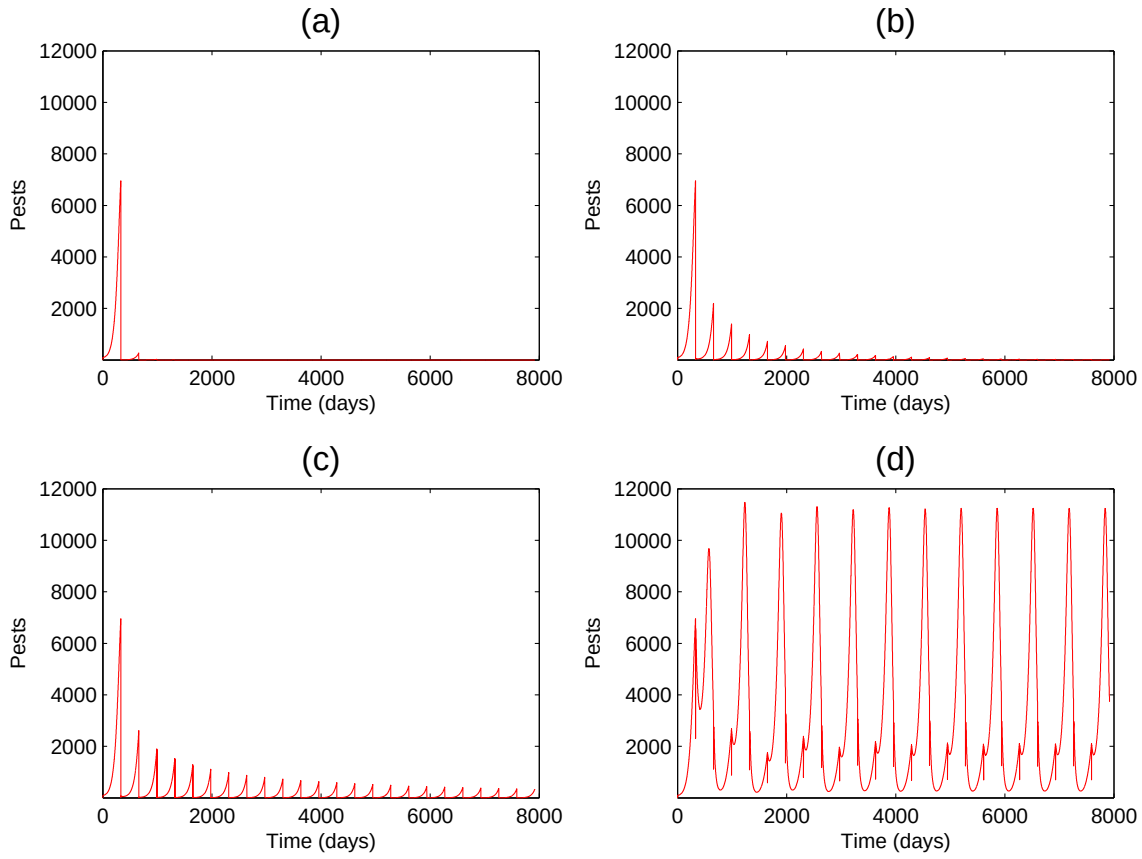

(a) $\lambda = 0.001$ and $\mathcal{R} = 0.1$; **(b)** $\lambda = 0.009$ and $\mathcal{R} = 0.9$; **(c)** $\lambda = 0.011$ and $\mathcal{R} = 1.1$; **(d)** $\lambda = 1$ and $\mathcal{R} = 97.7$.

Figure 4.6 – Infesting pest dynamics of model (4.2) - (4.7) over several cropping seasons for different values of λ. The infestation rate is $\beta = 0.1$, so that the reduced model approximates the full model well. Remaining parameter values are given in Table 4.1, leading to the threshold value $\lambda_0 = 0.010$ defined in equation (4.34).

These simulations show that the nematicide needs to destroy more than 99% of the pests at the beginning of each season to lead to their disappearance over time. Besides the fact that nematicides are harmful for the environment, studies show that most nematicides cannot reach such an efficacy. While a very efficient nematicide like tannic acid can have an efficient mortality rate that goes up to 94% in a "kind" soil like fine sand [51], Fenamiphos can only reach a mortality of 77% in *in vitro* tests, and high dosages of the biological nematicide "ABG-9008" barely reach a mortality of 70% [69]. It therefore appears that, in case of a single application per season, nematicides can only provide a partial remedy in terms of nematode control but cannot result in complete pest eradication. In case of multiple applications, plant growth is strongly impacted. Indeed,

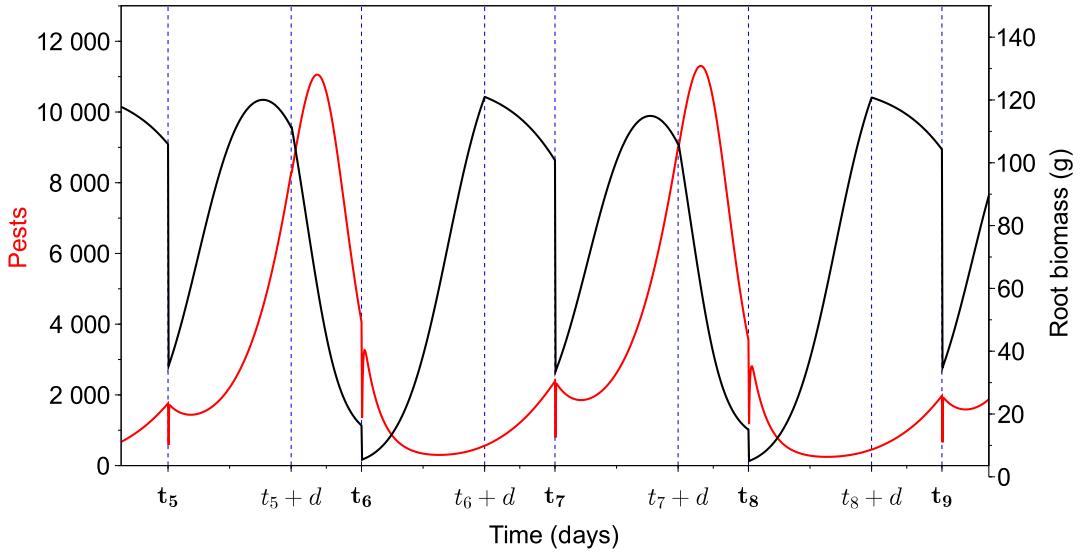

Figure 4.7 – Pest-root dynamics over four seasons without chemical control ($\lambda = 1$) of model (4.2) - (4.7). At the beginning t_i of each season, root biomass grows until either the growth stops (at $t_i + d$) or the pest populations are so high that they overeat the roots. The jumps in the root dynamics at t_i are due to the switch (4.7), where a portion of the root pool of the parent plant turns into a pool of old roots that die quickly by senescence. The remaining portion represents the root pool of the sucker from which the new plant grows. The jumps in the pest dynamics are also due to the switch (4.7), with in particular a proportion of the infesting pests which become free pests because of the senescence of the part of the roots they are in. The level of infesting pests goes up very quickly because the free pests return quickly in the fresh roots, since β is high.

pesticides reduce the symbiotic efficiency of nitrogen-fixing bacteria and host plants [37] and plants use fixed nitrogen (ammonia) to synthesize proteins. It is therefore necessary to study a more environment-friendly and possibly more efficient mean of control.

In the next section, we replace the pesticide by crop rotation with non-host plants or fallows.

4.2.2 Sufficient fallow deployment

In this subsection we study the system formed by equations (4.2) and (5.1). We remind that t_n, the starting point of the $(n+1)$-th season, here has the value $t_n = n(D+\tau)$; where τ stands for the duration of the fallow. Since the new-planted suckers are assumed to be pest-free, it seems coherent that here $X(0^+) = 0$.

Through this section, we are going to present significant results that will bring us to the computation of a threshold duration τ_0 of the fallow. The tropical character of the banana cultures gives us an important freedom for this fallow duration as synchronization with seasonality is not required.

The system (4.2,5.1) admits the following periodic pest free solution:

$$\bar{S}(t) = \begin{cases} \dfrac{S_0 K}{S_0 + (K - S_0)e^{-\rho(t-t_n)}} & \text{if } t \in (t_n, t_n + d] \\ \dfrac{S_0 K}{S_0 + (K - S_0)e^{-\rho d}} & \text{if } t \in (t_n + d, t_n + D] \\ 0 & \text{if } t \in (t_n + D, t_{n+1}] \end{cases} \tag{4.35}$$

As same as in Subsection 4.2.1, there is a sufficient condition of global stability of the pest-free solution.

Theorem 4.2. (Global stability of the pest-free solution)

The pest-free solution of the system (4.2,5.1) is globally asymptotically stable under the condition $\alpha a < \mu$.

Proof. As in the proof of Theorem 4.1 we can consider the growth rate of roots $\rho(t)$ as a state variable R. We write the system (4.2,5.1) as the autonomous 4-dimensions impulsive system (4.36 - 4.38) that follows :

$$\begin{cases} \dfrac{dP}{dt} = -\beta PS + \alpha a(1-\gamma)\dfrac{SX}{S+\Delta} - \omega P, \\ \dfrac{dS}{dt} = RS\Big(1 - \dfrac{S}{K}\Big) - a\dfrac{SX}{S+\Delta}, \\ \dfrac{dX}{dt} = \beta PS + \alpha a\gamma\dfrac{SX}{S+\Delta} - \mu, \\ \dfrac{dR}{dt} = 0, \\ \quad t \in (t_n, t_n + D], n \in \mathbb{N}, \text{and } P(0^+) = P_0,\ S(0^+) = S_0,\ X(0^+) = 0,\ R(0^+) = \rho. \end{cases} \tag{4.36}$$

$$\begin{cases} P(t_n + d^+) = P(t_n + d), \\ S(t_n + d^+) = S(t_n + d^+), \\ X(t_n + d^+) = X(t_n + d^+), \\ R(t_n + d^+) = 0. \end{cases} \tag{4.37}$$

$$\begin{cases} P(t_n^+) = \big(P(t_n + D) + rX(t_n + D)\big), \\ S(t_n^+) = S_0, \\ X(t_n^+) = 0, \\ R(t_n^+) = \rho. \end{cases} \tag{4.38}$$

Let us introduce the function $V(t) = P(t) + X(t)$

- When $t \neq t_n$ and $t_n \neq t_n + d$,

$$\begin{aligned} D^+V(t) &= \alpha a\frac{SX}{S+\Delta} - \mu X - \omega P \\ &\leq (\alpha a - \mu)X - \omega P, \end{aligned}$$

because, S being positive according to Lemma 4.1, we have $\frac{S}{S+\Delta} \leq 1$. Hence, $D^+V < 0$, since $\alpha a < \mu$. We can thus write :

$$D^+V(t) = -\zeta, \quad \zeta > 0. \tag{4.39}$$

- When $t = t_n + d$,

$$\begin{aligned} V(t_n + d^+) &= P(t_n + d^+) + X(t_n + d^+) \\ &= P(t_n + d) + X(t_n + d) \\ &= V(t_n + d). \end{aligned} \tag{4.40}$$

- When $t = t_{n+1}$,

$$\begin{aligned} V(t_{n+1}^+) &= P(t_{n+1}^+) + X(t_{n+1}^+) \\ &= \big(P(t_n) + rX(t_n)\big)e^{-\omega\tau} + 0 \\ &= P(t_{n+1}) \\ &= P(t_{n+1}) + X(t_{n+1}) \\ &= V(t_{n+1}). \end{aligned} \tag{4.41}$$

Equations (4.39), (4.40), (4.41) lead, for all $n \in N$, for all $t \in (t_n, t_{n+1}]$, to $V(t) \leq -\zeta t + P_0$, from which $V(t) \to 0$ when $t \to \infty$, since $V(t)$ is positive according to Lemma 4.1.

Therefore, $P(t)$ and $X(t)$ tend to 0 when $t \to \infty$. □

As in Subection 4.2.1, we reduce the first subsystem of equation (4.2) to a Rosenzweig-MacArthur model, by introducing a new state variable $N = P + X$ that represents the total number of nematodes and using the singular perturbation theory, to obtain equation (4.21) on $(t_n, t_n + d]$ intervals with this time the initial conditions $S(t_n^+) = S(0^+) = S_0,\ N(t_n^+) = P(t_n^+),\ N(0^+) = P_0$.

The reduced system admits the same pest free solution. With this knowledge, we can obtain the solutions of the reduced system of (4.2) - (5.1) on $(t_n, t_n + d]$ intervals, linearised around the pest free solution. The following proposition gives such result:

Proposition 4.4.

- For all $n \in \mathbb{N}$, the reduced equation (4.21), with initial conditions $S(t_n^+) = S(0) = S_0,\ N(t_n^+) = P(t_n),\ N(0^+) = P_0$, linearised around the pest free solution (4.35), admits for $t \in (t_n, t_n + d]$ the solution:

$$N(t) = P(t_n^+) \exp\left(-\mu(t \bmod (D + \tau)) + \int_{t_n}^{t} \frac{\alpha a \bar{S}(\tau)}{\bar{S}(\tau) + \Delta} d\tau\right) \tag{4.42}$$

$$\begin{aligned} S(t) = \bar{S}(t) - \int_{t_n}^{t} F(\xi) \exp\left(-\int_{t_n}^{\xi} \rho\left(1 - \frac{2\bar{S}(\tau)}{K}\right) d\tau\right) d\xi \\ \times \exp\left(\int_{t_n}^{t} \rho\left(1 - \frac{\bar{S}(\tau)}{K}\right) d\tau\right). \end{aligned} \tag{4.43}$$

- For all $n \in \mathbb{N}$ and $t \in (t_n + d, t_n + D]$.

  There exists a matrix $\Pi(t)$ detailed in the proof of Proposition 4.2. such that:

$$\begin{pmatrix} P(t) \\ X(t) \end{pmatrix} = \Pi\big(t \pmod{D + \tau} - d\big). \begin{pmatrix} 0 \\ N(t_n + d) \end{pmatrix} \tag{4.44}$$

and

$$S(t) = \bar{S}(t) - a\frac{S(t_n+d)}{S(t_n+d)+\Delta}\int_{t_n+d}^{t} X(\tau)d\tau + \big[S(t_n+d) - \bar{S}(t_n+d)\big], \tag{4.45}$$

Where $S(t_n+d)$ is obtained from (4.43).

The proof is the same as for Proposition 4.2, setting initial conditions X^+ to 0 and $\tilde{S}(t_n^+) = S_0 - S_0 = 0$.

The solution given by Proposition 4.4 is used to initialise the second subsystem of equation (4.2), from which we compute the basic reproduction number of the pest and the minimal duration τ_0 of fallow that leads to the decline of pests. That is the aim of the following proposition.

Proposition 4.5. (Pest eradication)

We have the following results:

1. For all $n \in \mathbb{N}$, the discrete pest dynamics in the neighbourhood of the pest free solution is defined by:

$$P(t_n^+) = P_0 e^{-n\omega\tau}\theta^n\big[\Pi_{1,2}(D-d) + q\Pi_{2,2}(D-d)\big]^n, \tag{4.46}$$

where

$$\theta = \exp\left(-\mu d + \int_0^d \frac{\alpha a\bar{S}(\tau)}{\bar{S}(\tau)+\Delta}d\tau\right).$$

2. The effective reproduction number is given by:

$$\mathcal{R} = e^{-\omega\tau}\theta\big[\Pi_{1,2}(D-d) + q\Pi_{2,2}(D-d)\big]. \tag{4.47}$$

3. The pest free solution is locally asymptotically stable for fallow durations $\tau > \tau_0$, with:

$$\tau_0 = \frac{ln\Big(\big[\Pi_{1,2}(D-d) + q\Pi_{2,2}(D-d)\big]\theta\Big)}{\omega}. \tag{4.48}$$

Proof. 1. From equation (4.42), we have

$$N(t_n+d) = P(t_n^+)e^{-\mu d + \int_0^d \frac{\alpha a\bar{S}(\tau)}{\bar{S}(\tau)+\Delta}d\tau}.$$

Hence, $N(t_n+d) = P(t_n^+)\theta$.

Equation (4.44) therefore involves

$$\begin{pmatrix} P(t_n+tf) \\ \\ X(t_n+D) \end{pmatrix} = \begin{pmatrix} \Pi_{1,1}(D-d) & \Pi_{1,2}(D-d) \\ \\ \Pi_{2,1}(D-d) & \Pi_{2,2}(D-d) \end{pmatrix} \begin{pmatrix} 0 \\ \\ \theta P(t_n^+) \end{pmatrix}$$

Hence,

$$\begin{cases} P(t_n+D) &= \Pi_{1,2}(D-d).P(t_n^+)\theta \\ \\ X(t_n+D) &= \Pi_{2,2}(D-d).P(t_n^+)\theta \end{cases}$$

So, according to the switching rule (5.1),

$$P(t_{n+1}^+) = \Big[\Pi_{1,2}(D-d) + q\Pi_{2,2}(D-d)\Big]P(t_n^+)\theta e^{-\omega\tau}$$

From where we deduce

$$P(t_n^+) = P_0 e^{-n\omega\tau}\theta^n\big[\Pi_{1,2}(D-d) + q\Pi_{2,2}(D-d)\big]^n.$$

2. Since $P(t_n^+) \to 0$ iff
$$\big(\Pi_{1,2}(D-d) + q\Pi_{2,2}(D-d)\big)\theta e^{-\omega\tau} < 1, \tag{4.49}$$
We deduce $\mathcal{R} = \big(\Pi_{1,2}(D-d) + q\Pi_{2,2}(D-d)\big)\theta e^{-\omega\tau}$.

3. We deduce τ_0 from the condition (4.49) above, by rearranging as $\tau > \frac{ln\Big(\Big[\Pi_{1,2}(D-d)+q\Pi_{2,2}(D-d)\Big]\theta\Big)}{\omega} \equiv \tau_0$.

□

In Proposition 4.5, equation (4.47) shows that the effective reproduction number $\mathcal{R}$ depends exponentially negatively on the duration τ of the fallow periods. Thereby, the larger the value of τ, the smaller the value of $\mathcal{R}$. When τ is greater than the threshold τ_0 given by equation (4.48), $\mathcal{R}$ will be smaller than 1 and the pests will decline. Whereas when τ is below the threshold τ_0, $\mathcal{R}$ will be greater than 1 and the pest will persist. We are going to illustrate this numerically.

Numerical simulations

As in Subsection 4.2.1 $\beta = 0.1$, so that the reduced system (4.21) approximates well the first subsystem of (4.2) such that the results of Proposition 4.5 are accurate for both. We consider the system (4.2,5.1).

We illustrate the behaviour of the population of nematodes, in terms of persistence or decline, according to the values taken by τ and $\mathcal{R}$ on both sides of the critical values $\tau = \tau_0$ and $\mathcal{R} = 1$.

The parameter values are given in Table 4.1. With these parameters, the critical duration of fallow is $\tau_0 = 36.79$ days. In Figure 4.8, four results are illustrated: (a) A high duration of fallow $\tau = 83.3$ days leads to a small effective reproduction number $\mathcal{R} = 0.1 \ll 1$. The pests therefore decline rapidly. (b) When the fallow period is set to $\tau = 38.92$ that remains higher than the threshold τ_0, the effective reproduction number $\mathcal{R} = 0.9$ is larger but remains less than 1. The pests decline more slowly. (c) When $\tau = 34.86$ days $< \tau_0$, the effective reproduction number takes the value $\mathcal{R} = 1.1 > 1$ that leads to the persistence of pests. (d) The highest value of the effective reproduction number, that is the basic reproduction number $\mathcal{R} = \mathcal{R}_0 = 6.18$, is obtained when there is no fallow ($\tau = 0$) and leads to the persistence of the pests with regular oscillation of their population.

It is well known that semi-discrete equations can give rise to periodic or oscillating solutions when modelling epidemics [64, 94]. Oscillations in Figure 4.8 can find a biological meaning since populations of *R. similis* also show oscillating behaviour in empirical studies. Indeed, some authors have shown that *R. similis* nematode populations on a banana plant can vary over time in line with banana root dynamics and the stage of the parent plant; nematode populations grow until banana flowering, are constant during inflorescence development, and are stable after bunch harvest [96, 97, 98, 108]. We would have preferred to find, in the simulations, intervals during which the populations are more or less constant, but it is not a feature of our model.

These simulations and the computed value of τ_0 show that for a reasonable 37 fallow days after each cropping season, the tendency of the pest population is the decline. In addition to being more environmental-friendly, controlling *R. similis* by deploying fallows also seems easier to implement than chemical control. Indeed, the latter requires the eradication of more than 99% of the nematodes each time the nematicide is used. Moreover, the use of fallow leads to a smaller highest possible value $\mathcal{R} = 6.18$ of the effective reproduction number, compared to the value $\mathcal{R} = 97.7$ obtained with chemical control. This huge difference can be easily explained by the size of pests reservoir. Indeed, in the case of deployment of fallow, only a few root tips constitute the reservoir of pests (portion $r = 5\%$) between cropping seasons, whereas a whole pool of roots inherited from the parent plant constitutes the reservoir of pests when there is no fallow (portion $1 - q = 2/3$).

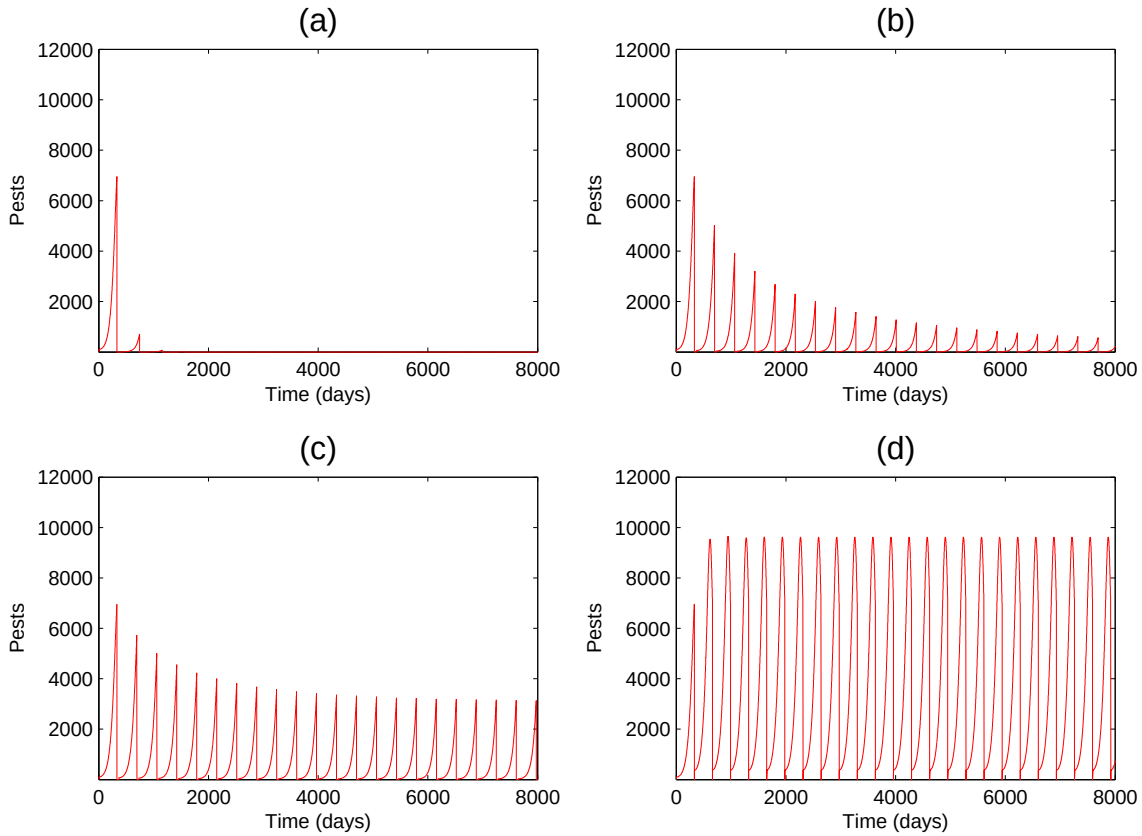

(a) $\tau = 83.3$ and $\mathcal{R} = 0.1$; **(b)** $\tau = 38.92$ and $\mathcal{R} = 0.9$; **(c)** $\tau = 34.86$ and $\mathcal{R} = 1.1$; **(d)** $\tau = 0$ and $\mathcal{R} = 6.18$.

Figure 4.8 – Infesting pest dynamics of model(4.2)-(5.1) over several cropping seasons for different values of τ. The infestation rate is $\beta = 0.1$, so that the reduced model approximates the full model well. Remaining parameter values are given in Table 4.1, leading to the threshold value $\tau_0 = 36.79$ defined in equation (4.48).

4.3 Discussion

We found in the literature only one study of *R. similis* populations with or without the use of nematicide [133]. The model has been named SIMBA-NEM, and showed that population-related parameters (limit capacities, growth rates) have a large impact on the population of *R. similis*, while in contrary, the parameters related to the use of pesticides had a little impact. This remark does not contradict our conclusion of Subsection 4.2.1, where it has been noted that large quantities of nematicide were needed to significantly reduce the infestation. SIMBA-NEM is a population model based on the cohort structure, which describes different stages of the nematode life cycle. As a result, it is a discrete and computational model that pioneers pest dynamics in cropping system models.

However, SIMBA-NEM being computational, it has no analytic result or qualitative description and its outputs and conclusions strongly depend on the value of the parameters and precision in their estimation, which often requires extensive data [3]. But we have not found in the literature quantitative studies that count nematodes by sorting them by age, stage or cohort; possibly because it is difficult to set up this type of experiment for microscopic worms. Also, the model does not allow fallowing or crop rotation with non-host plants, whereas it

has been shown empirically that these are effective strategies to fight the spread of R. similis [16, 15, 17].

The crop rotation models presented in our introduction [83, 127, 139] are not adapted to the dynamics of *R. similis* because the studied pests have different life cycles and sometimes different hosts that have different symptoms of the infestation. Also, since *R. similis* does not have a large diffusive spread in the soil [10], a spatially explicit model is not necessary when studying its dynamics. However, knowing that the spread of *R. similis* is mainly by water [10, 32], it might be interesting to study its spatial dynamics in highly irrigated environments. In this case, we can rely on excellent preliminary work found in reference [42].

The analysis of plant-pest dynamics subjected to interruptions is not new. Gubbins and Gilligan have studied the persistence of continuous plant-parasite systems in discrete disturbed environments [47]. The semi-discrete formalism has also been studied for SEIR models [65] and many other plant epidemic or more general dynamics including seasonality (see [67]). More precisely, a general framework for soilborne parasite models has been given by Mailleret et al. [66] and Hamelin et al. [49].

But those models remains general frameworks not precisely related to the dynamics of *R. similis*. For instance, they do not interrupt root growth after the flowering of the plant, giving rise to an additionnal switching within the continuous dynamics of the cropping season. Moreover, in such models, the specific off-season (e.g. winter) during which hosts lack has a fixed size that cannot be manipulated in order to control the pest. As the geographical area we analyse in Subsection 4.2.2 of this paper has a tropical climate that is well-suited for banana growing all year long, it does not suffer fixed-sized and fixed-distributed off-season. We can handle the size of such off-season that correspond here to a fallow. In this way, we differentiate from previous works, and therefore can see the effective reproduction number $\mathcal{R}$ under a new perspective. Indeed, it is now correlated with a threshold size τ_0 of the off-season, around which the pest dynamics show different behaviours.

This work was done after having reduced the model using singular perturbations, by considering that the infestation rate was markedly high, which satisfies biological observations [110, 31, 95, 79]. We then compared the pest population dynamics for different values of the infestation rate (Figure 4.5). For high enough values, the reduced model is an excellent approximation of the full model, as shown for instance in Figure 4.5 (c) for $\beta = 0.1$. However, for lower values such as $\beta = 0.001$ illustrated in Figure 4.5 (a), the approximation does not hold and the full model should be used.

4.4 Conclusion

Our work proposes a multi-seasonal framework which describes the infestation of banana (or plantain) roots by the burrowing nematode *R. similis*. In this work, we have studied two semi-discrete models based on impulsive ordinary differential equations, where the feeding of the pests has a saturated response. In both models, pests have two living stages: a free stage in the soil and an infesting stage in the roots. The difference between the two models lies in their control method: the first one includes the use of pesticides while the second one relies on fallow periods between seasons. We were able to provide local stability results for these new models, to compute effective reproduction numbers and link them to biological thresholds, while managing well the difficulties related to a step root growth function.

The two models bring out an obvious similarity: whether we use pesticides or fallows, the infestation can be reduced by playing on the thresholds that are related to the effective reproduction number. In the first model, it relies on the increase of the pesticide dosage, while in the second model it requires the increase of the duration

of the fallows between cropping seasons. However, we have shown that chemical control is not very effective. Indeed, the required pesticide efficiency which results from our computations and the value of our parameters is barely achieved in realistic environments, and would require large amounts of pesticide. The fallow deployment model has also allowed us to find an oscillation behaviour of nematode populations as found in the literature.

However, the two models showing similarities in study and pest management, both of them present implementation issues due to different factors:

(i) The first model implies the use of pesticides which have harmful ecological impact [43] and the nematode can evolve to develop resistance to their application. Besides, the effect of phytotoxicity of such pesticides has been identified in practice [100], but has not been included in our model yet. Such an effect would certainly eliminate the linearity in the basic pest reproduction number and induce the existence of an intermediate value of λ that minimizes the effective pest reproduction number, with no guarantee that the latter would be smaller than 1. Consideration of phytotoxicity could therefore change the control strategy. Also, nematicides have a cost and increasing the dosage also mean to increase the expense of chemical control.

(ii) The reproduction of the plant in the second model comes exclusively from the use of healthy vitro-plants which each have a financial cost. Hence, the cost of this strategy could be prohibitive for small farmers, while the natural asexual reproduction of the plants by lateral shot is free of cost. Besides, we have shown that long fallow periods reduce significantly the infestation; but long fallow periods can also decrease the number of cropping seasons over a fixed time horizon. The legitimate question is how far the duration of the fallow can be extended and still be accepted by planters? It appears that the development of sustainable strategies for the management and control of plant diseases, in general, requires an understanding of economic and social constraints that influence the deployment of control [39].

(iii) Although our second model has been able to highlight the population oscillations described in the literature, we were not able to obtain a simulation in which the population of *R. similis* seems to be constant during a certain period as observed by some authors [108, 96, 97, 98].

In order to solve issues (i) and (ii), we can think about linking fallow durations to an economical yield to identify optimal fallow deployments. An interest in linking epidemiological with economic modelling arises when there are constraints over the amount of control that can be applied, whether it is chemical, cultural, genetical or biological [39]. Concerning fallow deployment, the control is cultural and is related to the duration of fallow periods between cropping seasons. A constraint arises naturally from this control, since one cannot deploy too large fallow periods in order to maintain a reasonable yield.

The control relies on planting healthy vitro-plant at the beginning of each cropping season. Therefore, finding the optimal control strategy requires estimates for the cost of a healthy vitro-plant and crop yield losses induced by the infestation. An interesting metric to capture the yield of crops in compartmental models has been proposed in the literature [48]. In this metric, the yield depends on the biomass of healthy tissues and a weighting function over the time.

Finally, in order for optimal control strategies to be implemented, the parameters must be well-known. Poorly understood parameters can lead to systematic biases in decision-making and distort control. Unfortunately, we see in Table 4.1 that many parameters are poorly known, which could question the future results of

the optimization described above. To overcome such biases, we can rely on parameter estimation and sensitivity analysis. In case real-time data measurements are possible, we could use a Control Smart Algorithm (CSA) to know whether to wait to collect the data or to implement the control directly with the data as it is available [130]. This may improve the efficiency of our future optimal control models.

This chapter proposes a multi-seasonal framework which describes the banana (or plantain) roots infestation dynamics by *Radopholus similis*. In this chapter, we have studied two semi-discrete models based on impulsive ordinary differential equations, where the feeding of the pests has a saturated response. In both models, pests have two living stages: a free stage in the soil and an infesting stage in the roots. The difference between the two models lies in their control method: the first one includes the use of pesticides while the second one relies on fallow periods between seasons. We were able to provide local stability results for these new models, to compute basic reproduction numbers and link them to biological thresholds, while managing well the difficulties related to a step root growth function. This work has been done after having reduced the systems using singular perturbations.

The two models bring out an obvious similarity: whether we use pesticides or fallows, the infestation can be reduced by playing on the thresholds that are related to the basic reproduction rate. In the first model, it relies on the increase of the pesticide dosage, while in the second model it requires the increase of the duration of the fallows between cropping seasons. However, we have shown that the chemical control is not very effective. Indeed, the required pesticide efficiency which results from our computations and the value of our parameters is barely achieved in realistic environments, and would require large amounts of pesticides. The fallow deployment model has also allowed us to find an oscillation behaviour of nematode populations as found in the literature.

However, the two models showing similarities in study and pest management, both of them present implementation issues due to different factors:

(i) The first model implies the use of pesticides which have harmful ecological impact [43] and the nematode can evolve to develop resistance to their application. Besides, the effect of phytotoxicity of such pesticides has been identified in practice [100], but has not been included in our model yet. Such an effect would certainly eliminate the linearity in the basic pest reproduction number and induce the existence of an intermediate value of λ that minimizes the basic pest reproduction number, with no guarantee that the latter would be smaller than 1. Consideration of phytotoxicity could therefore change the control strategy. Also, nematicides have a cost and increasing the dosage also mean to increase the expense of chemical control.

(ii) The reproduction of the plant in the second model comes exclusively from the use of healthy vitro-plants which each have a financial cost. Hence, the cost of this strategy could be prohibitive for small farmers, while the natural asexual reproduction of the plants by lateral shot is free of cost. Besides, we have shown that long fallow periods reduce significantly the infestation; but long fallow periods can also decrease the number of cropping seasons over a fixed time horizon. The legitimate question is how far the duration of the fallow can be extended and still be accepted by planters?

(iii) Although our second model has been able to highlight the population oscillations described in the literature, we were not able to obtain a simulation in which the population of *Radopholus similis* seems to be constant during a certain period as observed by some authors [108, 96, 97, 98].

To solve most of these issues, we can think about (i) linking fallow durations to an economical yield and then identify optimal rotation strategies over a fixed time horizon, and (ii) combining the plant's reproduction strategies between new vitro-plant and natural lateral reproduction, and come out with better coordinated management of both. The definite goal is to put aside chemical control while ensuring economic viability.

CHAPTER FIVE

OPTIMAL FALLOW DEPLOYMENT FOR THE SUSTAINABLE MANAGEMENT OF *Radopholus similis*

In this chapter, we rely on the fallow deployment model in Chapter 4. Contrary to that model (subsection 4.2.1), the differences $t_{n+1} - t_n$, ($n \in \mathbb{N}$) are not constant, meaning that the falllow periods could be of different lengths. We formulate an optimization problem to determine the distribution of fallow periods that maximizes multi-seasonal crop profit. We show the existence of an optimal distribution of fallow periods and propose a stochastic algorithm that seeks the solution. We will also propose regulations to obtain solutions that are easier to deploy, and we provide numerical simulations to illustrate our results.

The within-season model is given by equation (4.2), and the switching between two season is given by the following equation :

$$\begin{cases} P(t_{n+1}^+) = \Big(P(t_n + D) + rX(t_n + D)\Big)e^{-\omega\tau_{n+1}}, \\ S(t_{n+1}^+) = S_0, \\ X(t_{n+1}^+) = 0. \end{cases} \tag{5.1}$$

Equations (4.2) and (5.1) form our multi-seasonal model for the dynamics of banana-nematodes interactions with a distribution $(\tau_n)_{n\geq 1}$ of fallow periods. We are now going to define what is the economical profit that can emerge from this model.

5.0.1 Yield and profit

Banana roots are responsible for the absorption of nutrients. After the flowering, these nutrients are mainly used for the growth of the banana bunch. If the economic yield of a bunch depends on its weight, then this yield is related to the biomass of fresh roots during the bunch's growth period. We make the hypothesis that a season is profitable only if it is complete. A metric to capture the yield of the $(k+1)$-th cropping season from the model (4.2,5.1) can therefore be given by the following formula:

$$Y_k = \int_{t_k+d}^{t_k+D} W(t)\, S(t)\, dt,$$

where $W(t)$ is a weighting function [48].

From reference [115], the weighting function $W(t)$ appears to be a constant $W(t) = m$. So we can rewrite the previous expression of yield as follows:

$$Y_k = m \int_{t_k+d}^{t_k+D} S(t)\, dt. \tag{5.2}$$

As each healthy sucker has a cost [82], we subtract the cost of a healthy sucker from the yield to obtain the profit:

$$R_k = m \int_{t_k+d}^{t_k+D} S(t)\, dt - c. \tag{5.3}$$

In equation (5.3), the biomass $S(t)$ depends of the infestation. Because of the switching law (5.1), this infestation depends on all the fallow periods that have preceded the current season. Hence, the cumulated profit after the deployment of n fallow periods is the sum of the corresponding $(n+1)$ cropping seasons and depends on the distribution of fallow periods. Its expression is given by:

$$R(\tau_1, \ldots, \tau_n) = \sum_{k=0}^{n} R_k \tag{5.4}$$

5.0.2 Parameter values

The form of the seasonal profit 5.3 induces two additional parameters (c and m). The other parameters are found in Table 4.1. Some data also come from different geographic regions, and we assume that they are compatible. For example, we graphically evaluated the parameter m of the weighting function intervening in the yield equation (5.2) based on plantations in Costa Rica, in a publication which relates the yield in boxes per hectare and per year (a box weighing 18.14 kg) to the functional root weight in grams per plant [115]. To convert this yield per hectare into the yield per plant, we used plant high-density data from plantations in Latin America and the Caribbean [103]; based on FAO data [36], we converted the yield into a monetary yield. The currency used is the Central African CFA franc (XAF). It has a fixed exchange rate with Euro : 1 Euro = 655.956 XAF. From the literature, we set the value of the yield factor of fresh roots (m) to 0.3 XAF.g^{-1}.day^{-1} [115, 137, 75]. The cost (c) of a banana healthy sucker is set to 230 XAF [82].

The value $P_0 = 100$ nematodes per volume of soil occupied by a plant considered in Table 4.1 is rather large and corresponds to heavily infested soils. Indeed, several authors have shown in the literature that the densities of *R. similis* in bare soils were very low [110, 31, 95, 79]. However, simulations in [126] show that soil infestations can reach such levels just after plant uprooting, i.e. before the nematode populations have had time to significantly decrease. It is this high infestation case that is analyzed in this paper.

We performed a local sensitivity analysis, based on the numerical derivatives of the single season profit R_k defined in Equation (5.3), calculated with the considered parameter values. Our method uses the iterative approximation based on directional derivatives, in a similar form to that used by Maly and Petzold [68]. Sensitivities are computed for each epidemiological parameter and for the economic parameter m as the directional derivative of the profit with respect to this parameter, and depicted in Figure 5.1. It turns out that the parameter a is largely the most influential. Further studies on the voracity of *R. similis* might be needed to have a more confident estimate of a. In addition to this parameter of great sensitivity, the values of the other relatively influential parameters are satisfactory. The parameter μ which represents the mortality rate of infesting nematodes

is rather well known, and the growth rate ρ of banana roots is well estimated. The other parameters have no or negligible influence.

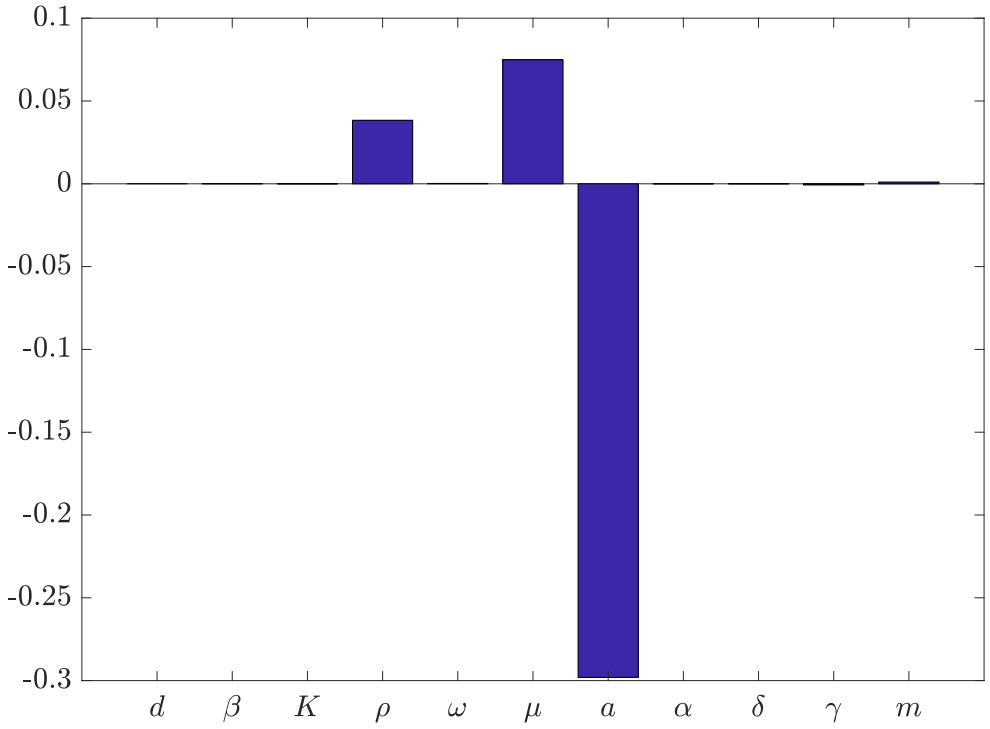

Figure 5.1 – Local sensitivity analysis to assess the impact of the epidemiological and economic parameters, on the single season profit R_k defined in Equation (5.3). Sensitivities correspond to the directional derivatives of the profit with respect to these parameters.

5.1 Optimization

From switching rule (5.1), long fallow durations τ_n lead to the reduction of the soil infestation. Equation (5.2) shows that the seasonal yield is linked to fresh root biomass that depends on the infestation level throughout the season. Increasing the fallow durations to drastically reduce the pest population increases the yield. However, on a fixed and finite time horizon that spans several seasons, increasing the fallow durations may reduce the number of cropping seasons and hence the multi-seasonal profit. For example, if we consider $D = 330$ days and a time horizon $T_{max} = 1000$ days, then 3 cropping seasons can be completed with short fallow periods, for instance of 2 and 5 days. However, the crops will be hampered by severe infestations that may reduce the profit. In contrast, if fallow periods are longer, for instance 20 and 50 days, the profits of the first two seasons increase, but the third cropping season cannot be completed within T_{max}.

The optimization problem here is to find a sequence of fallow durations that maximizes the total profit. For the problem to be relevant, the time horizon should allow to deploy at least one fallow period. Still denoting T_{max} the time horizon, it corresponds to the following assumption:

Assumption 5.1. The time horizon spans at least two seasons: $T_{max} > 2D$.

We hence state the following problem:

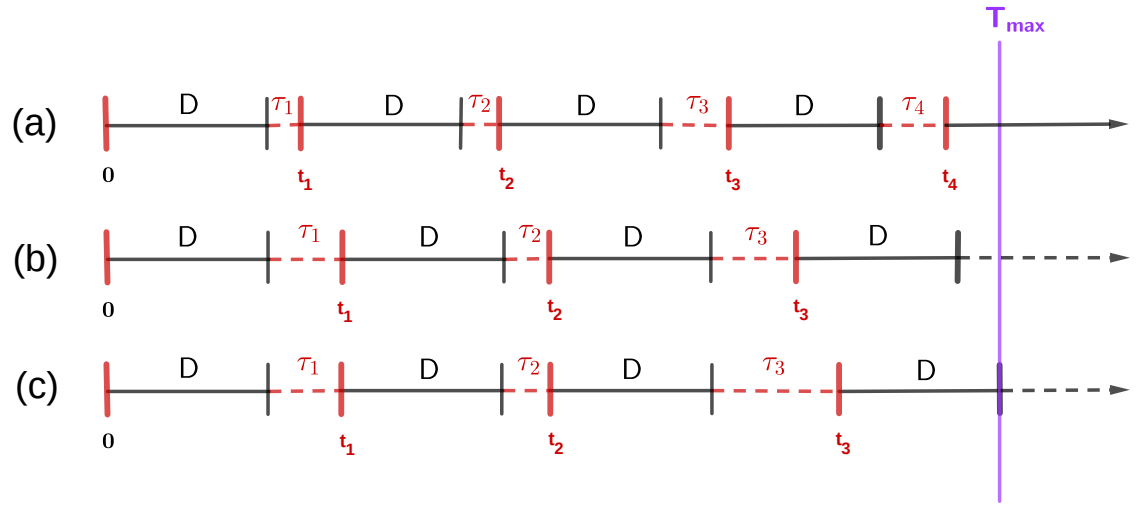

Figure 5.2 – Possible occurrences of T_{max}. In (a) T_{max} occurs in the middle of a cropping season, in (b) during a fallow period, and in (c) at the end of a cropping season, at the same time as the harvest.

Problem 5.1. Under assumption 5.1, find a sequence of fallow durations $(\tau_1^*, \ldots, \tau_n^*)$ such that maximizes R defined in equation (5.4).

5.1.1 Location of the optimal solutions

If T_{max} hits the middle of a cropping season (Figure 5.2(a)) then this season is useless in terms of profit because its harvest occurs after T_{max}. In the same way, if T_{max} hits a fallow period (Figure 5.2(b)), then this fallow is useless because it is not followed by a cropping season within T_{max}. In both cases, the time elapsed between the last harvest and T_{max} might be added to the last useful fallow such that T_{max} hits the end of a cropping season (Figure 5.2(c)). This might increase the yield of the crop. Indeed, according to the switching rule (5.1), increasing the length of the last fallow period leads to a reduced number of pests at the beginning of the last season. This reduction of pests is supposed to reduce the pest population throughout the season and therefore increase the root biomass and the profit. So the last harvest of the optimal solution should occur at T_{max}. But such ideal behaviour only holds in dynamical systems that show a certain "monotonicity". Definition 5.1 describes such monotonicity for system (4.2).

Definition 5.1. (Monotonicity)

System (4.2) is said to be monotone on the interval $(t_k, t_k + D]$ according to initial soil infestation $P(t_k^+) = P(t_k)$ if:

1. $\tilde{P}_k \geq P_k \Rightarrow P\big(t; t_k^+, (\tilde{P}_k, S_0, 0)\big) \geq P\big(t; t_k^+, (P_k, S_0, 0)\big)$ for all $t \in (t_k, t_k + D]$
2. $\tilde{P}_k \geq P_k \Rightarrow X\big(t; t_k^+, (\tilde{P}_k, S_0, 0)\big) \geq X\big(t; t_k^+, (P_k, S_0, 0)\big)$ for all $t \in (t_k, t_k + D]$
3. $\tilde{P}_k \geq P_k \Rightarrow S\big(t; t_k^+, (\tilde{P}_k, S_0, 0)\big) \leq S\big(t; t_k^+, (P_k, S_0, 0)\big)$ for all $t \in (t_k, t_k + D]$

Where $(P, S, X)\big(t; t_k^+, (P_k, S_k, X_k)\big)$ is the solution on $(t_k, t_k + D]$ of equation (4.2) with initial condition (P_k, S_k, X_k) at $t = t_k^+$.

We can reformulate the preceding argument as follows. Let t_n be the starting point of the last useful cropping season, i.e. the last season for which $\delta_n = T_{max} - (t_n + D) \geq 0$. If the last harvest occurs at T_{max}, then $\delta_n = 0$. Otherwise, let $\tilde{\tau}_n = \tau_n + \delta_n$ and let $\tilde{t}_n = t_{n-1} + \tilde{\tau}_n$.

Because of switching law (5.1), we have $P(t_n) = P(t_{n-1} + \tau_n) \geq P(t_{n-1} + \tilde{\tau}_n) = P(\tilde{t}_n)$. As a consequence, in case of monotonicity, we have $S(t_n + t) \leq S(\tilde{t}_n + t)$, for $t \in (0, D]$. Hence,

$$\int_{t_n+d}^{t_n+D} S(t)dt \leq \int_{\tilde{t}_n+d}^{\tilde{t}_n+D} S(t)dt \tag{5.5}$$

and the profit of season n is higher for fallow duration $\tilde{\tau}_n$.

We add the following assumption.

Assumption 5.2. System (4.2) is monotone according to definition 5.1.

Remark 5.1. Assumption 5.2 means that the fewer the initial pests, the lower the infestation throughout the season, and the larger the root biomass. However, for such a predator-prey-like system this property may not hold depending on the parameter values. Indeed, when the level of infestation is high, root biomass S undergoes overconsumption. Such overconsumption induces the decline of root biomass that is food for nematodes. This food decline leads to the decline of nematodes and therefore to the recovery of the root biomass, if the overconsumption occurs early enough during the root growth period $(t_k, t_k + d]$. Such dynamics give rise to cycles that induce the loss of monotonicity. If the pests are "not too abundant", this overconsumption scenario should not appear and the monotonicity holds at least for the finite duration D.

We surmise that there exists a reasonable level of infestation below which Assumption 5.2 is realistic and we illustrate it numerically. With parameters in Table 4.1 and Subsection 5.0.2, we plot in Figure 5.3 the curves of free pests (P), infesting pests (X) and fresh root biomass (S) on a single season, for a large range of infestation values $P(t_k^+)$ at the beginning of cropping season k that encompasses realistic values that are usually below 100. It shows that Assumption 5.2 holds for variables P, S and X, for realistic values of $P(t_k^+)$ below 200. Indeed, the curve order is conserved throughout the season (curves do not cross), so the monotonicity condition is verified for P, S and X.

Nevertheless, we could build a counterexample setting two parameters to unrealistic values by observing the system dynamics during the first two seasons. We considered a very high and unrealistic value of the initial infestation $P(t_0^+) = 300$, compared to the reference value $P_0 = 100$. Then by setting the proportion of pests released in the soil after uprooting to $r = 100\%$, we ensured that the infestation at the beginning of the second cropping season was higher than with the reference value $r = 5\%$. We varied the fallow duration τ. The higher the τ values, the lower $P(t_1^+)$ at the beginning of the second cropping season. If monotonicity Assumption 5.2 held, then we would expect a lower S curve for a lower τ and hence a lower profit. However, for instance for $\tau = 2$ and $\tau = 10$, that yield to $P(t_1^+) = 6860$ and $P(t_1^+) = 4617$ respectively, it did not hold, as shown in Figure 5.4: the S curves cross (Figure 5.4(a)) and, as a consequence, the profit is lower for the higher τ (Figure 5.4(b)). More generally, for low values of τ, the profit counter-intuitively decreases with τ (Figure 5.4(b)). However, this situation is quite unrealistic, since a proportion $r = 100\%$ simply means that there is no uprooting of the old plant and that all the nematodes remain in the soil.

According to the arguments above, we can state the following lemma:

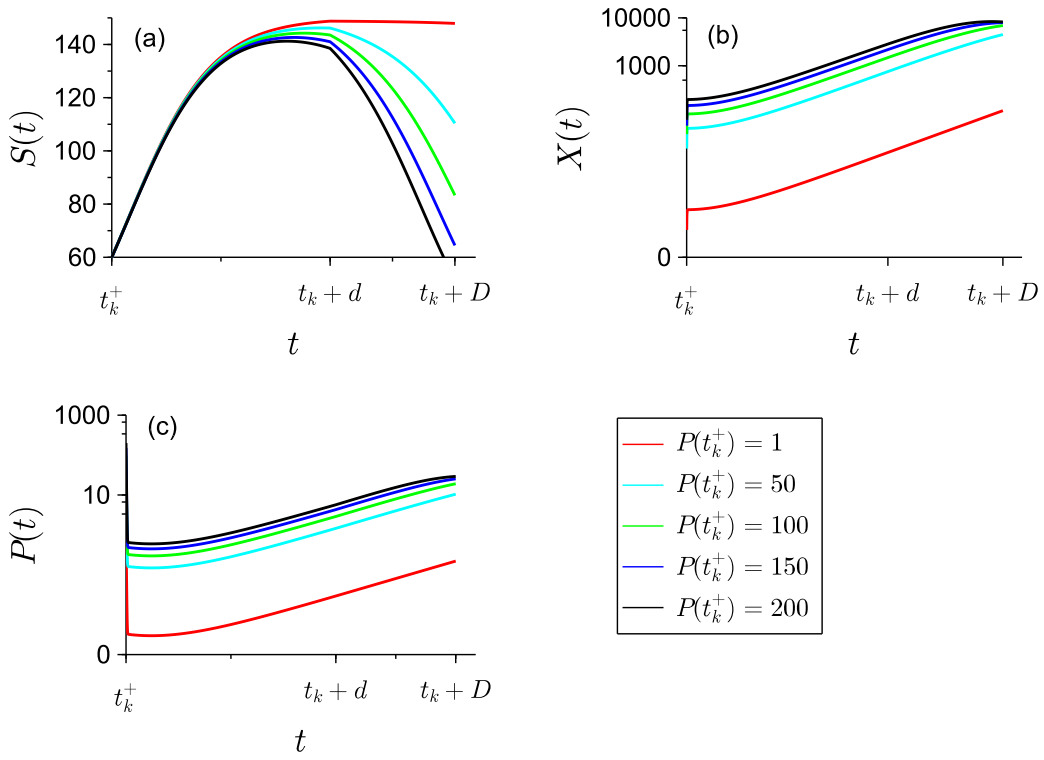

Figure 5.3 – Curves of pests populations (X and P) and fresh root biomass (S) for different values of the initial infestation $P(t_k^+)$. For initial infestations lower than 200, (a) the greater the initial infestation, the lower the curves of fresh root biomass on the domain $(t_k, t_k + D]$; (b) and (c) The greater the initial infestation, the higher the curves of pests on the domain $(t_k, t_k + D]$.

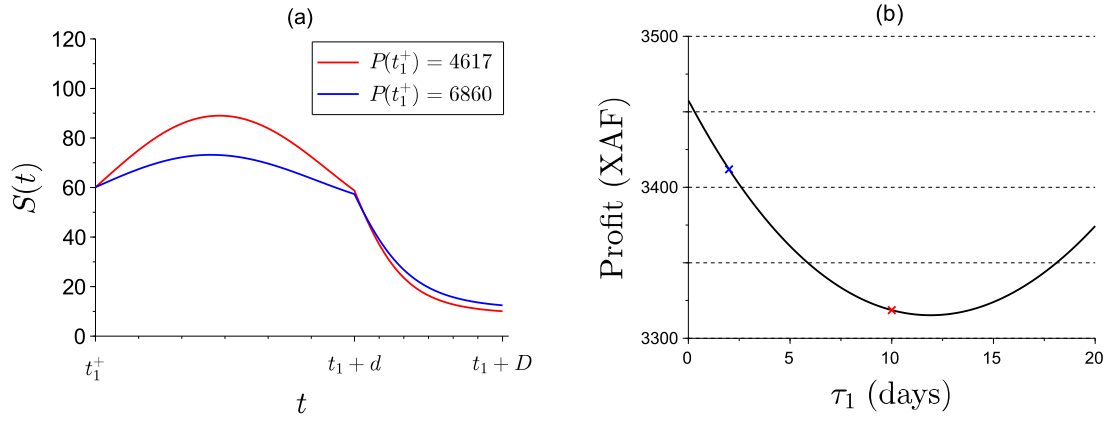

Figure 5.4 – Counterexample: loss of monotonicity when $r = 100\%$ and $P_0 = 300$. (a) Root biomass during the second cropping season for two different values of $P(t_1^+)$ arising from $\tau_1 = 2$ days (blue curve) and $\tau_1 = 10$ days (red curve). At the beginning, the blue curve is below the red curve, which is consistent with the monotonicity assumption as $P(t_1^+)$ is higher for the blue curve. However, shortly after $t_1 + d$, the relative position of the two curves switches and so the monotonicity Assumption 5.2 is not verified. (b) Profit for the first two seasons as a function of fallow duration τ_1. The fallow duration $\tau_1 = 2$ days (blue cross) yields a better profit than the fallow duration $\tau_1 = 10$ days (red cross), although the former corresponds to a higher infestation $P(t_1^+)$ than the latter. This is due to the loss of monotonicity.

Lemma 5.1. Under monotonicity Assumption 5.2, if Problem 5.1 admits a solution, then it belongs to one of the n-simplexes:

$$A^n = \{(\tau_1, \ldots, \tau_n) : \sum \tau_k = T_{max} - (n+1)D\}, \tag{5.6}$$

with $n = 1, ..., n_{max} \equiv \left\lfloor \frac{T_{max}}{D} \right\rfloor - 1$. It means that the last harvest needs to occur at T_{max}.

Problem 5.1 can be rewritten as:

Problem 5.2. Let $\mathcal{A}$ be the reunion of all the n-simplexes A^n ($n \in \{1, ..., n_{max}\}$). Under Assumptions 5.1 and 5.2, find the optimal sequence $(\tau_1^*, \ldots, \tau_n^*) \in \mathcal{A}$ of fallow durations that maximizes R defined in equation (5.4).

We prove the existence of solutions to Problem 5.2.

Theorem 5.1. (Existence of optimal fallow deployments)

For all $n_{max} \geq 1$, Problem 5.2 has a solution on the collection $\mathcal{A}$ of the n-simplexes A^n ($n \in \{1, ..., n_{max}\}$) defined in equation (5.6).

Proof. Let us consider from equation (5.4) the expression $R(\tau_1, \ldots, \tau_n) = \sum_{k=0}^{n} R_k$. First, $(n+1)$ is bounded by $\left\lfloor \frac{T_{max}}{D} \right\rfloor$. Besides,

(i) $Y_0 = m \int_{t_0+d}^{t_0+D} S(t)dt$ is finite and doesn't depend on any t_i.

(ii) For all $k \geq 1$, the bounds of the integral $Y_k = m \int_{t_k+d}^{t_k+D} S(t)dt$ continuously depends on $(\tau_1, \ldots, \tau_{k-1})$ as $t_k = D + \tau_1 + D + \tau_2 + \cdots + D + \tau_{k-1}$.

$S(t)$ continuously depends on the initial condition $(P(t_k + d^+), S(t_k + d^+), X(t_k + d^+))$ of the second subsystem of (4.2) that continuously depends on the initial condition $(P(t_k^+), S(t_k^+), X(t_k^+))$. From switching rule (5.1), this initial condition continuously depends on τ_k.

Hence, the yield Y_k continuously depends on $(\tau_1, \ldots, \tau_k)$ for all $k \geq 1$.

It follows that $\sum_{k=0}^{n} R_k$ is upper-bounded and lower-bounded. Therefore, R admits a minimum and a maximum on $\mathcal{A}$. □

Remark 5.2. The maximizing sequence might not be unique. If two or more solutions are optimal we would need to define a tie-break rule. For instance, we could prefer (i) a solution with less cropping seasons; (ii) within solutions with the same number of cropping seasons, the solution closer to the average fallow duration.

Remark 5.3. If $T_{max} < 3D$, then a maximum of two cropping seasons and one fallow can be deployed. Problem 5.2 admits a unique solution $\tau_1^* = T_{max} - 2D$.

5.1.2 Optimization algorithm

For values of T_{max} that are larger than $3D$, the solution could imply two or more fallow periods. In order to numerically solve the optimization problem (5.2), we propose an algorithm of adaptive random search as proposed in Walter and Pronzato [148], that we adapt to simplexes. This method is useful since the function R may have many local maximizers and it is highly desirable to find its global maximizer. The convergence of this kind of algorithm has been proven in the literature [118]. Algorithm 5.1 gives the solution of the optimization problem 5.2. The profits of the maximizers in each dimension are compared to obtain the optimum.

Data: T_{max}, D
$n_{max} := \left\lfloor \frac{T_{max}}{D} \right\rfloor - 1$ // maximum number of fallow periods that can be deployed on $[0, T_{max}]$
Result: optimal fallow sequence $\vec{\tau}^*$ of size n^*
$n^* = 1$ // initialization
$\vec{\tau}^* := \vec{\tau}^{1,*} = T_{max} - 2D$
for $n := 2$ *to* n_{max} **do**
  $\vec{\tau}^{n,*} :=$ ARS(n) // n-optimal fallow sequence of size n
  if $R(\vec{\tau}^{n,*}) > R(\vec{\tau}^*)$ **then**
    $n^* = n$
    $\vec{\tau}^* = \vec{\tau}^{n,*}$
  end
end

Algorithm 5.1: Optimization algorithm for the numerical resolution of Problem 5.2. Integer n corresponds to the number of fallow periods that are deployed on interval $[0, T_{max}]$. For each $n \leq n_{max}$, the n-optimal fallow sequence $\vec{\tau}^{n,*}$ is computed: for $n = 1$ the solution is trivial; for $n > 1$, the n-optimum is computed using an adaptive random search (ARS) algorithm, adapted to simplex A^n. The ARS algorithm is detailed in 1.3.2. The optimal fallow deployment $\vec{\tau}^*$ corresponds to the n-optimum that yields the highest profit R.

5.2 Numerical results

We provide the solution for small values of the time horizon T_{max} in Subsection 5.2.1 and for high values in Subsection 5.2.2. The latter relies on the optimization algorithm described above in Subsection 5.1.2.

5.2.1 Small dimensions

In small dimensions, when $T_{max} < 5D$, up to 3 fallow periods can be deployed. The 3-dimension simplex A^3, defined in equation (5.6), can be represented on a plane. Hence, we can have a good numerical understanding of the location of the optimal solution of problem (5.2), by building a graphical representation of the profit on the simplex and identifying its maximum. We name "size of the simplex" the length of each side of the simplex. We use parameter values in Table 4.1 and Subsection 5.0.2.

We first set $T_{max} = 1400$ days. Up to 4 cropping seasons, corresponding to 3 fallow periods covering $1400 - 4 \times 330 = 80$ days, can hence be deployed. Figure 5.5 is a representation of the profit, defined in equation (5.4), in the 3-simplex of size 80 days projected on its first coordinates (τ_1, τ_2). The duration of the third fallow period is then $\tau_3 = 80 - (\tau_1 + \tau_2)$. We notice that:

- The maximum is obtained for 3 fallow periods and is located at the summit $\tau_1 = 80$ days. This may be because, when there is enough fallow duration to be distributed (here 80 days), a long first fallow can lead to drastic pest reduction and hence better profits for the following cropping seasons.
- The profit is low near the point $\tau_3 = 80$ days (that corresponds to $\tau_1 = \tau_2 = 0$) and increases toward the edge $\tau_3 = 0$ (that corresponds to the hypotenuse). Higher profits hence correspond to shorter durations for the last fallow period, which is consistent with the previous remark.

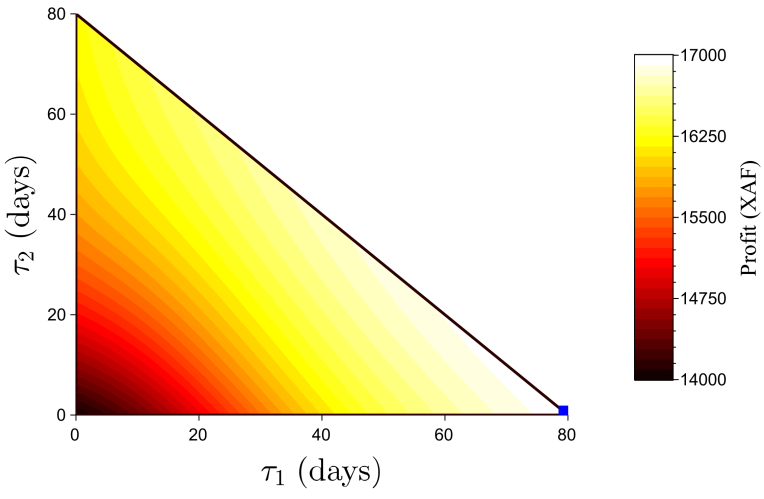

Figure 5.5 – Profit as a function of the fallow period distribution on the A^3 simplex of size 80 days ($T_{max} = 1400$ days). The simplex is projected on its first two coordinates (τ_1, τ_2) and $\tau_3 = 80 - (\tau_1 + \tau_2)$. The lighter the colour, the higher the profit. The maximum is indicated by a blue square and corresponds to $\tau_1 = 80$ days and $\tau_2 = \tau_3 = 0$ day.

The strategy may be very different with a different time horizon, which nevertheless admits the same number of deployable seasons. For example, let $T_{max} = 1340$ days instead of 1400 days. In this case, it

is preferable to deploy 3 cropping seasons (i.e. 2 fallow periods) and the optimal deployment is given by $(\tau_1, \tau_2) = (332, 18)$ days. However, a 332-days fallow period is somehow too long, so we introduce an upper bound of 60 days on each fallow period. This brings the optimal solution back to 3 fallow periods, illustrated in Figure 5.6. This figure shows that the maximum is located at the summit $\tau_3 = 20$ days. Since the total fallow duration ($\tau_1 + \tau_2 + \tau_3 = 20$ days) is small, it may be better to deploy it when the pest infestation is at its highest in order to maximize the fallow impact. In this case, a first 20-day fallow period is not long enough to sufficiently reduce the pest population, so it is more efficient to allocate these 20 days to the last fallow.

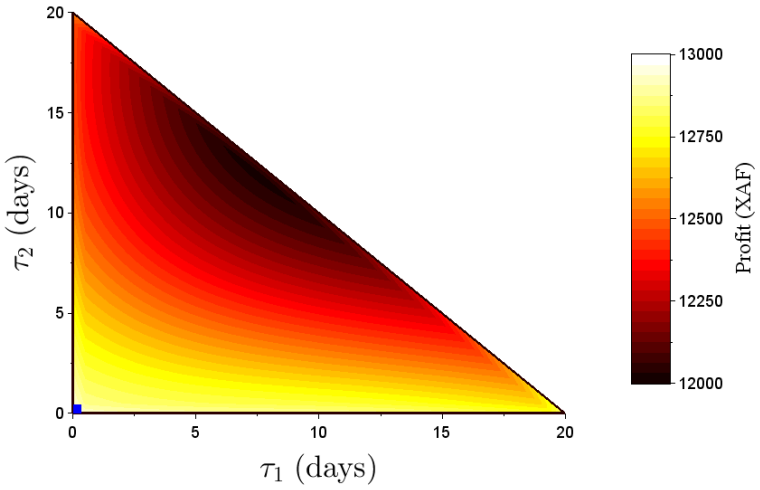

Figure 5.6 – Profit as a function of the fallow period distribution on the A^3 simplex of size 20 days ($T_{max} = 1340$ days). The simplex is projected on its first two coordinates (τ_1, τ_2) and $\tau_3 = 20 - (\tau_1 + \tau_2)$. The lighter the colour, the higher the profit. The maximum is indicated by a blue square and corresponds to $\tau_3 = 20$ days and $\tau_1 = \tau_2 = 0$ day.

Still, in the case of a time horizon of 1340 days, the optimum can be brought back from the summit $\tau_3 = 20$ days to the summit $\tau_1 = 20$ days when the initial infestation is large, and therefore the impact of the first fallow period is significant. We set $P_0 = 10000$ nematodes, instead of the reference value $P_0 = 100$ nematodes found in Table 4.1, and we illustrate the levels of infestation in Figure 5.7. As in Figure 5.5, the maximum consists of deploying the total fallow duration during the first period. In this case though, this strategy does not drastically reduce the pest population but prevents it from increasing too much. Profits are globally lower than in the previous cases, whatever the fallow distribution.

5.2.2 High dimensions

In high dimensions, i.e. when T_{max} is large, we cannot easily illustrate the profit as a function of the fallow distribution. Moreover, thoroughly exploring the space of all the possible sequences of fallow periods would require a great deal of computation. Therefore, we solve the optimization Problem 5.2 using the Algorithm 5.1 in subsection 5.1.2.

We still use parameter values in Table 4.1 and Subsection 5.0.2. We set $T_{max} = 4000$ days. Up to 12 cropping seasons, i.e. 11 fallow periods, can be deployed over this time horizon. However, the optimal deployment is obtained for 11 cropping seasons, which corresponds to a total of 370 days of fallow. It is

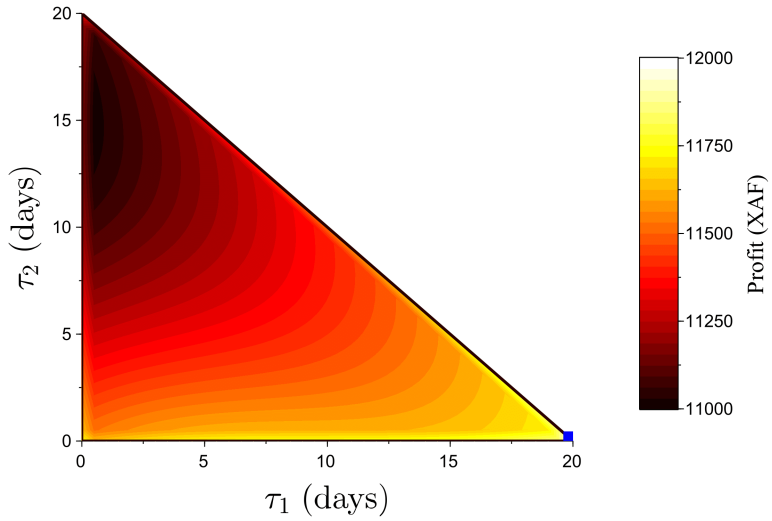

Figure 5.7 – Profit as a function of the fallow period distribution on the A^3 simplex of size 20 days ($T_{max} = 1340$ days), for a very high initial infestation ($P_0 = 10000$ nematodes). The simplex is projected on its first two coordinates (τ_1, τ_2) and $\tau_3 = 20 - (\tau_1 + \tau_2)$. The lighter the colour, the higher the profit. The maximum is indicated by a blue square and corresponds to $\tau_1 = 20$ days and $\tau_2 = \tau_3 = 0$ day.

illustrated in Figure 5.8. The corresponding optimal profit is $R(\vec{\tau}^*) = 54530$ XAF (83 euros) and the final soil infestation after the last harvest is $P(T^+_{max}) = 251$ nematodes.

5.2.3 Regulation of high dimension solutions

The optimal distribution of fallow periods found in Subsection 5.2.2 and Figure 5.8 is very dispersed around the average fallow duration. The first fallow period is huge whereas some others are null. Even if the strategy is optimal, farmers could be reluctant to implement such an irregular cropping strategy. Besides, the level of infestation (251 nematodes) after the last harvest is somehow high, which would be a problem if the grower then cropped a good host for *R. similis*. It is necessary to find a compromise between the balance of the fallow durations and the profit. In this subsection, we aim at limiting the durations of the fallow periods without penalizing the profit too much. First, we regulate the solution by bounding the duration of fallow periods. Then, we favour fallow periods that are close to the average duration (that depends on the number of cropping seasons deployed). Finally, we consider constant fallow periods. We still use parameter values in Table 4.1 and Subsection 5.0.2, and $T_{max} = 4000$ days for the numerical simulations.

5.2.3.1 Bounded fallows

The first regulation consists in bounding all fallow period durations τ_k by a maximal value τ_{sup}. This means that $\tau_k \leq \tau_{sup}$, $k = 1 \dots n$. Since $\sum_{k=1}^{n} \tau_k = T_{max} - (n+1)D$, we should have $n.\tau_{sup} \geq T_{max} - (n+1)D$. Hence:

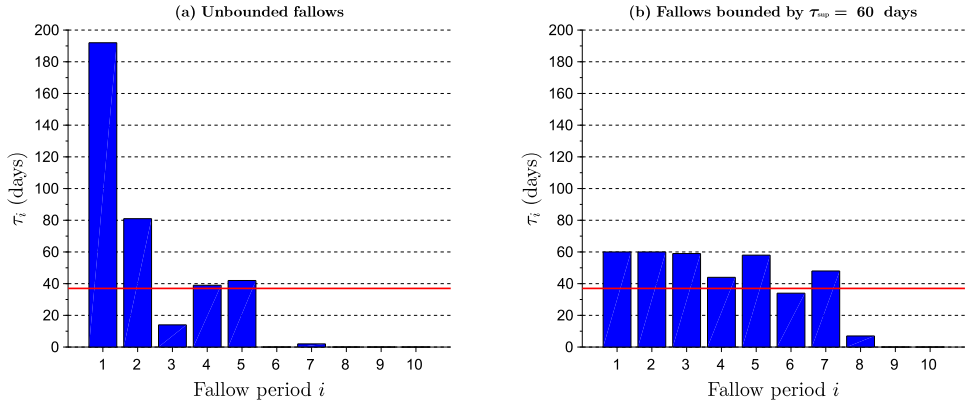

Figure 5.8 – Optimal distribution of fallow periods for time horizon $T_{max} = 4000$ days. The maximal profit is obtained for 11 cropping seasons and 10 fallows: $\vec{\tau}^* = (192, 81, 14, 39, 42, 0, 2, 0, 0, 0)$ (in days). The red line corresponds to the average fallow period $\tau = 37$ days.

$$n \geq \frac{T_{max} - D}{\tau_{sup} + D}.$$

The optimal fallow distribution $\vec{\tau}^*$ should then be sought for dimensions n between:

$$n_{min} = \left\lceil \frac{T_{max} - D}{\tau_{sup} + D} \right\rceil \quad \text{and} \quad n_{max} = \left\lfloor \frac{T_{max}}{D} \right\rfloor - 1$$

We run Algorithm) 5.1 for such dimensions and compare the profits obtained. When a τ_k, chosen randomly, is greater than τ_{sup} in the ARS algorithm (1.3.2), we simply discard it and draw another one.

With the parameter values in Table 4.1 and Subsection 5.0.2, $T_{max} = 4000$ days and a maximal fallow duration $\tau_{sup} = 60$ days, the algorithm converges to the solution illustrated in Figure 5.9. The associated profit is $R(\vec{\tau}^*) = 54285$ XAF, which is just 0.4% worse than the non-regulated solution obtained in Subsection 5.2.2. The final soil infestation after the last harvest is $P(T_{max}^+) = 223$ nematodes.

5.2.3.2 Penalizing dispersed fallows

The second regulation consists in limiting the dispersion of the fallow distribution $\vec{\tau}$ around the average fallow duration, i.e. the distance between $\vec{\tau}$ and the centre of the simplex denoted by $\vec{\tau}_0$. Thereby, we introduce a penalty function in the expression of the profit, which is proportional to this distance $d(\vec{\tau}, \vec{\tau}_0)$, and define the penalized profit by:

$$\tilde{R}(\vec{\tau}) = R(\vec{\tau}) - r\, d(\vec{\tau}, \vec{\tau}_0). \tag{5.7}$$

The regulation term r is taken such that the magnitude of the penalty term $r\, d(\vec{\tau}, \vec{\tau}_0)$ is an acceptable fraction of the magnitude of the unpenalized profit $R(\vec{\tau})$. Choosing $1/10$ for this faction, we deduce the value of r as follows:

$$r = \frac{R(\vec{\tau}_0)}{10 \times d_{max}},$$

where d_{max} stands for the longer distance to the centre of the simplex.

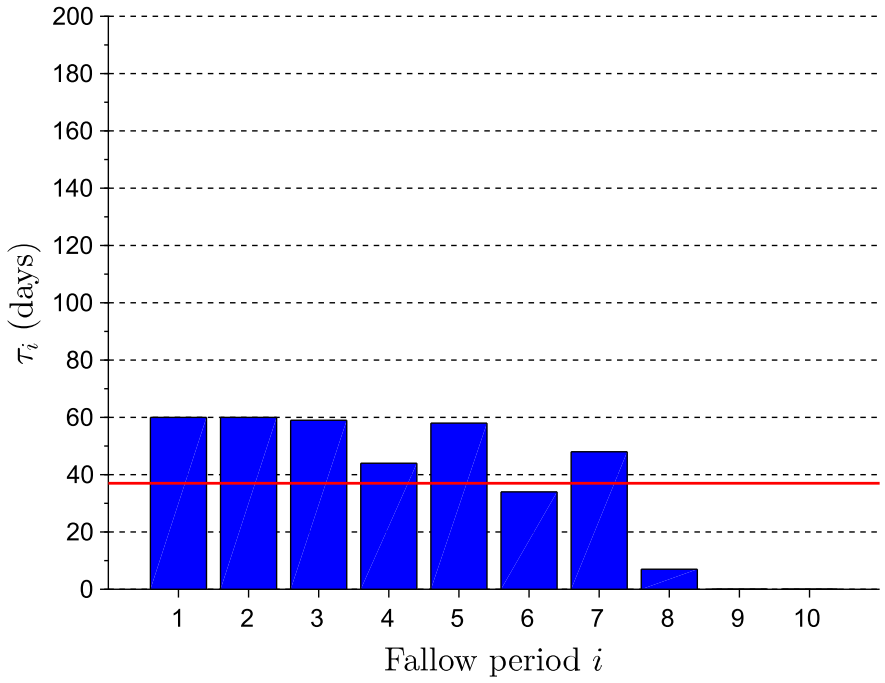

Figure 5.9 – Optimal distribution of fallow periods for time horizon $T_{max} = 4000$ days, when fallow durations are upper-bounded by $\tau_{sup} = 60$ days. The maximal profit is obtained for 11 cropping seasons and 10 fallows: $\vec{\tau}^* = (60, 60, 59, 44, 58, 34, 48, 7, 0, 0)$ (in days). The red line corresponds to the average fallow period $\tau = 37$ days.

We apply Algorithm 5.1 for the profit function $\bar{R}$ given by equation (5.7). The algorithm converges to the solution illustrated in Figure 5.10, using parameter values in Table 4.1 and Subsection 5.0.2, and $T_{max} = 4000$ days. The associated penalized profit is $\tilde{R}(\vec{\tau}^*) = 54250$ XAF, which is just 0.5% worse than the non-regulated optimum obtained in Subsection 5.2.2. The final soil infestation after the last harvest is $P(T_{max}^+) = 223$ nematodes.

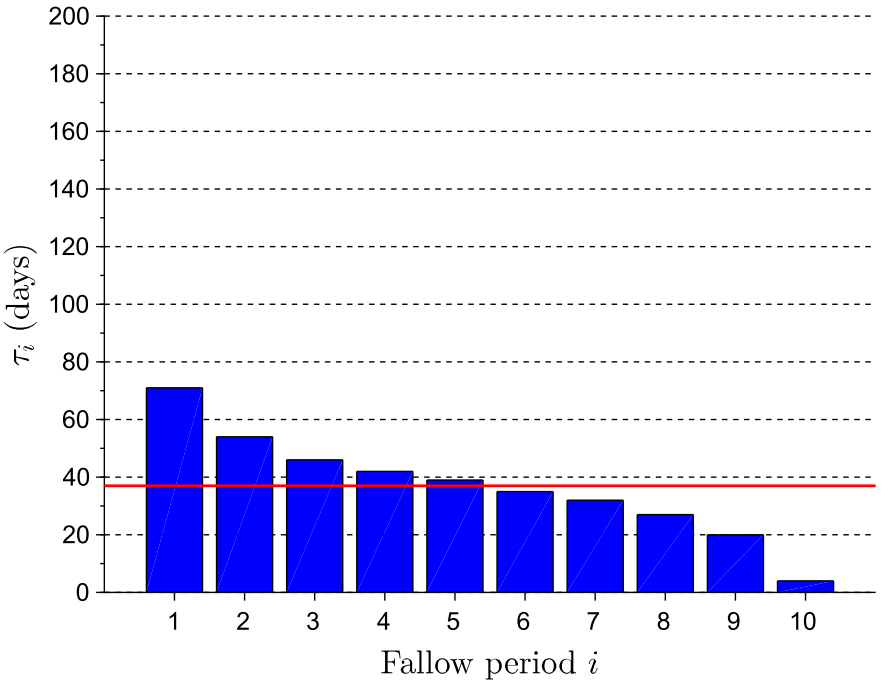

Figure 5.10 – Optimal distribution of fallow periods for time horizon $T_{max} = 4000$ days, when far from average fallow durations are penalized. The maximal profit is obtained for 11 cropping seasons and 10 fallows: $\vec{\tau}^* = (71, 54, 46, 42, 39, 35, 32, 27, 20, 4)$ (in days). The red line corresponds to the average fallow period $\tau = 37$ days.

5.2.3.3 Constant fallows

We previously deduced from monotonicity Assumption 5.2 that the last harvest should occur at T_{max} to optimize the profit. Indeed, since we could distribute the total fallow duration quite freely, it was always profitable to increase the fallow preceding the last cropping season, instead of deploying it at the end of the time horizon. In this section though, fallow durations are set to a constant value, which is an additional constraint that does allow the previous reasoning. We show below that, under the same Assumption 5.2, the last harvest of the optimal solution also occurs at T_{max}.

Given a fallow duration τ, the number of complete cropping seasons that can be deployed over time horizon T_{max} is given by:

$$N \equiv N(\tau) = sup\{n \in \mathbb{N} \mid T_{max} \geq nD + (n-1)\tau\}, \tag{5.8}$$

As an incomplete cropping season yields no income, because of the sucker cost it induces a negative profit.

Therefore, we assume that if τ leads to an incomplete season at the end end of the time horizon (corresponding to case (a) in Figure 5.2 but with constant fallows), the last sucker is not planted. We can then rewrite the profit (5.4) over T_{max} as:

$$R(\tau) = \sum_{k=1}^{N(\tau)} R_k, \tag{5.9}$$

and formulate the following optimization problem:

$$\tau^* = \arg\max_{\tau \geq 0} R(\tau). \tag{5.10}$$

Remark 5.4. Function $R(\tau)$ in equation (5.9) is not necessarily a continuous function of τ. A discontinuity may occur for τ values such that $N(\tau+\varepsilon) = N(\tau)-1 < N(\tau)$ for small positive values of ε. As an incomplete cropping season is not profitable and hence not implemented, this small increase of the fallow duration wastes a whole cropping season.

The previous remark shows that τ values such that $N(\tau+\varepsilon) < N(\tau)$ for small positive values of ε, locally maximize the profit "on the right": $R(\tau) > R(\tau+\varepsilon)$, provided that the yield of a cropping season is higher than the cost of a sucker. This assumption is reasonable as it ensures the viability of the cropping system. If it did not hold, the profit would be negative, and such τ values would minimize the profit "on the right".

Besides, if Assumption 5.2 holds, then such τ values maximize the profit "on the left". Indeed, when two different fallow durations correspond to the same number of cropping seasons, the longer fallow leads to a greater reduction of the pest population during the fallow, that in turn leads, by monotonicity, to a greater root biomass during the following cropping season and therefore to a better yield. Therefore, if Assumption 5.2 holds, the solution of Problem (5.10) belongs to the set:

$$\begin{gathered}\Xi = \left\{\tau \geq 0 : \frac{T_{max}-D}{D+\tau} \in \mathbb{N}\right\} = \left\{\frac{T_{max}-(n_{max}+1)D}{n_{max}}, \ldots, T_{max}-2D\right\}, \\ \text{with } n_{max} = \left\lfloor \frac{T_{max}}{D} \right\rfloor - 1.\end{gathered} \tag{5.11}$$

Still using parameter values in Table 4.1 and Subsection 5.0.2, and $T_{max} = 4000$ days, we plot in Figure 5.11 profit R as a function of fallow duration τ. The maximizer $\tau^* = 37$ days, leading to 10 fallow periods and 11 cropping seasons, belongs to Ξ as surmised. It corresponds to the average fallow period represented in Figures 5.8–5.10 (red line). The associated profit is $R(37) = 52000$ XAF, which is just 4.6% worse than the non-regulated optimum obtained in Subsection 5.2.2. The final soil infestation after the last harvest is $P(T_{max}^+) = 82$ nematodes, which is much lower than for the non-regulated optimum. Figure 5.11 also shows that this optimal constant fallow is 54% more profitable than no fallow ($R(0) = 32150$ XAF).

Using the unrealistic parameters of the monotonicity counterexample in Figure 5.4, for which Assumption 5.2 is no longer valid, we can build a counterexample in which the optimal fallow period duration is not an element of set Ξ defined above in equation (5.11). Indeed, setting $T_{max} = 680$, only one fallow period can be deployed and $\tau = 20$ is the only point of Ξ. However, as shown in Figure 5.4(b), $\tau = 20$ does not maximize (nor minimize) the profit.

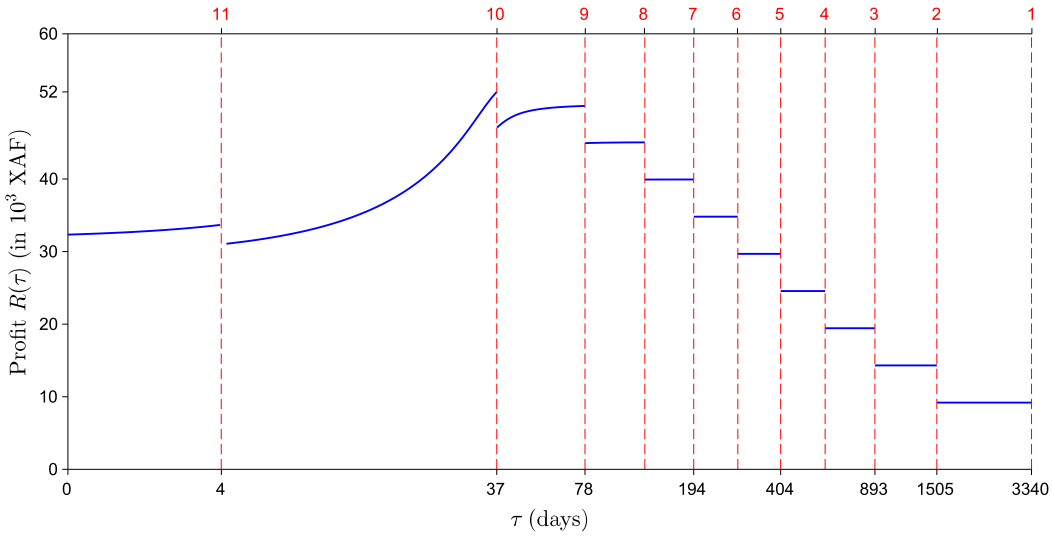

Figure 5.11 – Profit R as a function of fallow duration τ (logarithm scale) for time horizon $T_{max} = 4000$ days. The set $\Xi = \{4, 37, 78, 129, 194, 282, 404, 588, 893, 1505\}$ (in days), defined in equation (5.11), is represented by dashed red bars. Elements of Ξ correspond to discontinuities of the profit function, when the number of fallows n (upper axis) that fit in T_{max} is incremented (from right to left). The maximal profit $R^* = 52000$ XAF (79.27 euros) is obtained for $n = 10$ fallows of duration $\tau^* = 37$ days, which belongs to Ξ.

5.2.4 Comparisons

We compare the different optima obtained above when $T_{max} = 4000$ days, for the non-regulated and regulated strategies. In Figure 5.12, we represent the soil infestation after each harvest. In the most regular strategy, corresponding to constant fallows, the soil infestation follows a regular decrease over the seasons. For the other strategies, the soil infestation is first brought down, then rises again. The decrease and increase are sharper for the non-regulated strategy; in particular, the soil infestation is negligible right after the second harvest, but at its highest after the last harvest. The regulated strategies consisting of bounding or penalizing dispersed fallows induce similar soil infestations, especially after the last harvest at T^+_{max}. At this time, the soil infestation is much lower for constant fallows (up to three times lower).

The dynamical behaviour of soil infestation after each harvest is also reflected in the seasonal profits, since monotony (Assumption 5.2) makes lower infestations yield better profits. This is illustrated in Figure 5.13. Seasonal profits vary much less than soil infestations. As shown above in Subsection 5.2.3, bounding or penalizing dispersed fallows yields total profits that very similar to the optimal with no regulation. This holds also for seasonal profits. With constant fallows, the seasonal profit increases regularly; at the last season, it is higher than the profits generated by the other strategies.

5.3 Discussion and future work

We have shown in this paper that increasing the duration of fallow periods tends to reduce the pest population. In Chapter 4, we identified a threshold τ_0 above which constant fallows lead to the disappearance of the pest

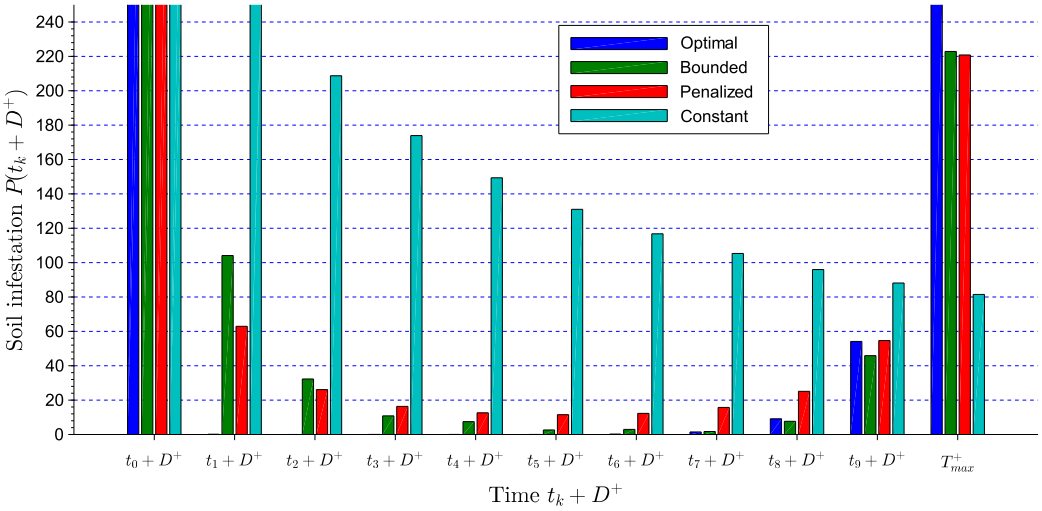

Figure 5.12 – Soil infestation after each harvest for the optimal non-regulated and regulated fallow deployment strategies over time horizon $T_{max} = 4000$ days. The non-regulated strategy (blue bars) corresponds to Figure 5.8. Regulations consist in bounding (green bars), penalizing (red bars) and setting constant (cyan bars) fallows; they correspond to Figures 5.9, 5.10 and 5.11, respectively. Soil infestations $P(t_0 + D^+)$ after the first harvest are the same for all strategies, as initial conditions are the same. All strategies involve 10 fallows, but as their durations differ among strategies, times t_k ($k = 1, \ldots, 9$) also differ.

asymptotically. With the parameters in Table 4.1, this threshold is $\tau_0 = 36.8$ days. However, the systematic deployment of fallow periods longer than this threshold may not be optimal in terms of profit. On the one hand, such a deployment ensures that the pest declines in the long run, but in the short to medium term, quite longer fallows may be needed to significantly reduce the pest population and ensure higher seasonal profits. On the other hand, deploying long fallow periods could induce the loss of one or more cropping seasons on a given finite time horizon, which in turn could affect the total profit. Our optimization problem aimed at finding the right balance. For a time horizon of a little less than 11 years, we showed that it is preferable to deploy 11 rather than 12 cropping seasons in order to increase the total fallow time. The optimal solution consists of deploying a very long fallow after the first harvest, to drastically reduce the soil infestation, and then intermediate fallows during four more years (Figure 5.8). Pests remain relatively low until the end of the second to last cropping season, when they increase considerably (Figure 5.12). The last seasonal profit hence decreases (Figure 5.13), but further consequences of this optimal strategy would occur later, beyond the time horizon, which is a common issue for finite horizon optimization problems. In future work, to overcome this issue, we could penalize the final soil infestation.

In this work, we chose to tackle another issue exhibited by this optimal solution, which is the dispersal of the fallow distribution around the average fallow duration (Figure 5.8). The first long fallow of the unconstrained optimal strategy allows to drastically sanitize the soil, which is initially heavily infested. For several reasons, this solution may not be adopted by growers. First, this solution implies an irregular crop calendar. The crop calendar is the schedule of cultural operations needed in crop production with respect to time, such as sowing, fertilizing, harvesting. A regular schedule allows a better planning of farm activities, including the distribution

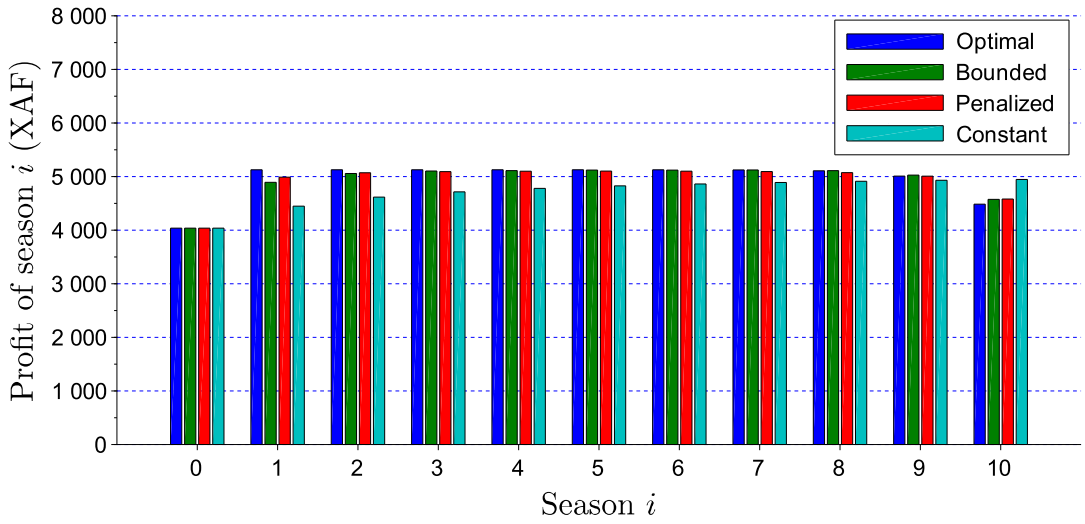

Figure 5.13 – Seasonal profits of banana crop under different strategies of fallow deployment. for the optimal non-regulated and regulated fallow deployment strategies over time horizon $T_{max} = 4000$ days. The non-regulated strategy (blue bars) corresponds to Figure 5.8. Regulations consist in bounding (green bars), penalizing (red bars) and setting constant (cyan bars) fallows; they correspond to Figures 5.9, 5.10 and 5.11, respectively. Profits of the first season are the same for all strategies, as initial conditions are the same.

of labour. Second, a long period without crop also means a long period with reduced earnings. Another crop could be planted between banana cropping seasons instead of a fallow, provided that this inter-crop is a poor host of the pest. Otherwise, it would not help to control the pest population. To implement such rotation, intervals between banana cropping seasons should long enough to grow the inter-crop. This is why the optimal solution was regularized by bounding fallows (Figure 5.9), penalizing dispersed fallows (Figure 5.10) or setting constant fallows (Figure 5.11). Regulating the fallow duration requires to maintain the sanitation effort longer but induces limited profit losses. Constant fallows, besides being perfectly regular, leads to the lowest soil infestation after the last harvest, with only a small reduction of the total profit. Hence, the crops that are planted afterwards will benefit from less infested soil. Constant fallows, possibly replaced by a poor host inter-crop, are therefore a good trade-off between profit and cultural constraints. A naïve method of obtaining constant fallow distributions could be to set a desired number of cropping seasons, then subtract from the time horizon the total time these cropping seasons cover, and equally distribute the result to the different fallow periods. However, we can see in Figure 5.11 that the profits are very variable depending on the number of cropping seasons. We observe that for this example, 11 growing seasons would give a terribly lower profit than 12 growing seasons. It is even worst for 3, 4 or 5 cropping seasons. The problem of choosing the right number of cropping seasons would therefore arise and would bring us once again to the optimization of the profit defined by Equation 5.4.

We opted for a purely “profit-based" optimal cost because those were the terms we could quantify. Penalizing the density of nematodes at the end of the time horizon in the objective function would require a weighting parameter that would not be easy to adjust. We could say that the cost we optimize is the one that really matters to the grower, and that, after the end of the considered time period, he can choose to change the crop to a non-host crop for a while in order to sanitize the soil. However, if the grower wanted to keep growing banana

plants after the time-period of interest, including such a term including the final nematode density would be necessary, so as to ensure that his field has not become unsuitable for bananas by that time.

Determining such optimal fallow deployment strategies requires a good knowledge of the plant-pest interaction parameters, as well as the initial infestation. In this study, we gathered data from various published studies to inform our model parameters. Still, more quantitative experimental work on banana–nematode dynamics would help strengthen our conclusions.

There are some limitations in our model that could lead to further developments. Firstly, we do not take into account the possible toppling of the plant. Indeed, above a certain damage level, the plant falls and the yield for that season is then totally lost [16, 14]. This goes hand in hand with the monotonicity Assumption 5.2 that ensures the "good properties" of our optimization problem. An infestation level high enough to induce the loss of monotonicity could lead to the toppling of the plant. Secondly, the use of nursery-bought healthy vitro-plants comes at a fairly high cost. Third, the measurement of the initial infestation of soils, which is an input parameter of our optimization, is difficult. It could, however, be based on estimates made using methods of counting free-living nematodes in the soil that can be found in the literature. The count can be done by a quantitative estimate of nematodes in small soil samples [74], the Galleria-trap method [4, 56] which seems more suitable for entomophagous nematodes, or geostatistical analysis [149]. Nevertheless, these techniques are often destructive of the biotope as they require the removal of soil samples. It would also be interesting to know how a bad measurement of the initial infestation influences the yields. On the other hand, the infestation can be influenced by the factors of the dissemination of *R. similis*. Nematodes can indeed be transported by tillage machinery [77], and water in very flooded plantations [33]. But the transport of contaminated banana strains and suckers is considered to be the main mode of dissemination of *R. similis* [44, 25] and active dissemination in the soil remains very marginal [86]. Thus, if the vitro-plants planted at the beginning of each season are not completely healthy, they could lead to values of $X(t_k^+)$ more or less different according to the seasons. Taking into account possible variations in these values of $X(t_k^+)$ should lead to systems with impulsive noise or discontinuous Markov processes, and it will be a question of finding new methods of analysis and optimization.

Finally, banana producers are well aware that the vegetative reproduction of bananas does not need growers to sow new suckers at the beginning of each season. In fact, banana and plantain have their own natural reproduction that relies on the growth of a lateral bud, which gives a new plant. Therefore, they may not need to plant new suckers at the beginning of each season, especially since healthy suckers have a cost. It is advisable to combine the planting of healthy suckers with the growth of the banana plant by lateral shot. This leads to more complex strategies in order to manage in the same time the moments where fallow periods occur and their distribution. This is the aim of the following chapter.

CHAPTER SIX

TOWARD A MIXED CONTROL STRATEGY

In Chapter 4, we built two models with two different banana plant reproduction means: the natural reproduction that relies of outgrowths of the vegetative buds, and the planting of healthy vitro-plants after eventually a fallow period. In Chapter 5, we relied on the latter reproduction mean, and we optimized the durations of fallow periods between cropping seasons. In this chapter, the plant reproduces naturally during several seasons. After these successive seasons, a fallow is implemented. Following this fallow, the reproduction necessarily relies on planting a healthy vitroplant. We name *chain*[1] the set of successive cropping seasons and the single fallow that follows.

Let us denote by;

1. C_i the i-th chain;
2. t_i the starting point of chain $C_{(i+1)}$;
3. t_i^j the starting point of the $(j+1)$-th season within chain $C_{(i+1)}$;
4. l_i the number of cropping seasons within chain $C_{(i)}$, defining the *size of the chain*;
5. τ_i the fallow duration of chain C_i, which follows the l_i cropping seasons;
6. T_i the duration of chain C_i.

Hence, cropping season j within chain C_i holds on the interval $(t_{i-1}^{j-1}, t_{i-1}^{j}]$.

Remark 6.1. $t_i^j = t_i + jD$, for all $j = 1, \ldots, l_i - 1$ and $T_i = l_i D + \tau_i$.

Remark 6.2. A chain depends on its size l_i and its fallow duration τ_i, $C_i \equiv C_i(l_i, \tau_i)$.

A mixed strategy consists in a succession of chains and is illustrated in Figure 6.1.

6.1 Optimization problem

According to the definitions in Section 5.0.1, we define the profit of one cropping chain C_i as follows:

$$R(C_i) = R(l_i, \tau_i) = -c + \sum_{j=1}^{l_i} \int_{t_{i-1}^{j-1}}^{t_{i-1}^{j}} mS(t)dt. \tag{6.1}$$

[1] We could have called it *cycle*, but in the banana farming literature, the word *cycle* more commonly designates the growth time of a single banana plant from the time it is a viable sucker until the time it dies, in a context of natural reproduction.

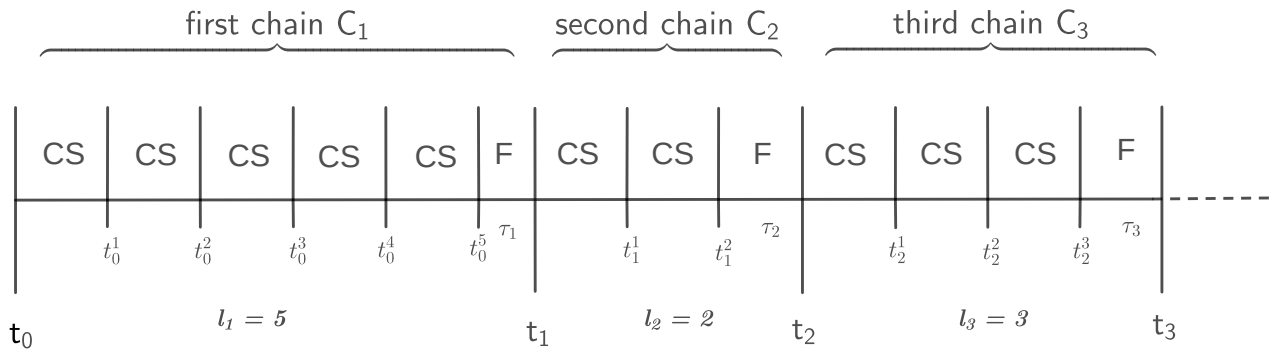

Figure 6.1 – Illustration of the first three chains of a mixed strategy. Each chain C_i contains l_i cropping seasons (CS) and one fallow (F). Cropping seasons have a fixed duration (D) but fallow durations τ_i may vary.

Hence, the profit of $n+1$ chains $C_0, C_1, \ldots, C_n$ is given by:

$$R(C_0, C_1, \ldots, C_n) = R\big((l_i, \tau_i)_{i=0,\ldots,n}\big) = \sum_{i=0}^{n} R(l_i, \tau_i). \tag{6.2}$$

On a finite time horizon T_{max}, the (l_i, τ_i) are such that $\sum_{i=0}^{n}(l_i D + \tau_i) \leq T_{max}$. With this condition, R admits a maximum according to the same arguments as in Chapter 5. If we name $\mathbb{A}^n$ the set of $(l_i, \tau_i)_{i=0,\ldots,n}$ in $\mathbb{N}^* \times \mathbb{R}^*$, and $\mathcal{A}$ the reunion of $\mathbb{A}^n$, $n \geq 0$, then we state the general optimization problem as follows:

Problem 6.1. Find the optimal sequence $(l_i^*, \tau_i^*)_{i=0,\ldots,n} \in \mathcal{A}$ of chain sizes and fallow durations that maximizes R defined in equation (6.2) on a finite time horizon T_{max}.

Problem 6.1 admits a solution, but determining an optimal deployment strategy without any constraint is not obvious. Therefore, we concentrate on solving the problem on the case of fixed-size chains, with either constant or varying fallows.

6.2 Optimization with fixed-size chains and constant fallow

This subsection deals with the solution of Problem 6.1 with fixed-size chains of size l when fallow durations are set to a constant value τ. Hence, mixed deployment strategies consist of a succession of identical chains.

6.2.1 Resolution

The maximal chain size l_{max} corresponds to a cropping strategy in which fallow periods are never deployed over T_{max}. Hence we have $l_{max} = \left\lfloor \frac{T_{max}}{D} \right\rfloor$.

Given a chain size $l \in \{1, \ldots, l_{max}\}$ and a fallow duration τ, the number of complete chains that fit within the time horizon T_{max} is given by:

$$N \equiv N(l, \tau) = \left\lfloor \frac{T_{max} + \tau}{lD + \tau} \right\rfloor, \tag{6.3}$$

with the last chain allowed to have no fallow period.

Example 6.1. Let $T_{max} = 4000$ days and $D = 330$ days as in Table 4.1. The number of chains of size $l = 3$ and fallow duration $\tau = 10$ days is given by:

$$N(3, 10) = \left\lfloor \frac{4000 + 10}{3 * 330 + 10} \right\rfloor = 4.$$

If $\tau = 12$ days, still $N = 4$ both the 4^{th} chain ends with a 4-day fallow.

N is bounded as follows:

$$1 \leq N(l, \tau) \leq N(1, 0) = \left\lfloor \frac{T_{max}}{D} \right\rfloor. \tag{6.4}$$

If $T_{max} - (lD + \tau)N > D$, then an incomplete chain, i.e. a chain with less than l cropping seasons, can be introduced at the end of the complete chains. Formally, let $M = T_{max} - (lD + \tau)N$. If $M > D$ then let $p = \lfloor \frac{M}{D} \rfloor$. On can deploy an additional chain of size p and write profit (6.2) in this particular framework as follows:

$$R(l, \tau) = -c(N + 1) + m \sum_{i=1}^{N} \sum_{j=1}^{l} \int_{t_i^{j-1}}^{t_i^j} S(t)dt + m \sum_{j=1}^{p} \int_{t_N^{j-1}}^{t_N^j} S(t)dt, \tag{6.5}$$

where $N = N(l, \tau)$.

The profit $R(l, \tau)$ has a maximum for $(l, \tau) \in \Omega = \{1, \ldots, l_{max}\} \times [0, T_{max} - (l_{max} + 1)D]$.

The optimization problem with fixed-size chains and constant fallow can therefore be written as follows:

Problem 6.2. Find $(l^*, \tau^*) \in \Omega$ such that $R(l^*, \tau^*) = \max_{(l,\tau)\in\Omega} Y(l, \tau)$, with $R(l, \tau)$ defined in equation (6.5).

Since the set of values of l is countable, we seek the solution τ^* of Problem (6.2) for each $l \in \{1, \ldots, l_{max}\}$ and compare them.

Remark 6.3. If $l = l_{max}$, there can be only one chain and the solution is trivial.

Remark 6.4. The solution is highly likely to be unique. If not, we could choose the solution that has the highest total fallow duration $\tau N(l, \tau)$ [2]. Different tie-break rules could be defined, depending on agricultural needs.

6.2.2 A case study

We solved Problem 6.2 numerically using the same parameter values than in Chapter 5. Table 6.1 summarizes the optimal fallow durations for all possible chain sizes l over the time horizon $T_{max} = 4000$, and the yields that they generate. The optimum is obtained for $l^* = 1$, meaning that the chains consist of one cropping season followed by a fallow period. The optimal fallow duration obtained is $\tau^* = 37$ days and it generates a profit of 52,000 XAF (79.3 euros). It corresponds to the optimum obtained with systematic and constant fallows.

Several conclusions can be drawn from Table 6.1:

1. The most profitable deployment is obtained for chains of size 1. This means that the cost of the vitroplant that could be saved by adopting vegetative reproduction is not sufficient to compensate for the loss of yield due to the infestation.

[2] The longer the fallow, the fewer crops are planted, thus reducing the cropping effort

Chain size l	Optimal fallow duration τ^*	Optimal number of complete chains N^*	Max number of complete chains	Number of cropping seasons of the incomplete chain p^*	Profit(XAF)
1	**37**	**11**	**12**	**0**	**52,000**
2	175	5	6	0	47,550
3	233	3	4	1	46,400
4	350	2	3	2	43,020
5	700	2	2	0	42,105
6	370	1	2	5	42,240
7	370	1	1	4	42,690
8	370	1	1	3	39,035
9	370	1	1	2	37,830
10	40	1	1	2	35,150
11	40	1	1	1	38,180
12	0	1	1	0	34,960

Table 6.1 – Optimal fallow durations and generated profits for different chain sizes obtained for mixed deployment strategies with fixed-size chains and constant fallows. The line in bold print indicates the overall optimum, obtained here for chains of size 1.

2. The optimal chains of size 6 are more profitable than the optimal chains of size 5, although the infestation is likely to get higher with 6 successive cropping seasons. This is because the former allows one more season (11) than the latter (10). However, the optimal chain of size 7, which allows the same number of cropping seasons (11), gives a better yield although it has more successive cropping seasons. In the same way, the optimal chain of size 11 gives a better yield than the ones of size 10.

3. The previous cases aside, increasing the chain size decreases the profit. This partly depends on the cost of the vitroplant. If we increase this cost tenfold, such that its value becomes $c = 2300$ XAF, we obtain the results depicted in Table 6.2. In this case, the profit reaches its optimal value R = 38550 XAF for a single chain of size $l = 7$, a single fallow period of duration $\tau = 370$ days, and a 4-season incomplete chain, in stark contrast with the previous case.

6.3 Optimization with fixed-size chains and varying fallows

In this subsection, chains still have a constant size, but fallow durations vary. To simplify matters, rather than seeking for an optimal fixed-size chain, we aim at optimizing the fallow distribution, based on the optimal chains obtained in Subsection 6.2 with constant fallows.

Chain size l	Optimal fallow duration τ^*	Optimal number of complete chains N^*	Max number of complete chains	Number of cropping seasons of the incomplete chain p^*	Profit (XAF)
1	37	11	12	0	29,230
2	175	5	6	0	37,200
3	233	3	4	1	38,120
4	350	2	3	2	36,810
5	700	2	2	0	37,965
6	370	1	2	5	38,100
7	**370**	**1**	**1**	**4**	**38,550**
8	370	1	1	3	34,875
9	40	1	1	3	33,860
10	40	1	1	2	31,010
11	40	1	1	1	34,040
12	0	1	1	0	32,890

Table 6.2 – Optimal fallow durations and profits obtained for different chain sizes obtained for mixed deployment strategies with fixed-size chains and constant fallow. The vitroplant cost here is $c = 2300$ XAF. The line in bold print indicates the overall optimum, obtained here for chains of size 7.

6.3.1 Resolution

For a chain of size l, if N is the number of complete chains of size l and p the number of complete cropping seasons of the incomplete chain, then we look for a distribution $(\tau_i)_{i=1,\dots,N}$ of fallow periods such that:

$$\sum_{i=1}^{N} \tau_i = T_{max} - (NlD + pD), \tag{6.6}$$

which means that the last harvest occurs at T_{max}, with the last chain possibly being incomplete.

Let us define the simplex:

$$A_l^{N,p} \equiv \{(\tau_i)_{i=1,\dots,N} \subset \mathbb{R}^+ : \sum_{i=1}^{N} \tau_i = T_{max} - (klD + pD)\} \tag{6.7}$$

We define the profit for N chains of size l with an incomplete chain of size p, namely the profit of $(\tau_i)_{i=1,\dots,N}$ on $A_l^{N,p}$, as follows:

$$R_l^p(\tau_0, \dots, \tau_{N-1}) = -(N+1)c + \sum_{i=1}^{N}\sum_{j=0}^{l-1} \int_{t_i^j}^{t_i^{j+1}} mS(t)dt + \sum_{j=0}^{p-1} \int_{t_N^j}^{t_N^{j+1}} mS(t)dt. \tag{6.8}$$

The optimization problem we want to solve is the following.

Problem 6.3. Given $l \in \{1, \dots, l_{max}\}$, $p^* < l$, and $N^* > 0$ such that $T_{max} - (N^*lD + p^*D) \geq 0$, find $\vec{\tau}^* = (\tau_i^*)_{i=1,\dots,N} \in A_l^{N^*,p^*}$ such that

$$R_l^{p^*}(\vec{\tau}^*) = \max_{\vec{\tau} \in A_l^{N^*,p}} R_l^{p^*}(\vec{\tau})$$

,

where N^* and p^* are the optimal values obtained solving Problem 6.2 with l fixed.

After having determined the solution with constant fallow durations τ^*, we capture the values of l, N^* and p^* from this solution. We then find the optimal fallow distribution with N^* fallow periods, chains of size l and a last chain of size p^* by running an adaptive random search algorithm (see Appendix 1.3.2) on the simplex $A_l^{N^*,p^*}$.

6.3.2 A case study

We solve Problem 6.3 numerically, using the same parameter values than in Chapter 5. We find the optimum for each $l \in \{1, \ldots, l_{max}\}$ in order to perform comparisons. The optimum is obtained for $l^* = 1$. It corresponds to the solution obtained with systematic fallow deployment represented in Figure 5.8(a). Figure 6.2 gives a visual representation of this optimal solution. Table 6.3 summarizes the optimal distributions of fallow durations for all possible chain sizes and the profits that they generate.

Chain size l	Optimal fallow distribution τ^*	Optimal number of complete chains N^*	Number of cropping seasons of the incomplete chain p^*	Profit (XAF)
1	**(192, 81, 14, 39, 42, 0, 2, 0, 0, 0)**	**11**	**0**	**54,530**
2	(664, 0, 0, 0, 36)	5	0	47,615
3	(699, 0, 1)	3	1	46,625
4	(698, 2)	2	2	43,075
5	(610, 90)	2	0	42,105
6	(370)	1	5	42,240
7	(370)	1	4	42,690
8	(370)	1	3	39,035
9	(370)	1	2	37,830
10	(40)	1	2	35,150
11	(40)	1	1	38,180
12	(0)	1	0	34,960

Table 6.3 – Optimal fallow duration distributions and profits obtained for different chain sizes for the mixed deployment strategy with fixed-size chains and varying fallow. The line in bold print indicates the overall optimum, obtained here for chains of size 1.

Several conclusions can be drawn from Table 6.3:

1. As in the previous subsection, the most profitable deployment is obtained for chains of size 1. It corresponds to 11 cropping seasons, whereas the time horizon can span up to 12 cropping seasons.

2. Table 6.4 gives the optimal fallow distributions and profits for all possible chain sizes when we increase the cost of vitroplants tenfold. The optima are obtained for the same distributions as in Table 6.3, but the profits are lower due to the higher vitroplant cost. The optimal deployment is obtained for 3 complete chains of size 3, whereas it is obtained for chains of size 7 when fallows are constant, as shown in Table 6.2. The optimal deployment with variable fallows allows for a very long fallow period (699 days)

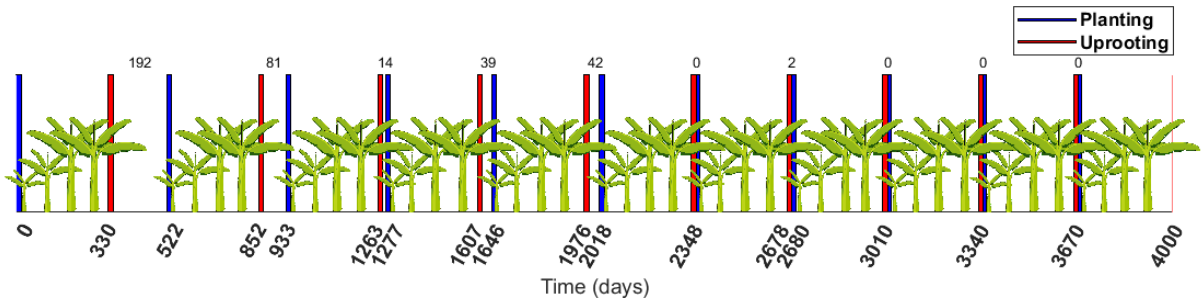

Figure 6.2 – Visual representation of the optimal mixed deployment strategy with fixed-size chains and variable fallows. The optimum is obtained for chains of size 1 and the fallow distribution (192, 81, 14, 39, 42, 0, 2, 0, 0, 0). The blue bars correspond to the planting of nematode-free vitroplant while the red bars correspond to the uprooting of plants after the harvest of the fruit bunch. The filled spaces over the course of time correspond to banana cropping seasons while the white spaces correspond to fallows whose durations are indicated at the top. Some fallows last 0 days and in these cases, the old plant is still uprooted and a nematode-free vitroplant is planted.

early on, which drastically reduces the nematode infestation. Figure 6.3 gives a visual representation of this optimal solution.

3. For the longer chain sizes ($l \geq 6$), which only allow 1 complete chain and hence 1 fallow period, results with fixed (Tables 6.1 and 6.2) and varying fallows (Tables 6.3 and 6.4) are identical in terms of optimal fallow duration and profit.

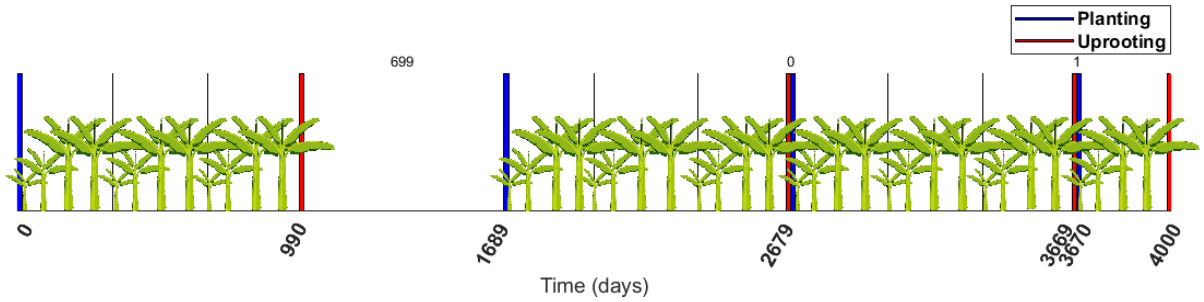

Figure 6.3 – Visual representation of the optimal mixed deployment strategy with fixed-size chains and variable fallows. The optimum is obtained for chains of size 3 and the fallow distribution (699, 0, 1). The vitroplant cost here is $c = 2300$ XAF. The blue bars correspond to the planting of nematode-free vitroplant while the red bars correspond to the uprooting of plants at the end of the chain. The filled spaces over the course of time correspond to banana cropping seasons while the white spaces correspond to fallows whose durations are indicated at the top. In this strategy, a single 370-day long fallow is deployed.

Chain size l	Optimal fallow distribution τ^*	Optimal number of complete chains N^*	Number of cropping seasons of the incomplete chain p^*	Profit (XAF)
1	(192, 81, 14, 39 42, 0, 2, 0, 0, 0)	11	0	31,760
2	(383, 274, 0, 43, 0)	5	0	37,265
3	**(699, 0, 1)**	**3**	**1**	**38,845**
4	(698, 2)	2	2	36,865
5	(610, 90)	2	0	37,965
6	(370)	1	5	38,100
7	(370)	1	4	38,550
8	(370)	1	3	34,895
9	(370)	1	2	33,690
10	(40)	1	2	31,010
11	(40)	1	1	34,040
12	(0)	1	0	32,890

Table 6.4 – Optimal fallow durations and yields obtained for different chain sizes in the mixed control strategy with fixed-size chains and varying fallow when the cost of a healthy vitroplant is $c = 2300$ XAF. The line in bold print indicates the overall optimum, obtained here for chains of size 3.

6.4 Conclusion

In sections 6.2 and 6.3, we have seen that the optimal solutions with fixed-size chains are obtained with chains of size 1. This is because with larger chains, the infestation quickly becomes very high, which significantly reduces the yield. We have thus shown that the gain obtained by saving the cost of vitroplants when the seasons are allowed to chain by vegetative reproduction is not significant enough to compensate for the profit loss due to a higher infestation. We analysed nevertheless the solutions with different chain sizes, which showed profit losses of at least 8.56% compared to the optimal solution (size 1 chains). However, the conclusions changed when we increased the price of the vitroplant tenfold because the gain was much higher. In such case, the optima were found for chains of size 7 for constant fallows (Table 6.2) and chains of size 3 for variable fallows (Table 6.4).

The result of this optimization might be different if we admit different chain sizes from one chain to another. In this case, the size of the chains and the duration of the fallow periods must be optimized dynamically. Controlling chain sizes, which are necessarily integer values, could give rise to combinatorial problems. Several perspectives therefore emerge from this first approach to mixed deployment:

- We could control both the fallow durations and the size of the chains, so that the strategy decides at the end of each season, whether to let the plant reproduce or deploy a fallow (possibly of null duration), and in the latter case, how long a fallow. This amounts to finding the general solution to Problem 6.1. Enumerating all the possible distributions $(l_i)_i$ of chain sizes and optimizing these distributions is not feasible over long time horizons as the number of distributions can explode very quickly. Also, it depends on the distribution of fallow periods. It is therefore necessary to optimize both simultaneously.

- When the seasons follow one another without uprooting, the infestation increases significantly, which

has the effect of bringing the root biomass to very low levels (see Chapter 4, Fig.7). A low level of root biomass, which seems easy to obtain in this model, could lead to the fall of the plant [8, 120]. Moreover, banana suckers have a critical minimum level of root biomass to insure their survival [115]. As discussed in Chapter 5 could model the fall of plants by introducing an Allee effect in root growth, so that below this critical level the fresh root biomass would tend to perish.

The key input parameters of our optimization are the time horizon T_{max} and the initial soil infestation P_0. Hence, in order to apply our strategy in an operational context, the soil infestation has to be measured. Counting free-living soilborne nematodes is not an easy task but some methods are often adopted like the quantitative estimate of nematodes in small soil samples or geostatistical analysis [74, 149]. After these measurements, and provided that the model parameters are well-calibrated, our optimization algorithm describes when to plant and when to leave the soil bare to have the best economic returns by the horizon T_{max}. Also, before applying such strategies in the field, agricultural constraints should be taken into consideration in our optimization problem. For instance, fallow durations would certainly need to be upper-bounded, as long periods without crops also mean long periods with reduced earnings. These strategies would probably meet with low acceptability among banana producers, who might prefer using nematicides. Fallow durations could also be lower-bounded, so as to implement crop rotations between banana plants and other crops that could provide an extra income. This approach could be extended to other soil-borne pests that are obligate root parasites, as fallow deployment would similarly impact their development. The seasonal model would need to be adapted to take into account the pest population dynamics and its interactions with the plant host.

Part V

Conclusion

Conclusion

This thesis focused on the mathematical modelling and control of the plantain plant parasitic nematode *Radopholus similis*. Since there is no sharp distinction between banana and plantain, as their of the same specie (Musa spp.), we named both of them "banana" throughout this thesis. The main objective was to give a first modelling approach of its interaction with its host using dynamical systems, and also to model eco-friendly means of control. We reviewed literature about the biologies of *R. similis* and banana plants in Chapter 2. Since there was, to our knowledge, only one mathematical and computational model adapted to *R. similis* in the literature [133], we enlarged our literature review to encompass soilborne pests in general. Hence, we proposed in Chapter 3 a literature review on mathematical modelling of soilborne pests - including *R. similis* - and crop rotation models for such soilborne pests. The main contributions of the work are found in Chapters 4, 5 and 6. Chapter 4 is related to publication of the papers [124] and [126]. Chapter 5 is related to a manuscript published in Applied Mathematics and Computations in 2021 [122] and has been presented in many symposia and conferences [135, 46, 125]. Chapter 6 is related to an ongoing work whose first results have been published in Journal of Interdisciplinary Methods and Issues in Sciences [123].

Our first contribution, presented in Chapter 4, consists in two deterministic semi-discrete models of plant-nematode interaction over multiple seasons. The models differ each to other by the control strategies implemented therein, and the mean of reproduction of the crops. In the first model, the infestation was controlled by pesticides, which are still widely used, and the banana plant reproduced itself vegetatively by producing a lateral sucker. In the second model, the infestation was controlled by introducing a fallow period after each cropping season, and the reproduction of the plant was insured by planting of a new nematode-free vitro-plant. The objective was, on the one hand, to understand the interaction of the burrowing nematode *R. similis* with banana roots, namely the oscillatory levels of pest population. On the other hand, we wanted to compare the chemical control and the fallowing, in order to analyse their effectiveness. For both models, the basic reproduction number was computed in order to determine the local long-term stability of the systems. Whether we used pesticides or fallow, the basic reproduction could be brought below the threshold 1, such that the pest population tends to disappear on a more or less long time. However, we showed that the chemical control was not very effective because of the large amounts required.

Our second contribution, presented in Chapter 5, focused on the control of the pest through optimal fallow deployment, which has a greater respect for the environment than chemical methods. The optimization was based on the multi-seasonal model with fallow presented in Chapter 4. The aim was to find the best way, in terms of profit, to allocate the durations of fallow periods between the cropping seasons, over a fixed time horizon spanning several seasons. The existence of an optimal allocation was proven and an adaptive random search algorithm was proposed to solve the optimization problem. It arose that for a relatively long time

horizon, deploying one season less than the maximum possible number of cropping seasons allows to increase the fallow period durations and results in a better multi-seasonal profit. For regular fallow durations, the profit was lower than the optimal solution, but the final soil infestation was also lower.

In our last contribution, presented in Chapter 6, we proposed a framework to generalize the control proposed in Chapter 5. We introduced the notion of cropping chain, that is a family a successive cropping seasons that are not interrupted by a fallow period. At the end of a chain, the plant is uprooted after the harvest of its bunch and a fallow is deployed until the beginning of the following chain. Introducing this notion, our model encompassed both of the two reproduction strategies presented in Chapter 4. Our aim was to know when and how to fallow. Namely, we stated an optimization problem aiming to know how many cropping seasons should be have each cropping chain and how long should be the fallow periods between the chains. We obtained first results for fixed-size chains, for which the optimal solutions was always the solution with chains of one cropping season, and therefore coincided with the results in Chapter 6. We established comparisons with different size of chains and analysed the difference. We have in perspective to go further by considering chains with different sizes, such that we are going to couple a combinatoric optimization and a dynamical optimization.

The fallow deployment strategies developed in this thesis may well be exported for a wider range of soil pathogens, subject to possibly modifying the dynamics of interaction of the pathogen with the plant, or the specific dynamics of the plant. For example, stopping root growth after plant flowering may not occur for other plant species. Also, the laying of the pathogen could be done exclusively inside or exclusively outside the roots. A review of the literature [57] allows us to list a range of soilborne pathogens that a deployment of fallow, with sowing of healthy seeds, allows to control. In the large *Brassicaceae* family in which we find cabbage, turnip, rapeseed, mustard, horseradish, watercress, the control of cyst nematodes of *Heterodera* species can rely on crop rotation, possibly with fallow periods. The same is true for the control of charcoal rot caused by the fungus *Macrophomina phaseolina*, which mainly attacks cucurbits or solanaceae and whose management can be based on crop rotations and fallow deployments. Solonaceae and legumes such as lentils, beans, and in particular peas, are threatened by soilborne pathogens such as root-knot nematodes of the *Meloidogyne* species, and whose management can be based on crop rotations with possibly fallow deployments. It is the same for the stem and bulb nematode *Ditylenchus dipsaci* which attacks liliaceae such as garlic and hyacinth.

Infections from multiple soilborne pathogens sometimes result in a disease complex that can further damage the crops. Positioning *R. similis* in its ecological community [93] therefore becomes a crucial issue in the extension of our models. It is necessary to extend our models in the future, in order to include the dynamics of competing or facilitating organisms, which interact with *R. similis* and potentially with plant roots. The conclusions in terms of strategy that the ecological community of pests may surprise us.

Part VI

Bibliography

Bibliography

[1] P. Arias, C. Dankers, P. Liu, and P. Pilkauskas. *The world banana economy, 1985-2002*, volume 1. Food & Agriculture Org., 2003.

[2] *Banana Cultivation Guide*, Consulted on March 23, 2018.

[3] S. Basu and J. Andrews. Complexity in mathematical models of public health policies: A guide for consumers of models. *PLOS Medicine*, 10(10):1–6, 10 2013.

[4] R. Bedding and R. Akhurst. A simple technique for the detection of insect parasitic rhabditid nematodes in soil. nematol. 21, 109–110, 1975.

[5] R. Bellman. Dynamic programming. *Science*, 153(3731):34–37, 1957.

[6] M. Beugnon and J. Champion. Etude sur les racines du bananier. *Fruits*, 21(7):309–327, 1966.

[7] C. D. Blake. The histological changes in banana roots caused by *Radopholus similis* and *Helicotylenchus multicinctus*. *Nematologica*, 12:129–137, 1966.

[8] C. D. Blake. *Nematode diseases of banana plantations*. London, UK: Academic Press, 1972.

[9] D. Blake, C. Root rot of bananas caused by *Radopholus similis* (Cobb) and its control in New South Wales. *Nematologica*, 6(4):295–310, 1961.

[10] A. Burr and A. Robinson. *Locomotion Behavior*, chapter 2, pages 25–62. CAB International, 01 2004.

[11] J. Cauthen, D. B. Jones, M. K. Gugerty, and C. L. Anderson. Banana and plantain value chain: West Africa. In *Evans School Policy Analysis And Research (EPAR)*, 2019.

[12] C. Chabrier. *Survie et dissémination du nématode Radopholus similis (Cobb) Thorne dans les sols bruns-rouilles à halloysites (nitisols): effets de l'état hydrique et des flux hydriques*. PhD thesis, Université des Antilles-Guyane, 2008.

[13] C. Chabrier, C. Carles, P. Quénéhervé, and Y.-M. Cabidoche. Nematode dissemination by water leached in soil: Case study of *Radopholus similis* (Cobb) Thorne on nitisol under simulated rainfall. *Applied Soil Ecology*, 40(2):299–308, 2008.

[14] C. Chabrier, J. Hubervic, and P. Quénéhervé. Evaluation de l'efficacité de deux formulations d'oxamyl contre les nématodes et charançons des bananiers à la Martinique. *Nematropica*, 35(1):11–22, 2005.

[15] C. Chabrier, H. Mauléon, P. Bertrand, A. Lassoudière, and P. Quénéhervé. Banane antillaise, les systèmes de culture évoluent: en Martinique, méthodes alternatives pour réduire l'utilisation des nématicides et insecticides en bananeraies. *Phytoma - La défense des végétaux*, 584:12–16, 2005.

[16] C. Chabrier and P. Quénéhervé. Control of the burrowing nematode (*Radopholus similis* Cobb) on banana: impact of the banana field destruction method on the efficiency of the following fallow. *Crop protection*, 22(1):121–127, 2003.

[17] C. Chabrier, P. Tixier, P.-F. Duyck, Y.-M. Cabidoche, and P. Quénéhervé. Survival of the burrowing nematode *Radopholus similis* (Cobb) Thorne without food: Why do males survive so long? *Applied Soil Ecology*, 45(2):85 – 91, 2010.

[18] D. L. Coyne, L. Cortada, J. J. Dalzell, A. O. Claudius-Cole, S. Haukeland, N. Luambano, and H. Talwana. Plant-parasitic nematodes and food security in sub-saharan Africa. *Annual review of phytopathology*, 56:381–403, 2018.

[19] N. J. Cunniffe, B. Koskella, C. J. E. Metcalf, S. Parnell, T. R. Gottwald, and C. A. Gilligan. Thirteen challenges in modelling plant diseases. *Epidemics*, 10:6–10, 2015.

[20] O. Diekmann and J. A. P. Heesterbeek. *Mathematical epidemiology of infectious diseases: model building, analysis and interpretation*, volume 5. John Wiley & Sons, 2000.

[21] DSCE. Cadre de référence de l'action gouvernementale pour la période 2010-2020. Technical report, Doc/INS, 2009.

[22] N. K. Dubey, R. Shukla, A. Kumar, P. Singh, and B. Prakash. Global scenario on the application of natural products in integrated pest management programmes. In *Natural products in plant pest management*, volume 1, pages 1–20. CABI Preston, 2011.

[23] L. W. Duncan. *Nematode parasites of citrus*, chapter 12, pages 437–466. CAB International Edit., Wallingford Oxon, U.K., 2005.

[24] L. W. Duncan, D. T. Kaplan, and J. W. Noling. Maintaining barriers to the spread of *Radopholus citrophilus* in Florida citrus orchards. *Nematropica*, 20:71–87, 1990.

[25] L. W. Duncan and M. Moens. Migratory endoparasitic nematodes. *Plant nematology*, pages 123–152, 2006.

[26] K. Eckstein and J. C. Robinson. The influence of the mother plant on sucker growth, development and photosynthesis in banana (Musa AAA; Dwarf Cavendish). *The Journal of Horticultural Science and Biotechnology*, 74(3):347–350, 1999.

[27] D. I. Edwards and E. J. Wehunt. Host range of Radopholus similis from banana areas of Central America with indications of additional races. *Plant disease reporter*, 55(5):415–418, 1971.

[28] M. Ehwaeti, M. Elliott, J. McNicol, M. Phillips, and D. Trudgill. Modeling nematode population growth and damage. *Crop Protection*, 19:739–745, 09 2000.

[29] G. Fallas and J. Sarah. Effect of temperature on the in vitro multiplication of seven Radopholus similis isolates from different banana producing zones of the world. *Fundamental and Applied Nematology*, 18:445–449, 1995.

[30] FAO. Banana market review and banana statistics 2012–2013. *Market and Policy Analyses of Raw Materials, Horticulture and Tropical (RAMHOT) Products Team. Rome*, 2014.

[31] M. Fargette and P. Quénéhervé. Populations of nematodes in soils under banana, cv. Poyo, in the Ivory Coast. the nematofauna occurring in the banana producing areas. *Revue de Nématologie*, 51(2):239–244, 1988.

[32] L. R. Faulkner and W. J. Bolander. Acquisition and distribution of nematodes in irrigation waterways of the Columbia Basin in Eastern Washington. *Journal of nematology*, 2(4):362–367, 1970.

[33] L. C. C. B. Ferraz and D. J. F. Brown. *An Introduction to Nematodes*. Plant Nematology. A student's textbook. Pensoft (edit.), Sofia, Bulgarie, 2002.

[34] S. A. Ferreira, E. Eduardo, and E. Trujillo. Banana bunchy top virus. *Plant Disease*, 12:1–4, 1997.

[35] R. Fogain. Effect of Radopholus similis on plant growth and yield of plantains (Musa, AAB). *Nematology*, 2:129–133, 05 2000.

[36] Food and Agriculture Organization of the United Nations (FAO). Banana facts and figures, 2020. Accessed 24 March 2020.

[37] J. E. Fox, J. Gulledge, E. Engelhaupt, M. E. Burow, and J. A. McLachlan. Pesticides reduce symbiotic efficiency of nitrogen-fixing rhizobia and host plants. *Proceedings of the National Academy of Sciences*, 104(24):10282–10287, 2007.

[38] A. Gelman, J. B. Carlin, H. S. Stern, D. B. Dunson, A. Vehtari, and D. B. Rubin. *Bayesian data analysis*. Chapman and Hall/CRC, 1996.

[39] C. Gilligan. Sustainable agriculture and plant diseases: An epidemiological perspective. *Philosophical transactions of the Royal Society of London. Series B, Biological sciences*, 363:741–59, 03 2008.

[40] C. Gilligan and A. Kleczkowski. Population dynamics of botanical epidemics involving primary and secondary infection. *Philosophical Transactions of the Royal Society B: Biological Sciences*, 352:591–608, 05 1997.

[41] C. A. Gilligan. *Mathematical Modeling and Analysis of Soilborne Pathogens*, pages 96–142. Springer Berlin Heidelberg, Berlin, Heidelberg, 1990.

[42] C. A. Gilligan. Modelling soil-borne plant pathogens: reaction-diffusion models. *Canadian Journal of Plant Pathology*, 17(2):96–108, 1995.

[43] S. Gowen. Chemical control of nematodes: efficiency and side-effects. In M. A. Maqbool and B. Kerry, editors, *Plant nematode problems and their control in the Near East region*, pages 59–65. FAO, 1997.

[44] S. R. Gowen, P. Quénéhervé, and R. Fogain. *Nematode Parasites of Bananas and Plantains*, pages 611–643. CAB International Edit., Wallingford Oxon, U.K., 2005.

[45] P. Gregory. *Plant Roots: Growth Activity and Interactions with Soils*. Bio-Green Elsevier (Exc), 2006.

[46] F. Grognard, I. Tankam Chedjou, Y. Fotso Fotso, and S. Touzeau. Modelling, control, and optimization for tropical agriculture. In *CMPD5 - Computational and Mathematical Population Dynamics*, Fort Lauderdale, United States, May 2019.

[47] S. Gubbins and C. A. Gilligan. Biological control in a disturbed environment. *Philosophical Transactions of the Royal Society of London. Series B: Biological Sciences*, 352(1364):1935–1949, 1997.

[48] R. J. Hall, S. Gubbins, and C. A. Gilligan. Evaluating the performance of chemical control in the presence of resistant pathogens. *Bulletin of mathematical biology*, 69(2):525–537, 2007.

[49] F. M. Hamelin, M. Castel, S. Poggi, D. Andrivon, and L. Mailleret. Seasonality and the evolutionary divergence of plant parasites. *Ecology*, 92(12):2159–2166, 2011.

[50] A. Hamzah, N. Shamsidah, M. Mamat, S. C. Lee, and N. Ahmad. Impulsive differential equations by using the Euler method. *Applied Mathematical Sciences*, 4(65):3219–3232, 2010.

[51] T. E. Hewlett, E. Hewlett, and D. W. Dickson. Response of Meloidogyne spp., Heterodera glycines, and *Radopholus similis* to tannic acid. *Journal of nematology*, 29(4S):737, 1997.

[52] C. S. Holling. The Functional Response of Invertebrate Predators to Prey Density. *Memoirs of the Entomological Society of Canada*, 98(S48):5–86, 1966.

[53] R. Hugon and H. Picard. Relations spatiales entre taches et nécroses racinaires et nématodes endoparasites chez le bananier. *Fruits*, 43(9):491–498, 1988.

[54] F. N. Jesus, J. C. A. Damasceno, D. H. S. G. Barbosa, R. Malheiro, J. A. Pereira, and A. C. F. Soares. Control of the banana burrowing nematode using sisal extract. *Agronomy for Sustainable Development*, 35(2):783–791, Apr 2015.

[55] D. T. Kaplan and C. H. Opperman. Reproductive strategies and karyotype of the burrowing nematode, *Radopholus similis*. *Journal of Nematology*, 32(2):126, 2000.

[56] J. Kehres, D. Denon, and H. Mauléon. A simple technique to estimate, in situ, population densities of an entomopathogenic nematode (heterorhabditis indica) in sandy soils. *Nematology*, 3(3):285 – 287, 2001.

[57] S. Koike, K. Subbarao, R. M. Davis, and T. Turini. *Vegetable diseases caused by soilborne pathogens*. UCANR Publications, 2003.

[58] P. K. Koshy, P. Sundararaju, V. K. Sosamma, and K. Ravikumar. Efficacy of four systemic nematicides against Radopholus similis in coconut nursery. *Indian Journal of Nematology*, 15(2):148–151, 1985.

[59] V. Lakshmikantham, D. D. Bainov, and P. S. Simeonov. Impulsive differential equations: periodic solutions and applications. *Pitman monographs and surreys in pure and applied mathematics*, 66, 1993.

[60] S. A. Lomov. *Introduction to the general theory of singular perturbations*, volume 112. American Mathematical Soc., 1992.

[61] C. A. Loos. Studies on the life history and habits of the burrowing nematode, *Radopholus similis*, the cause of the blackhead disease of banana. *Proceeding of the Helminthological Society of Washington*, 29(1):43–56, 1962.

[62] C. A. Loos and S. Loos. The blackhead disease of bananas (Musa acuminata). In *Proceeding of the Helminthological Society of Washington*, volume 27 (2), pages 189–193, 1960.

[63] P. Loridat. Etude de la microflore fongique et des nématodes associés aux nécroses de l'appareil souterrain du bananier en Martinique. mise en évidence du pouvoir pathogène du genre *Cylindrocladium*. *Fruits*, 44(11):587–598, 1989.

[64] Z. Ma and J. Li. *Dynamical Modeling and Analysis of Epidemics*. World Scientific, 01 2009.

[65] L. V. Madden and F. Van Den Bosch. A Population-Dynamics Approach to Assess the Threat of Plant Pathogens as Biological Weapons against Annual Crops: Using a coupled differential-equation model, we show the conditions necessary for long-term persistence of a plant disease after a pathogenic microorganism is introduced into a susceptible annual crop. *BioScience*, 52(1):65–74, 2002.

[66] L. Mailleret, M. Castel, M. Montarry, and F. Hamelin. From elaborate to compact seasonal plant epidemic models and back: Is competitive exclusion in the details? *Theoretical Ecology*, 5:311–324, 2011.

[67] L. Mailleret and V. Lemesle. A note on semi-discrete modelling in the life sciences. *Philosophical Transactions of the Royal Society of London A: Mathematical, Physical and Engineering Sciences*, 367(1908):4779–4799, 2009.

[68] T. Maly and L. R. Petzold. Numerical methods and software for sensitivity analysis of differential-algebraic systems. *Applied Numerical Mathematics*, 20(1):57 – 79, 1996. Method of Lines for Time-Dependent Problems.

[69] D. H. Marin, K. R. Barker, and T. B. Sutton. Efficacy of ABG-9008 against burrowing nematode (*Radopholus similis*) on bananas. *Nematropica*, 30(1):1–8, 2000.

[70] D. H. Marín, R. A. Romero, M. Guzmán, and T. B. Sutton. Black sigatoka: An increasing threat to banana cultivation. *Plant Disease*, 87(3):208–222, 2003. PMID: 30812750.

[71] D. H. Marin, T. B. Sutton, and K. R. Barker. Dissemination of bananas in Latin America and the Caribbean and its relationship to the occurrence of *Radophouls similis*. *Plant disease*, 82(9):964–974, 1998.

[72] S. F. Masri, G. A. Bekey, and F. B. Safford. A global optimization algorithm using adaptive random search. *Applied Mathematics and Computation*, 7(4):353 – 375, 1980.

[73] R. McSorley. Adaptations of nematodes to environmental extremes. *Florida Entomologist*, 86(2):138 – 142, 2003.

[74] G. Minderman. New techniques for counting and isolating free living nematodes from small soil samples and from oak forest litter. *Nematologica*, 1(3):216 – 226, 1956.

[75] Ministère du Commerce, Ministère de l'Agriculture et du Développement Rural, Ministère de la Recherche Scientifique et de l'Innovation, Ministère de l'Economie de la Planification et de l'Aménagement du Territoire. *Stratégie de développement de la filière banane plantain au Cameroun*, Visited on May 07, 2018.

[76] B. Moreau and J. Le Bourdelles. Etude du système racinaire du bananier Gros Michel en Equateur. *Fruits*, 18(2):71–74, 1963.

[77] G. D. Morgan, A. E. MacGuidwin, J. Zhu, and L. K. Binning. Population dynamics and distribution of root lesion nematode (pratylenchus penetrans) over a three-year potato crop rotation. *Agronomy Journal*, 94(5):1146–1155, 2002.

[78] C. C. Mundt. Durable resistance: A key to sustainable management of pathogens and pests. *Infection, Genetics and Evolution*, 27:446–455, 2014.

[79] J. M. Namaganda, I. N. Kashaija, and R. Maslen. Host status of the common weeds of banana establishments to banana nematodes in Uganda. *International Journal of Fundamental and Applied Nematological Research*, 4(2):271, 2002.

[80] National Horticulture Board, India. *BANANA*, Visited on May 04, 2018.

[81] A. H. Nayfeh. *Perturbation methods*. John Wiley & Sons, 1973.

[82] E. Ngo-Samnick. *Production améliorée du bananier plantain*. CTA, 2011.

[83] S. Nilusmas, M. Mercat, T. Perrot, C. Djian-Caporalino, P. Castagnone-Sereno, S. Touzeau, V. Calcagno, and L. Mailleret. A multi-seasonal model of plant-nematode interactions and its use to identify optimal plant resistance deployment strategies. *bioRxiv*, 2019.

[84] R. Nkendah and E. Akyeampong. Socioeconomic data on the plantain commodity chain in west and central Africa. *InfoMusa*, 12(1):8–13, 2003.

[85] J. Noling. Movement and toxicity of nematicides in the plant root zone. *ENY-041 (formerly RF-NG002)*, 1997.

[86] D. C. Norton. *Ecology of plant-parasitic nematodes*. Number SB998. N45. N6713 1978. Wiley New York, 1978.

[87] J. O'Bannon. Worldwide dissemination of *Radopholus similis* and its importance in crop production. *Journal of Nematology*, 9(1):16, 1977.

[88] J. N. Okolle, G. H. Fansi, F. M. Lombi, P. Sama Lang, and P. M. Loubana. Banana entomological research in Cameroon: how far and what next. *The African Journal of plant science and Biotechnology*, 3(1):1–19, 2009.

[89] J. Pinochet. Occurrence and spatial distribution of root-knot nematodes on bananas and plantains in Honduras. *Plant Disease Reporter*, 61(6):518–520, 1977.

[90] J. Pinochet, C. Fernandez, and J.-L. Sarah. Influence of temperature of in vitro reproduction of pratylenchus coffeae, *P. goodeyi*, and *Radopholus similis*. *Fundamental and applied Nematology*, 18(4):391–392, 1995.

[91] R. Plowright, J. Dusabe, D. Coyne, and P. Speijer. Analysis of the pathogenic variability and genetic diversity of the plant-parasitic nematode radopholus similis on bananas. *Nematology*, 15:41–56, 01 2013.

[92] J. Pretty. *The pesticide detox: towards a more sustainable agriculture*. Earthscan, 2012.

[93] R. J. Putman. *Community Ecology*. Springer Science, 1994.

[94] D. Qian and D. Li. Periodic solutions for ordinary differential equations with sublinear impulsive effects. *Journal of Mathematical Analysis and Applications*, 303(1):288–303, 2005.

[95] P. Quénéhervé. Population of nematodes in soil under banana, cv. Poyo, in the Ivory Coast. 5. Screening of nematicides and horticultural results. *Rev. Nématol.*, 14:231–249, 1989.

[96] P. Quénéhervé. Population of nematodes in soils under banana, cv. Poyo, in the Ivory Coast. 3. seasonal dynamics of populations in mineral soil. *Revue de Nématologie*, 12(2):149–160, 1989.

[97] P. Quénéhervé. Population of nematodes in soils under banana, cv. Poyo, in the Ivory Coast. 4. seasonal dynamics of populations in organic soil. *Revue de Nématologie*, 12(2):161–170, 1989.

[98] P. Quénéhervé. Nematode management in intensive banana agrosystems: comments and outlook from the Côte d'Ivoire experience. *Crop Protection*, 12(3):164 – 172, 1993.

[99] P. Quénéhervé, C. Chabrier, A. Auwerkerken, P. Topart, B. Martiny, and S. Marie-Luce. Status of weeds as reservoirs of plant parasitic nematodes in banana fields in Martinique. *Crop Protection*, 25(8):860–867, 2006.

[100] N. V. Ravichandra and K. Krishnappa. Effect of various pesticides on the control of the burrowing nematode, *Radopholus Similis* infecting banana. *Indian J. Nematol.*, 15(1):26–29, 1985.

[101] G. Reversat, J.-P. Rossi, and P. Bernhard. Analyse des courbes de survie de nématodes phytoparasites selon le modèle de teissier. *C. R. Acad. Sci. Paris, Sciences de la vie/Life Sciences*, 320(3):259–266, 1997.

[102] J. C. Robinson and V. G. Saúco. *Bananas and plantains*, volume 19. Cabi, 2010.

[103] F. E. Rosales, J. M. Alvarez, and A. Vargas. *Guide pratique pour la production de bananes plantains sous haute densité de plantation: retours d'expériences d'Amérique latine et des Caraïbes*. Bioversity International, 2010. French version of: Guía práctica para la producción de plátano con altas densidades: experiencias de América Latina y El Caribe.

[104] M. L. Rosenzweig and R. H. MacArthur. Graphical representation and stability conditions of predator-prey interactions. *The American Naturalist*, 97(895):209–223, 1963.

[105] A. Ryss and W. M. Wouts. The genus Radopholus (Nematoda: Pratylenchidae) from native vegetation in New Zealand, with descriptions of two new species. *International Journal of Nematology*, 7:1–17, 01 1998.

[106] D. Salguero, G. Rudon, R. Blanco, C. Moya, W. Ramclam, L. Medina, D. Azofeifa, and M. Araya. Effect of different nematicide applications per year on banana (musa aaa) root nematode control and crop yield. *Journal of Applied Biosciences*, pages 9598–9609, 01 2016.

[107] J. A. Sanders, F. Verhulst, and J. A. Murdock. *Averaging methods in nonlinear dynamical systems*, volume 59. Springer, 2007.

[108] J.-L. Sarah. Répartition spatiale des infestations racinaires de *Radopholus similis* (COBB) en relation avec la croissance et le développement du bananier Poyo en Côte d'ivoire. *Fruits*, 41:427–435, 1986.

[109] J.-L. Sarah. Variabilité du pouvoir pathogène de *Radopholus similis* entre populations provenant de différentes zones de production du monde. *Infomusa (Ed. Française)*, 2(2):6, 1993.

[110] J.-L. Sarah, A. Lassoudière, and R. Guérout. La jachère nue et l'immersion du sol: deux méthodes intéressantes de lutte integrée contre *Radopholus similis* (cobb.) dans les bananeraies des sols tourbeux de Côte d'Ivoire. *Fruits*, 38(1):35–42, 1983.

[111] J.-L. Sarah and X. Perrier. Sampling *Radopholus similis* in banana-sample size and accuracy. In *XIX International Nem. Symp. ESN.*, Uppsala, Sweden, August 1988.

[112] J.-L. Sarah, J. Pinochet, and J. Stanton. *Radopholus similis Cobb, nématode parasite des bananiers*. Fiche technique n1, INIBAP, Montpellier, France, 1996.

[113] J.-L. Sarah and A. Vilardebo. L'utilisation du miral en Afrique de l'Ouest pour la lutte contre les nématodes du bananier. *Fruits*, 34(12):729–741, 1979.

[114] G. B. Schaalje. Dynamic Models of Pesticide Effectiveness. *Environmental Entomology*, 19(3):439–447, 06 1990.

[115] E. Serrano. Relationship between functional root content and banana yield in costa rica. In D. W. Turner and F. E. Rosales, editors, *Banana root system: towards a better understanding for its productive management*, pages 25–34. Bioversity International, 2003.

[116] E. Shchepakina, V. Sobolev, and M. Mortell. *Singular perturbations. Introduction to system order reduction methods with applications*, volume 2114. Springer, 01 2014.

[117] M. R. Siddiqi. On the classification of the Pratylenchidae (Thorne, 1949) nov. grad.(Nematoda: Tylenchida), with a description of Zygotylenchus browni nov. gen. et nov. sp. *Parasitology Research*, 23(4):390–396, 1963.

[118] F. J. Solis and R. J.-B. Wets. Minimization by random search techniques. *Mathematics of Operations Research*, 6(1):19–30, 1981.

[119] I. Stamova. *Stability analysis of impulsive functional differential equations*, volume 52. Walter de Gruyter, 2009.

[120] R. H. Stover. *Banana, plantain and abaca diseases*. Kew, UK, Commonwealth Mycological Institute, 1972.

[121] S. Tang, Y. Tan, L. Juhua, and A. Cheke, R. Threshold conditions for integrated pest management models with pesticides that have residual effect. *Journal of Mathematical Biology*, 66(1):1–35, 2011.

[122] I. Tankam-Chedjou, F. Grognard, J. J. Tewa, and S. Touzeau. Optimal and sustainable management of a soilborne banana pest. *Applied Mathematics and Computation*, 397:125883, 2021.

[123] I. Tankam-Chedjou, F. Grognard, J. J. Tewa, and S. Touzeau. When and how to fallow: first steps towards banana crop yield improvement through optimal and sustainable control of a soilborne pest. *J. of Interd. Method. and Issues in Science*, 8:–, 2021.

[124] I. Tankam Chedjou, S. Touzeau, F. Grognard, L. Mailleret, and J.-J. Tewa. A multi–seasonal model of the dynamics of banana plant–parasitic nematodes. In E. Badouel, N. Gmati, and B. Watson, editors, *14. Colloque Africain sur la Recherche en Informatique et en Mathématiques Appliquées (CARI'2018)*, 2018.

[125] I. Tankam Chedjou, S. Touzeau, L. Mailleret, F. Grognard, and J. J. Tewa. Agricultural control of Radopholus similis in banana and plantain plantations. In *BIOMATH 2019 - International Conference on Mathematical Methods and Models in Biosciences*, Bedlewo, Poland, June 2019.

[126] I. Tankam-Chedjou, S. Touzeau, L. Mailleret, J. J. Tewa, and F. Grognard. Modelling and control of a banana soilborne pest in a multi-seasonal framework. *Mathematical Biosciences*, 322:108324, 2020.

[127] C. R. Taylor and R. Rodrìguez-Kábana. Optimal rotation of peanuts and cotton to manage soil-borne organisms. *Agricultural Systems*, 61(1):57–68, 1999.

[128] G. Teissier. Recherches sur le vieillissement et sur les lois de la mortalité. *Annales de physiologie et de physicochimie biologique*, 10:237–284, 1934.

[129] L. Temple, J. Chataigner, and F. Kamajou. Le marché du plantain au Cameroun, des dynamiques de l'offre au fonctionnement du système de commercialisation. *Fruits*, 51(2):83 – 98, 1996.

[130] R. N. Thompson, C. A. Gilligan, and N. J. Cunniffe. Control fast or control smart: When should invading pathogens be controlled? *PLOS Computational Biology*, 14(2):1–21, 02 2018.

[131] R. N. Thompson, K. Jalava, and U. Obolski. Sustained transmission of ebola in new locations: more likely than previously thought. *The Lancet Infectious Diseases*, 19(10):1058–1059, 2019.

[132] A. N. Tikhonov. Systems of differential equations containing small parameters in the derivatives. *Matematicheskii sbornik*, 73(3):575–586, 1952.

[133] P. Tixier, J.-M. Risède, M. Dorel, and E. Malézieux. Modelling population dynamics of banana plant–parasitic nematodes: A contribution to the design of sustainable cropping systems. *Ecological Modelling*, 198(3):321–331, 2006.

[134] A. Törn and A. Žilinskas. *Global optimization*, volume 350. Springer, 1989.

[135] S. Touzeau, I. Tankam Chedjou, Y. Fotso, J.-J. Tewa, B. Tsanou, S. Bowong, L. Mailleret, F. Grognard, and et al. Modélisation et contrôle en épidémiologie de cultures tropicales : application aux nématodes phytoparasites du bananier plantain et aux scolytes du caféier. In P. Bonnet, M. Roche, and H. Kirchner, editors, *AgriNumA'2019. Résumés des communications*, Dakar, Sénégal, 28 Avril - 30 Avril 2019. CIRAD.

[136] W. Tushemereirwe, A. Kangire, F. Ssekiwoko, L. C. Offord, J. Crozier, E. Boa, M. Rutherford, and J. J. Smith. First report of Xanthomonas campestris pv. musacearum on banana in Uganda. *Plant Pathology*, 53(6):802–802, 2004.

[137] S. M. Ulloa Cortazar, E. D. Wolf, and I. Armendáriz González. Effect of plant density on growth and yield in barraganete plantain (musa paradisiaca (l.) aab cv. curare enano) for a single harvest cutting in provincia de los ríos, ecuador. *Acta agronómica*, 66(3):367–372, 2017.

[138] R. V. Valmayor, S. H. Jamaluddin, B. Silayoi, S. Kusumo, L. D. Danh, O. C. Pascua, and R. R. C. Espino. *Banana cultivar names and synonyms in Southeast Asia.* INIBAP Regional Office for Asia and the Pacific, Laguna, Philippines, 2000.

[139] W. Van den Berg and W. Rossing. Generalized linear dynamics of a plant-parasitic nematode population and the economic evaluation of crop rotations. *Journal of nematology*, 37:55–65, 04 2005.

[140] W. Van Den Berg, W. A. H. Rossing, and J. Grasman. Contest and scramble competition and the carry-over effect in Globodera spp. in potato-based crop rotations using an extended Ricker model. *Journal of nematology*, 38(2):210–220, 2006.

[141] W. Van den Berg, J. Vos, and J. Grasman. Multimodel inference for the prediction of disease symptoms and yield loss of potato in a two-year crop rotation experiment. *International Journal of Agronomy*, 2012:9 pages, 2012.

[142] L. G. Van Weerdt. Studies on the biology of *Radopholus similis* (Cobb, 1893) Thorne, 1949. Part II, Morphological variation within and between progenies of single females. *Nematologica*, 3:184–196, 1958.

[143] L. G. Van Weerdt. Studies on the Biology of *Radopholus similis* (Cobb, 1893) Thorne, 1949. Part III, Embryology and Post–Embryonic Development. *Nematologica*, 5:43–52, 1960.

[144] A. B. Vasil'eva, V. F. Butuzov, and L. V. Kalachev. *The Boundary Function Method for Singular Perturbed Problems*, volume 14. Siam, 1995.

[145] F. Verhulst. Singular perturbation methods for slow–fast dynamics. *Nonlinear Dynamics*, 50(4):747–753, 2007.

[146] A. Vilardebo. Méthode d'essai d'efficacité pratique de nématicides étudiés sur *Radopholus similis* COBB en bananeraie, 1974.

[147] N. A. Walker and S. E. Smith. The quantitative study of mycorrhizal infection. *New Phytologist*, 96(1):55–69, 1984.

[148] E. Walter and L. Pronzato. *Identification of parametric models from experimental data*. Springer Verlag, 1997.

[149] R. Webster and B. Boag. Geostatistical analysis of cyst nematodes in soil. *Journal of Soil Science*, 43(3):583–595, 1992.

[150] N. Wuyts, A. Elsen, E. Van Damme, W. Peumans, D. De Waele, R. Swennen, and L. Sági. Effect of plant lectins on the host-finding behaviour of *Radopholus similis*. *Nematology, 2003*, 5(2):205–212, 2003.

[151] Y. Yates. The analysis of experiments containing different crop rotations. *Biometrics*, 10(3):324–346, 1954.

[152] G. Yeates and B. Boag. Female size shows similar trends in all clades of the phylum Nematoda. *Nematology*, 8(1):111–127, 2006.

[153] C. Zhang, H. Xie, C. Xu, X. Cheng, K.-M. Li, and Y. Li. Differential expression of rs-eng-1b in two populations of radopholus similis (Tylenchida: Pratylecnchidae) and its relationship to pathogenicity. *European Journal of Plant Pathology*, 133:899–910, 08 2012.

[154] A. zum Felde, L. Pocasangre, and R. A. Sikora. The potential use of microbial communities inside suppressive banana plants for banana root protection. In *Banana Root System: towards a better understanding for its productive management: Proceedings of an international symposium/Sistema Radical del Banano: hacia un mejor conocimiento para su manejo productivo: Memorias de un simposio internacional*, pages 169–177, 2005.